UCSF
UC San Francisco Electronic Theses and Dissertations

Title
NFATc1 controls skeletal muscle fiber type and is a negative regulator of MyoD transcriptional activity

Permalink
https://escholarship.org/uc/item/1sc5t4kg

Author
Ehlers Stewart, Melissa Laura

Publication Date
2012

Peer reviewed|Thesis/dissertation

eScholarship.org Powered by the California Digital Library
University of California

NFATc1 controls skeletal muscle fiber type and is a negative regulator of MyoD transcriptional activity

by

Melissa Stewart

DISSERTATION

Submitted in partial satisfaction of the requirements for the degree of

DOCTOR OF PHILOSOPHY

in

Biomedical Sciences

in the

GRADUATE DIVISION

of the

Dedication:

This work is dedicated to my husband, Ross William Stewart, for his unwavering love, support, and encouragement throughout my graduate studies. And to my loving parents, Ron and Jacqueline Ehlers, who are always proud of me, no matter what.

Acknowledgements:

First, I would also like to thank my graduate advisor, Dr. Brian Black for the opportunity to work in his lab. Brian has the highest expectations of his graduate students and post-docs. Though at times I perceived them to be unreasonable, they have made me not only a better scientist, but also a better professional. Brian is a critical scientist, enthusiastic speaker, and great scientific writer. I feel that I have been well trained in all of these areas having had him as an advisor. I would also like to thank my thesis committee members, Dr. Tamara Alliston and Dr. Harold Bernstein, for their support and mentorship. I greatly appreciate all of their helpful suggestions and discussions about my thesis work over the years.

The Black lab has always had extraordinary people, and Brian has done a nice job of putting together a group of people that have been great scientists, collaborators, and friends. I would especially like the thank Sarah de Val for being a great mentor to me during my first few years of graduate school. She has been a wonderful role model for me to this day. I would also like to especially thank Barbara (Piccola) Celona for all her help and encouragement during my final months of graduate school, not only with experiments to finish up the manuscript, but with her enthusiasm and reassurance that we would succeed. And to those who have been in the lab during the majority of my time here, Ashley Robinson, Kelly Lammerts Van Bueren, Will Schachterle and Dave McCulley have been wonderful co-workers and friends and have always been supportive of me. Lastly, to Luiza Savin for being a very dependable lab manager, both in the day to day needs of the lab, and especially for all her hard work and dedication in managing our mouse colony.

I would like to thank my parents, Ron and Jackie Ehlers, and my sister, Kristen Ehlers. I will never take for granted the love and support they have given me throughout my life, and especially during graduate school. They have always been proud of me, no matter how big or small an achievement I have made, and for that, I am forever grateful.

Finally, I would also like to thank my wonderfully awesome husband, Ross Stewart. Without his unfailing and unconditional love and support over the past seven years, I would not have had the fortitude and perseverance to complete this work. Throughout the past seven years Ross has always been my number one supporter. He has always had the patience to listen to my many worries and has always brought me back to reality when I needed it most. He is an amazing companion, who inspires me and makes me laugh, and I would not be the person I am today without him.

Abstract

The NFAT family of transcription factors regulates cell differentiation programs in a variety of cellular contexts, including immune cell activation, cardiac valve development, osteoclast differentiation, and fiber type in skeletal muscle. NFAT proteins are activated by the phosphatase calcineurin in response to increases in intracellular calcium levels, and can function as either activators or repressors, depending on co-factor interactions. Four of the five known NFAT transcription factors are expressed in skeletal muscle, of which NFATc2 and NFATc3 have a known function in skeletal muscle *in vivo*. However, studies interrogating the role of NFATc1 in skeletal muscle *in vivo* have been limited because *Nfatc1*-null mice die around E12.5 due to cardiac valve defects. We identified a novel function for NFATc1 in skeletal muscle as a repressor of the skeletal muscle specific bHLH transcription factor MyoD. We found that NFATc1, but not other NFAT isoforms, inhibits MyoD transactivation function. We found that NFATc1 physically interacts with MyoD via the N-terminal transactivation domain of MyoD and inhibits MyoD-mediated conversion of C3H10T1/2 fibroblasts into myosin expressing myotubes. We show that, and that NFATc1 is able to inhibit the transactivation ability of MyoD. To further verify NFATc1 repression of MyoD and to study the role of NFATc1 *in vivo,* we used Cre-Lox technology to generate a skeletal-muscle specific *nfatc1* knockout mouse (*nfatc1*$^{SkM\text{-}KO}$). We show that ^{NFATc1} controls skeletal muscle fiber type composition in adult mice. The balance between Type I (slow) and Type II (fast) myofibers is altered in mice lacking *nfatc1*, with these mice exhibiting an increase in the number of Type II (fast) myofibers compared to wild type mice. In addition, we found that NFATc1 is required for proper fiber type switching of myofibers from the fast-to-

slow fiber type phenotype in response to endurance exercise training. Finally, we examined the expression levels of several known MyoD target genes in muscle of *nfatc1* $^{SkM\text{-}KO}$ mice, and found that the majority of genes analyzed are upregulated, providing *in vivo* support of our findings that NFATc1 negatively regulates MyoD. We propose a model whereby NFATc1 represses MyoD transactivation ability, at least in part, to promote the slow fiber phenotype through repression of fast fiber genes regulated by MyoD.

Table of Contents:

Dedication…….. iii

Acknowledgements……... iv

Abstract……..... vi

List of Figures and Tables…… ix

Chapters:

1. Introduction……... 1

2. NFATc1 negatively regulates MyoD activity and controls skeletal muscle fiber type composition…… 21

3. Conclusions and Implications……..81

4. Materials and Methods……93

5. References……119

List of Tables and Figures

Figure 1: The *Mef2c* skeletal muscle specific enhancer contains multiple NFAT sites……58

Figure 2: NFATc1 inhibits Transactivation of the *Mef2c* enhancer by MyoD……59

Figure 3: NFATc1 inhibition of MyoD transactivation does not require NFAT sites……60

Figure 4: *MRF4* and *myogenin* promoter transactivation by MyoD is inhibited by NFATc1……62

Figure 5: NFATc1 inhibits MyoD-mediated conversion of fibroblasts into myotubes…63

Figure 6: MyoD and NFATc1 physically interact……64

Figure 7: NFATc1 does not affect MyoD nuclear localization……66

Figure 8: NFATc1 does not inhibit MyoD DNA binding or dimerization with E-proteins…….....67

Figure 9: NFATc1 inhibits MyoD-mediated transactivation via the N-terminal activation domain…….....69

Figure 10: Generation of a skeletal muscle-specific knockout of *nfatc1*……70

Figure 11: *nfatc1*$^{SkM\text{-}KO}$ mice do not have growth deficits……71

Figure 12: *nfatc1*$^{SkM\text{-}KO}$ mice do not have exercise deficits……..72

Figure 13: NFATc1 is required for proper fiber type balance and fiber type switching in response to exercise……...73

Figure 14: *nfatc1*$^{SkM\text{-}KO}$ muscle may have an increase in muscle regeneration in post-exercised muscle……75

Figure 15: NFATc1 is expressed in slow and fast myofiber nuclei……..76

Figure 16: NFATc1 and MyoD co-localize in skeletal muscle nuclei……77

Figure 17: *nfatc1*$^{SkM\text{-}KO}$ muscle has a defect in fast fiber gene expression at baseline….78

Figure 18: NFATc1 is required for proper expression of several MyoD target genes

in skeletal muscle……...79

Figure 19: Schematic model: NFATc1 inhibits MyoD in order to promote the slow fiber phenotype……..80

Table 1: Expression vectors and control probes for EMSA……105

Table 2: List of *mef2c* enhancer probes……..106

Table 3: List of primer sets used for qRT-PCR experiments……117

Chapter 1: Introduction

Skeletal muscle development

Skeletal muscle comprises up to 50% of total body mass, making it the largest organ in the body. Being such a large percentage of the human body, skeletal muscle plays a very important role in whole body metabolism. Skeletal muscles also allow the movement of the body, maintain posture, and hold the skeleton in the correct position, thereby preventing joint dislocation. In addition, skeletal muscles generate heat as a by-product of muscle activity, which is vital for maintaining normal body temperature.

During vertebrate embryogenesis, skeletal muscle of the trunk and limbs forms from progenitor cells originating in the somites. The somites are transient, segmentally organized mesodermal structures that bud off as epithelial spheres from the cranial end of the unsegmented presomitic mesoderm located on either side of the neural tube and notochord (Brent and Tabin 2002; Buckingham et al. 2003). The ventral part of the somite, known as the sclerotome, will differentiate into the cartilage and bone of the ribs and vertebrae, whereas the dorsal part of the somite, the dermomyotome, gives rise to the dorsal dermis and to the skeletal muscles of the body and limbs (Buckingham et al. 2003).

The first muscle mass to form, under the dermomyotome, is the myotome, which has an epaxial and a hypaxial component (Tajbakhsh and Buckingham 2000). The epaxial myotome forms the intercostal and abdominal wall muscles and the muscles of the back, whereas the hypaxial myotome is responsible for the formation of the muscle of the limbs, diaphragm, tongue, and the muscles of some branchial arch derived tissue

(Kablar et al. 1998). In the region of the embryo opposite the limb buds, skeletal muscle progenitor cells delaminate from the epithelium of the hypaxial dermomyotome and migrate into the limb bud, where they proliferate, express myogenic determination factors and subsequently differentiate into skeletal muscle (Buckingham et al. 2003).

Once mesodermal progenitor cells have been specified to the myogenic lineage, skeletal muscle development requires the differentiation and fusion of progenitors to form contractile, multinucleated myofibers. A number of regulatory factors involved in skeletal muscle specification and differentiation have been identified. These include Pax3, Lbx1 and Mox2 as well as the myogenic regulatory factors (MRFs)- MyoD, Myf5, myogenin, and MRF4- also referred to as the MyoD family of basic helix–loop–helix (bHLH) transcription factors. Myf5 and MyoD are considered myogenic determination factors, whereas myogenin is required for terminal differentiation, and MRF4 plays a role in both specification and differentiation (Buckingham et al. 2003; Tapscott 2005). In addition to the MRFs, the myocyte enhancer factor 2 (MEF2) family of transcription factors have also been shown to be important in the activation of muscle-specific gene expression in mice (Black and Olson 1998; Naya et al. 1999).

In particular, the MyoD family of transcription factors plays a critical role in the formation of skeletal muscle during embryogenesis. In the mouse, gene manipulation has made it possible to test the function of this family of factors, and therefore, the molecular regulation of myogenesis has been particularly well established (Buckingham 2001). Mice lacking *Myf5* display delayed embryonic myogenesis, which proceeds normally once MyoD expression is initiated (Braun et al. 1992). Interestingly, a later study showed that in *Myf5*-null mice, cells in the somite that would normally become myoblasts, do not

locate correctly to sites of myogenesis and therefore, adopt alternative cell fates (Tajbakhsh et al. 1996). *MyoD* knockout mice have largely normal skeletal muscle development due to prolonged and increased *Myf5* expression, which normally declines in wild-type mice at the more advanced developmental stage when MyoD expression begins (Rudnicki et al. 1992). These results have been shown to be due to redundancy of *Myf5* and *MyoD* during myogenesis. This redundancy became apparent from the complete lack of skeletal muscle and *myogenin* expression in *Myf5*/*MyoD* double-null mice (Rudnicki et al. 1993). In *Myf5*/*MyoD* double mutants, skeletal muscle does not form due to the absence of the myoblast precursor population (Rudnicki et al. 1993). Taken together, these findings establish MyoD and Myf5 as myogenic determination factors.

The differentiation of myoblasts into muscle fibers also depends on members of the MyoD family of transcription factors, specifically MRF4 and myogenin. Myogenin functions downstream of Myf5 and MyoD to activate skeletal muscle gene expression, and appears to be crucial for the differentiation of muscle cells *in vivo* (Tapscott 2005). Analysis of *myogenin* null mice revealed that the expression of several differentiation markers, such as myosin heavy chain and MRF4, was reduced, whereas MyoD levels remained unchanged (Hasty et al. 1993; Nabeshima et al. 1993). Phenotypically, this resulted in normal somitic compartmentalization during development but manifested in diffuse myofiber formation and an abundance of undifferentiated myoblasts in the later stages of myogenesis, resulting in perinatal death as a result of a severe loss of differentiated muscle fibers (Hasty et al. 1993; Nabeshima et al. 1993). MRF4 was initially established as a differentiation factor, however later studies using an allelic series

of three *Myf5* mutants that differentially affect the expression of the genetically linked *Mrf4* gene, showed that skeletal muscle is present in the *Myf5*/*MyoD* double-null mice only when *Mrf4* expression is not compromised (Kassar-Duchossoy et al. 2004). This finding revealed that MRF4 plays a role not only in muscle differentiation, but in myogenic specification as well.

Other transcription factors also play an important role in skeletal muscle development, notably the MEF2 family, which is characterized by the presence of a MADSbox motif (Black and Olson 1998). There are four *Mef2* gene products in mice termed *mef2a* through *mef2d*. A number of studies suggest that MEF2 factors function as essential myogenic co-factors required by myogenic bHLH proteins to initiate myogenesis (Molkentin et al. 1995; Ornatsky et al. 1997; Black et al. 1998). Analysis of the control regions of several muscle-specific genes has revealed that MEF2 proteins cooperate with myogenic bHLH proteins to activate transcription in skeletal muscle cells (Molkentin and Olson 1996). MEF2 proteins lie within a regulatory cascade downstream of the myogenic bHLH proteins, as demonstrated by the finding that overexpression of myogenin or MyoD in non-muscle cells can induce MEF2 DNA binding activity (Cserjesi and Olson 1991; Lassar et al. 1991). In addition, *mef2* transcription is regulated by myogenic bHLH proteins. During skeletal muscle development, *mef2c* is the first member of the MEF2 family to be expressed (Black and Olson 1998). Studies highlighting the transcriptional regulation of *mef2c* identified an evolutionary conserved skeletal muscle-specific enhancer from the mouse *mef2c* gene and showed that *mef2c* is a direct transcriptional target of the MyoD family *in vivo* (Wang et al. 2001; Dodou et al. 2003). This activation occurs via an essential E-box binding element found within the

skeletal muscle enhancer of *mef2c* that is required for enhancer activity both *in vivo* and *in vitro* (Wang et al. 2001; Dodou et al. 2003).

The MyoD family of transcription factors is also important in the formation and growth of adult muscle fibers. In postnatal life, adult skeletal muscles retain a heterogeneous population of muscle progenitors, known as satellite cells, which are under the control of a transcriptional network reminiscent of that which functions during somitogenesis (Parker et al. 2003; Snider and Tapscott 2003). Satellite cells are quiescent cells that contribute to muscle growth, maintenance, repair, and regeneration, and are identified largely by their location under the basal lamina of skeletal muscle fibers and by their expression of the transcription factor Pax7 (Gnocchi et al. 2009; Wang and Rudnicki 2012). These cells are capable of repairing damaged segments of fibers or fusing together to generate entirely new multinucleated muscle fibers. Satellite cells arise during the late stages of mouse and chicken embryogenesis and are highly active during the postnatal growth of muscle tissue; therefore they provide most of the myonuclei to adult muscles (Schultz 1996). During the processes of proliferation and differentiation into myofibers, the satellite cell partially recapitulates the myogenic program. Myf5, MyoD, MRF4, and myogenin are expressed in similar during regeneration as in muscle development (Wang and Rudnicki 2012). Quiescent satellite cells do not express detectable levels of MRF protein or transcripts (Smith et al. 1994; Cornelison and Wold 1997). However, in response to exercise or muscle injury, satellite cells become activated and migrate to the site of injury where they commit to the myogenic lineage, subsequently expressing either MyoD or Myf5 before entering the cell cycle, allowing for expansion of the myogenic cell population (Smith et al. 1994; Seale and Rudnicki 2000; Hawke and Garry 2001).

Upon activation, the majority of satellite cells down-regulate Pax7 expression and ultimately undergo terminal muscle cell differentiation, whereas a small proportion of cells down-regulate MyoD expression, maintain Pax7 expression, and return to the quiescent state to sustain the satellite cell pool (Le Grand and Rudnicki 2007; Olguin et al. 2007; Biressi and Rando 2010). Activation of the downstream MRFs, myogenin and MRF4, is associated with terminal differentiation and fusion of satellite cells to new or existing fibers (Parker et al. 2003).

MyoD is an essential regulator in skeletal muscle

The basic helix-loop-helix (bHLH) transcription factor MyoD functions not only as an essential regulator of myogenesis, but is reutilized for multiple distinct roles in postnatal muscle as well. When expressed in primary fibroblasts or in a wide variety of other cell types, such as pigment, nerve, fat and liver, MyoD has the remarkable ability to convert these cells to skeletal muscle (Davis et al. 1987; Weintraub et al. 1989). These findings provided the first direct evidence that a single gene can initiate a complex program of differentiation, acting as a master switch. This potential largely depends on the ability of MyoD to penetrate and remodel chromatin at previously silent muscle loci (Gerber et al. 1997; de la Serna et al. 2005).

In undifferentiated myoblasts, the spontaneous activation of the differentiation program is prevented by recruitment of histone deacetylases (HDACs) on the chromatin of muscle genes. Class I HDACs preferentially associate with MyoD (Mal et al. 2001; Puri et al. 2001), while class II HDACs act as repressors of MEF2-dependent transcription (McKinsey et al. 2000). These interactions prevent hyperacetylation on the

regulatory elements of muscle genes. During muscle differentiation, HDACs are displaced from muscle bHLH and MEF2 proteins by distinct mechanisms (McKinsey et al. 2002), thereby allowing interactions with the acetyltransferases p300 and PCAF (Sartorelli et al. 1997; Sartorelli et al. 1999). The role of p300 in myogenic differentiation is independent of its acetyl transferase activity, and involves targeting PCAF for interaction with MyoD (Puri et al. 1997) and subsequent MyoD acetylation, which plays an important role in MyoD activity (Sartorelli et al. 1999).

Genetic studies have indicated that the four members of the MyoD family play distinct but overlapping roles in the embryo and participate in a mutually reinforcing transcriptional network to activate myogenesis appropriately (Sabourin and Rudnicki 2000; Buckingham et al. 2003; Tajbakhsh 2003). In order to activate gene transcription, MyoD and the other members of the myogenic bHLH family function as heterodimers with the ubiquitously expressed E2A gene products (E12, E47 and HEB), which are also basic helix-loop-helix proteins (Lassar et al. 1991). MyoD and E-proteins function as heterodimers through the interaction of their HLH domains (Murre et al. 1989). The basic regions act as sequence-specific DNA-binding domains that recognize a binding site on target genes with the core consensus sequence of CANNTG, termed an E-box (Blackwell and Weintraub 1990; Davis et al. 1990). MyoD protein contains a potent amino-terminal acidic-activation domain, as determined by its fusion to the heterologous DNA-binding domain of the Gal4 protein (Weintraub et al. 1991). This N-terminal activation domain also contains a specific motif, referred to as the C/H domain (Gerber et al. 1997) that facilitates interactions with p300/CBP and other chromatin remodeling enzymes (Puri et al. 1997; Puri et al. 1997; Sartorelli et al. 1997; Sartorelli et al. 1999; Polesskaya et al.

2001) to confer "pioneer" activity to MyoD. The MyoD C-terminal region contains an alpha helix that is critical for the efficient initiation of skeletal muscle gene expression through facilitation of chromatin remodeling (Gerber et al. 1997; Bergstrom and Tapscott 2001; Tapscott 2005). Recently, this was found to involve interaction of the MyoD C-terminus with BAF60c (Forcales 2012), a structural component of the SWI/SNF chromatin-remodeling complex that is required for the activation of muscle gene transcription (de la Serna et al. 2001; Simone et al. 2004; de la Serna et al. 2005).

During the early stages of skeletal muscle differentiation, during both myogenesis and in adult skeletal muscle, MyoD is not only involved in muscle-specific gene induction, but also in regulating the transition from proliferation to the orderly exit from the cell cycle. This key step in skeletal muscle differentiation involves the down-regulation of several cell cycle activators such as cyclins and cdks, and up-regulation of cell cycle inhibitors such as Rb, p21, p27, and p57 (Kitzmann and Fernandez 2001). Particularly, the cyclin-dependent kinase inhibitors Rb and p21 have been shown to play an important role in the growth arrest of differentiating myoblasts. The activity of p21 and Rb, while being negatively controlled by growth factors, appears to be positively linked with MyoD, which initiates cell cycle withdrawal by directly inducing the expression of these two factors (Crescenzi et al. 1990; Sorrentino et al. 1990; Guo et al. 1995; Halevy et al. 1995; Kitzmann and Fernandez 2001) leading to subsequent activation of muscle-specific gene transcription (Weintraub et al. 1991).

Loss-of-function studies in mice not only highlight MyoD's important role in development (Rudnicki et al. 1993), but also illustrated the important function of MyoD postnatally (Megeney et al. 1996). During embryonic myogenesis, MyoD can

compensate for the absence of Myf5, whereas postnatally, the unique role of MyoD in the process of muscle regeneration cannot be substituted by Myf5 (Megeney et al. 1996). These features indicate that MyoD expression and activity must be controlled by different regulatory pathways during development versus in the adult. However these pathways are not as well known. *MyoD*-null mice have severely deficient muscle regeneration due to excessive proliferation and defective differentiation of adult satellite cells (Sabourin et al. 1999; Yablonka-Reuveni et al. 1999; Schuierer et al. 2005). Increased numbers of satellite cells and deficient regenerative processes in the muscle of mice that lack *MyoD*, indicates that *MyoD*-deficient satellite cells might have an increased propensity for self-renewal rather than differentiation (Megeney et al. 1996). Several studies have gone on to show that myoblasts derived from cultured *MyoD*-deficient satellite-cells have a greater than 90% reduction in differentiation efficiency relative to wild type cells, and observed that these mutant cells form unusual aggregate structures and fail to fuse efficiently (Sabourin et al. 1999; Yablonka-Reuveni et al. 1999; Cornelison et al. 2000).

An additional function of MyoD in muscle is to regulate the balance of slow and fast fiber types (Hughes et al. 1993; Hughes et al. 1997; Macharia et al. 2010). The idea that MyoD may regulate aspects of fiber type began with the finding that MyoD mRNA levels differ between fast and slow muscles, and that *lacZ* expression controlled by a *cis*-regulatory region of the *MyoD* gene was mainly observed in fast glycolytic muscle fibers. (Hughes et al. 1993). In addition, during development, MyoD protein becomes largely restricted to the nuclei of the fastest classes of fibers in fast muscles (Hughes et al. 1993). Mice with a disruption in the *MyoD* gene show subtle shifts in fiber type of fast muscles

toward a slower phenotype, suggesting that MyoD is involved in the maintenance of the fast fiber phenotype (Hughes et al. 1997; Macharia et al. 2010).

Skeletal muscle fiber type

Skeletal muscle is composed of a heterogeneous population of muscle fibers that display distinctive metabolic properties, rates of contraction, and susceptibility to fatigue (Bassel-Duby and Olson 2006; Schiaffino and Reggiani 2011). The heterogeneity of muscle fibers permits the same muscle to be used for a wide variety of tasks ranging from continuous low-intensity activity (posture), to repeated moderate contractions (locomotion), and to fast and strong contractions (jumping and kicking). The contractile properties of individual muscle fibers correlate with the myosin heavy chain (MyHC) isoform expressed. The central role of myosin as a molecular motor in muscle cell physiology and the existence of several MyHC isoforms differentially distributed in various fibers make MyHC the best available marker for fiber typing. Skeletal muscle fibers are therefore classified by the MyHC isoform expressed within an individual fiber. Thus, a useful classification divides muscle fibers into four types: Type I (slow-twitch) fibers that express MyHC I, and three subtypes of Type II (fast-twitch) fibers that express MyHC IIa, IId/x, or IIb, respectively (Pette and Staron 2000), with Type IIb fibers being the fastest. Type I (slow twitch) fibers are rich in mitochondria, display increased vascularization, and are fatigue-resistant due to the utilization of oxidative metabolism for energy production (Wang et al. 2004; Schiaffino and Reggiani 2011; Yan et al. 2011). The use of oxidative metabolism provides a stable and long-lasting supply of ATP to the myofiber, and therefore, Type I fibers are generally more suited to endurance type

activities, such as running a marathon. In contrast, Type II (fast twitch) fibers have low levels of mitochondria, fewer blood vessels, and rely on glycolytic metabolism as the main energy source. The use of glycolytic metabolism results in Type II fibers being more susceptible to rapid fatigue (Schiaffino and Reggiani 2011; Yan et al. 2011). Therefore, they are generally more suited to short burst of activity, such as sprinting or jumping.

In the mouse, muscle fiber type diversification is first observed during late embryonic development (Rana et al. 2009). Prior to E16, all muscle fibers co-express MyHC-emb and MyHC-β/slow (Narusawa et al. 1987; Condon et al. 1990; Lyons et al. 1990), as well as both fast- and slow-type isoforms of many other muscle genes (Niro et al. 2010). At E16, fiber type diversification is first observed with the loss of MyHC-β/slow expression in some muscle fibers, which then begin to express MyHC-neo. These two populations of muscle fibers expressing either MyHC-emb and MyHC-neo or MyHC-emb and MyHC-β/slow will give rise to fast or slow muscle fibers, respectively (Condon et al. 1990). In the neonate, skeletal muscles are still not fully mature, and significant changes in the fiber type profile occur during early stages of postnatal development, mainly as a result of neuromuscular system maturation (Slater 1982; Fladby and Jansen 1990; Jansen and Fladby 1990). During the first few weeks of postnatal development, as mice are beginning to walk and use coordinated movements, muscles mainly receive unpatterned neural activity (Rana et al. 2009). It is not until the second week after birth that differential patterns of neural activity become apparent (Pette and Vrbova 1985; Pette and Vrbova 1999; Personius and Balice-Gordon 2001), and by P15 they resemble those of adult muscle fibers (Hennig and Lomo 1985; Personius and

Balice-Gordon 2001). Fast and slow motor neurons are thought to undergo a simultaneous maturation process, and specific motor neuron firing patterns are established so that the properties of fast and slow motor neurons are closely matched to those of the muscle fibers they innervate (Schiaffino and Reggiani 2011). The contractile and metabolic properties of fast and slow muscle fibers largely depend on the pattern of motor nerve innervation and contractile activity. Slow twitch myofibers maintain relatively high intracellular calcium levels (100–300 nM) in contrast to fast twitch fibers, which are characterized by brief, high amplitude calcium transients and lower intracellular calcium levels (50 nM) (Crabtree and Olson 2002). The role of innervation in muscle fiber type differentiation is especially evident in the postnatal development of slow muscle fibers. Following denervation in neonates, myosin slow expression progressively declines in the rat soleus muscle fibers and is no longer detectable 4 weeks after denervation (Gambke et al. 1983).

The structural and functional properties of myofibers, referred to as fiber phenotype, can change in response to multiple stimuli, including hormones, physical demand, and neural activity (Garry et al. 1996; Schiaffino and Reggiani 2011). The ability of a muscle fiber to change from one fiber type to another is termed muscle plasticity. Adult skeletal muscle displays extraordinary plasticity and can undergo conversion between different fiber types in response to a variety of stimuli, including exercise training and motor neuron activity (Booth and Thomason 1991; Jarvis et al. 1996; Pette 1998; Olson and Williams 2000; Hood 2001; Schiaffino and Reggiani 2011). Changes in fiber type are largely regulated by the selective transcriptional activation or repression of genes encoding contractile proteins, making transcriptional control an

important regulatory mechanism controlling fiber type switching (Buonanno and Rosenthal 1996; Gundersen 1998; Spangenburg and Booth 2003; Schiaffino et al. 2007). The regulation of fiber type switching has been highlighted in several studies using electrical stimulation designed to mimic motor neuron firing. A fast-to-slow switch in the direction 2B → 2X → 2A → 1 can be induced by tonic low-frequency electrical stimulation, resembling the firing pattern of slow motor neurons. Alternatively, a slow-to-fast switch in the direction 1 → 2A → 2X → 2B can be induced by phasic high-frequency electrical stimulation, resembling the firing pattern of fast motor neurons (Pette and Vrbova 1999; McCullagh et al. 2004; Mu et al. 2007; Calabria et al. 2009).

The proportions of type I and type II fibers in the adult animal play a pivotal role in whole-body metabolism. There are two major aspects to the relationship between fiber type and whole body metabolism. First, skeletal muscle is the primary protein reservoir in the body, and release of amino acids from muscle during prolonged starvation is vital for maintaining plasma glucose concentration and for the synthesis of new proteins. During periods of fasting, as well as in other situations of muscle wasting, such as cancer cachexia or sepsis, Type IIb glycolytic muscle fibers show greater atrophy than type I oxidative fibers (Li and Goldberg 1976; Matsakas and Patel 2009). The greater sensitivity of the type IIb fibers might be due to their lower levels of the transcriptional coactivator PGC-1α, as suggested by the finding that PGC-1α overexpression partially prevents muscle atrophy by reducing the FoxO-dependent upregulation of ubiquitin ligases atrogin-1 and MuRF1 (Sandri et al. 2006). A second aspect of the relationship between muscle fiber type and whole body metabolism involves plasma glucose disposal. Skeletal muscle is the major sink for plasma glucose following a meal. This function is mediated

by the insulin-dependent translocation of the glucose transporter GLUT4 to the sarcolemma (Huang and Czech 2007). Hyperglycemia occurs when glucose uptake by muscle fibers is defective, such as seen in insulin resistance and type 2 diabetes. Slow-oxidative muscle fibers are more active than fast-glycolytic fibers in removing glucose from blood, and it has been suggested that an altered fiber type distribution with prevalence of fast-glycolytic fibers, often associated with obesity, may contribute to insulin resistance and type 2 diabetes (Patti et al. 2003; Wang et al. 2004; Lowell and Shulman 2005; Long et al. 2007).

Several studies have examined the link between fiber type and metabolism as it relates to disease. For instance, rats that gained the most weight on high-fat diets were found to possess fewer type I fibers (Abou Mrad et al. 1992), and skeletal muscle from obese or type 2 diabetic humans, has been observed to have reduced oxidative capacity and fewer type I fibers (Lillioja et al. 1987; Hickey et al. 1995; Tanner et al. 2002). Furthermore, a predominance of Type I fibers has been shown to enhance insulin-mediated glucose uptake, protect against glucose intolerance, and reduce adipocyte size (Luquet et al. 2003; Ryder et al. 2003; Oberbach et al. 2006). There is also emerging evidence that muscle diseases such as sarcopenia and atrophy affect type II fibers specifically (Porter et al. 1995; Kim et al. 2005; Dreyer et al. 2006; Kosek et al. 2006; Verdijk et al. 2007). Taken together, these finding provide important evidence that the composition of skeletal muscle fiber type may be a very important determinant of overall health.

There are a several key factors known to be important in the regulation of fiber type. However, relatively few factors have been shown to promote the fast fiber

phenotype. As discussed previously, MyoD is important for promoting the fast fiber phenotype (Hughes et al. 1997; Macharia et al. 2010), as is the transcription factor Sox6. Analysis of developing skeletal muscle from *Sox6*-null mice during the late stages of embryogenesis showed a lack of fast myofibers (Hagiwara et al. 2005; Hagiwara et al. 2007). Several factors involved in promoting the slow fiber phenotype have been identified, and studied in much more detail. MEF2 proteins have been shown to promote the slow fiber phenotype (Wu et al. 2000; Potthoff et al. 2007) and function together with the peroxisome proliferator activated receptor-γ co-activator-1α (PGC-1α) and NFAT proteins (discussed in detail below) to drive slow-muscle-specific gene expression in adult muscle (Crabtree and Olson 2002; Lin et al. 2002). The role of PGC-1α as a regulator of the slow-muscle phenotype unveiled a new mechanism for transcriptional regulation whereby co-factors that lack intrinsic DNA-binding activity make use of tissue specific transcription factors to activate target genes (Puigserver 2005). MEF2-dependent pathways and the calcineurin-NFAT pathway are thought to display some degree of crosstalk as suggested by the finding that MEF2 activity is strongly activated by calcineurin (Wu et al. 2000). In one study of avian medial adductor muscle fibers, MEF2 and NFAT binding sites were shown to be required for innervation-induced slow MyHC promoter activity (Jiang et al. 2004).

NFAT proteins in skeletal muscle

The nuclear factor of activated T-cells (NFAT) proteins are a family of 5 transcription factors (NFATc1-4 and NFAT5) related to the Rel/NFkB family (Graef et al. 2001). The distinguishing feature of NFAT proteins is their regulation by Ca^{2+} and the Ca^{2+}/calmodulin-dependent serine phosphatase calcineurin (Rao et al. 1997; Hogan et al.

2003). NFAT proteins are heavily phosphorylated and are located in the cytoplasm in resting cells. Following an increase in intracellular calcium levels, calcineurin becomes activated (Schulz and Yutzey 2004), and subsequently, dephosphorylates multiple serine/threonine residues on NFAT proteins, leading to NFAT nuclear translocation (Hogan et al. 2003). Once in the nucleus, NFAT proteins become transcriptionally active, and bind to target genes, thereby providing a direct link between intracellular Ca^{2+} signaling and gene expression (Hogan et al. 2003).

All NFAT proteins contain a transactivation domain (TAD), located at the N-terminus, adjacent to a regulatory domain that contains sequences required for calcineurin binding (Crabtree and Olson 2002). This regulatory domain is also referred to as the Ca^{2+}/calcineurin-dependent translocation (CAT) domain, and is similar for all four NFATc family members. In resting cells, the CAT domain is heavily phosphorylated at multiple serine residues which are distributed among four classes of conserved serine-rich sequence motifs (SRR-1, SPxx repeat, SRR-2, and KTS motifs) (Beals et al. 1997; Okamura et al. 2000). Calcineurin dephosphorylates three of the four classes of motifs, consequently triggering NFAT nuclear accumulation and increasing the affinity of NFAT for its target sites on DNA (Shaw et al. 1995; Okamura et al. 2000; Porter et al. 2000; Neal and Clipstone 2001). Adjacent to the CAT domain, toward the C-terminus, is the DNA binding domain (DBD), which is highly conserved between NFAT family members and is of the Rel homology class (Rel/DBD domain) (Rao et al. 1997; Schulz and Yutzey 2004). An NFATc1–c4 consensus binding sequence of (A/T)GGAAA has been defined based on target sequences in the regulatory regions of cytokine genes (Rao et al. 1997). NFAT proteins display low DNA binding affinity and therefore, usually act in

conjunction with other transcription factors such as AP-1, MEF2, or GATA4 (Rao et al. 1997; Molkentin et al. 1998; Macian et al. 2001). NFAT proteins can be deactivated and translocated back to the cytoplasm through phosphorylation by several protein kinases including glycogen synthase kinase-3 (GSK-3), protein kinase A, p38 MAPK, JNK, and casein kinase (Beals et al. 1997; Chow et al. 1997; Zhu and McKeon 1999; Sheridan et al. 2002; Yang et al. 2002). Selective activation of export kinases might explain how individual NFAT proteins might be differentially regulated in a single cell type.

The phosphatase that activates NFAT proteins, calcineurin, has been shown to play a role in a broad spectrum of developmental processes in a variety of organ systems, including skeletal muscle (Crabtree and Olson 2002). Calcineurin is composed of a catalytic A subunit and a calcium-binding regulatory B subunit. Three catalytic genes (A subunit) have been identified in vertebrate species, of which *calcineurin Aα* and *calcineurin Aβ* are ubiquitously expressed (Crabtree 1999). Calcineurin Aα is the predominant catalytic isoform expressed in nearly all skeletal muscles (Parsons et al. 2003). In mice lacking either *calcineurin Aα* or *Aβ*, no gross growth-related alterations in skeletal muscle are evident, and the size and number of fibers is unaltered in glycolytic/fast muscle types (Parsons et al. 2003). In contrast, in mice lacking *calcineurin Aα* and *Aβ,* an alteration in myofiber number was observed in the oxidative/slow-type soleus muscle (Parsons et al. 2003). More significantly, *calcineurin Aα* and *Aβ* double-null mice showed a dramatic down-regulation in the oxidative/slow fiber type gene program in both fast and slow muscles (Parsons et al. 2003). Several additional lines of evidence suggest that calcineurin plays a role in the slow fiber phenotype. Inhibition of calcineurin using the immunosuppressive drugs Cyclosporin A and FK506 results in a

slow to fast fiber type switch (Chin et al. 1998; McCullagh et al. 2004). In addition, transgenic mice with muscle-specific overexpression of calcineurin exhibit increased slow fiber content (Naya et al. 2000).

Despite the findings that calcineurin signaling plays a key role in the activation of muscle-specific genes associated with the slow fiber phenotype (Crabtree and Olson 2002), relatively little is known about the specific downstream factors involved in fiber type determination. It is generally accepted that NFAT proteins regulate the transcription of some slow fiber genes and repress some fast muscle genes in response to nerve-activity (Rana et al. 2008; Calabria et al. 2009). In skeletal muscle, *in vivo* transfection of a constitutively active mutant of NFATc1 activates MyHC-slow but deactivates MyHC-IIb promoter activity (McCullagh et al. 2004). In addition, studies of fast troponin I gene regulation show that direct binding of NFAT to the fast troponin I intronic regulatory element mediates the activity-dependent transcriptional repression of this element (Rana et al. 2008). Because NFAT proteins are well-established effectors of calcineurin signaling, it has been postulated that NFAT proteins would play an essential role in fiber type determination and switching *in vivo* (Chin et al. 1998; Schiaffino et al. 2007; Yan et al. 2011). However, to date, a role for NFAT proteins in control of fiber type *in vivo*, has not been firmly established. Phenotypic analyses of myofibers from *nfatc2*-null mice show a normal formation of nascent myofibers, however these fibers contain a limited number of nuclei due to a lack of further growth-promoting myoblast fusion, and are therefore smaller in size, resulting in overall reduced muscle size (Horsley et al. 2001). The mechanism underlying this phenotype was suggested by the finding that NFATc2 plays a role in the expression of the cytokine IL-4, which is secreted by nascent myotubes

and attracts IL-4α receptor positive myoblasts, thereby promoting cell fusion and formation of mature myotubes (Horsley et al. 2003). *nfatc3*-null mice exhibit skeletal muscle hypoplasia due to a decrease in the number of myofibers of both the slow and fast type (Kegley et al. 2001). Defects in muscle formation were traced back to early stages of myogenesis, specifically a decrease in the total number of primary myofibers (Kegley et al. 2001). However, despite all the evidence to suggest that NFAT proteins are involved in fiber type determination, neither the *nfatc2* nor *nfatc3*-null mice display a defect in fiber type composition. Mice with a targeted disruption of *nfatc4* exhibit no overt muscle phenotype (Graef et al. 2001).

All four NFAT isoforms (c1-c4) are expressed in muscle, with NFATc1 being the predominant isoform expressed in adult skeletal muscle (Rana et al. 2008; Calabria et al. 2009), but studies interrogating the role of NFATc1 in skeletal muscle *in vivo* have been limited because *nfatc1*-null mice die around day E12.5 due to cardiac valve defects (de la Pompa et al. 1998; Ranger et al. 1998), precluding studies on the requirement of NFATc1 in skeletal muscle *in vivo*. Although *in* vivo studies of NFATc1 in skeletal muscle are limited, one study showed that NFATc1-GFP has a predominantly cytoplasmic localization in the fast tibialis anterior muscle but a predominantly nuclear localization in the slow soleus muscle (Tothova et al. 2006), suggesting a role for active NFATc1 in slow muscle.

Summary

The work presented in this thesis describes the role of NFATc1 in skeletal muscle and the ability of NFATc1 to negatively regulate MyoD activity. Studies interrogating the role of NFATc1 in skeletal muscle in vivo have been limited because *Nfatc1*-null mice die around E12.5 due to cardiac valve defects (de la Pompa et al. 1998; Ranger et al. 1998). We used Cre-Lox technology to generate a skeletal-muscle specific *Nfatc1* knockout mouse and found that NFATc1 controls the balance between slow Type I and fast Type II myofibers, and does so, at least in part, through inhibition of MyoD-dependent fast fiber genes. In addition, we found that NFATc1, but not other NFAT isoforms, inhibits MyoD activity by physically interacting with and blocking the function of the N-terminal activation domain of MyoD. We also show that NFATc1 is required for a fast-to-slow fiber type switch in response to endurance exercise. Thus, the data presented in this thesis show that NFATc1 is an essential regulator of both fiber type composition at baseline and fiber type switching in response to exercise, and establish NFATc1 as a negative regulator of MyoD function through functional blockade of the MyoD N-terminal transactivation domain.

Chapter 2: NFATc1 negatively regulates MyoD activity and controls skeletal muscle fiber type composition

The *Mef2c* skeletal muscle specific enhancer contains multiple NFAT sites

Previous studies have identified an evolutionarily conserved promoter and enhancer region from the mouse *mef2c* gene that is sufficient to direct expression to skeletal muscle during murine development (Wang et al. 2001; Dodou et al. 2003). This skeletal muscle promoter resides upstream of exon 1 in mouse *mef2c* (Wang et al. 2001; Dodou et al. 2003). Sequence alignment of the mouse, human, and chicken *mef2c* loci shows an evolutionarily conserved 429bp region upstream of the first transcribed exon (Fig. 1A). Evolutionary conservation of noncoding regions suggests that a DNA sequence that has been conserved across species may have important regulatory elements necessary for activation or repression of a gene. A few key *cis*-acting sequences, which are essential for expression of the enhancer *in vivo,* have been identified within the *mef2c* skeletal muscle promoter. Among the *cis*-acting elements in the skeletal muscle promoter of *mef2c* is an E box, which is bound by myogenic bHLH proteins with extremely high affinity and is required for expression *in vivo* and *in vitro* (Wang et al. 2001; Dodou et al. 2003).

Examination of the sequence of the *mef2c* skeletal muscle enhancer revealed the presence of five potential NFAT bonding sites, four of which are perfectly conserved NFAT consensus binding sites among human, mouse, and chicken, and one of which is perfectly conserved between human and mouse (Fig. 1A). Identification of five putative

NFAT consensus binding sites within the *mef2c* promoter suggested that NFAT proteins might be candidates for regulating the *mef2c* gene.

The NFAT family of transcription factors encompasses five proteins evolutionarily related to the Rel/NFκB family (Chytil and Verdine 1996; Graef et al. 2001). NFAT proteins recognize the consensus binding site GGAAA (Hogan et al. 2003). NFAT factors c1, c2, c3, and c4, have all been identified in skeletal muscle tissue. Given the presence of multiple potential NFAT sites in the *mef2c* promoter, we tested the hypothesis that NFAT proteins may bind to these sites and regulate activity of the enhancer. We decided to focus on NFATc1 binding, as the function of NFATc1 *in vivo* is largely unknown, and identification of a transcriptional target of NFATc1 might give us insight into the role of NFATc1 in skeletal muscle *in vivo*. We first tested the ability of NFATc1 to bind to each of these sites in an electromobility shift assays (EMSA). Recombinant NFATc1 protein was used with a radiolabeled double-stranded oligonucleotide encompassing each of the five potential *mef2c* NFAT sites, termed *mef2*-N1 through *mef2*-N5. Indeed, NFATc1 protein bound to three of the five NFAT sites within the *mef2c* enhancer, as tested by EMSA (Fig. 1B). Specifically, NFATc1 efficiently bound to the *mef2c* NFAT sites 2, 4, and 5, with the most robust binding occurring on NFAT site 2. For each of these sites, this binding was competed by an excess of unlabeled wild type *mef2c* NFAT probe, but not by an excess of unlabeled mutant *mef2c* NFAT probe (Fig. 1B).

Transactivation of the *Mef2c* enhancer by MyoD is inhibited by NFATc1

Given that NFATc1 can bind to several of the identified NFAT sites within the *mef2c* enhancer, we next wanted to know whether NFATc1 could transactivate the *mef2c* enhancer *in vivo*. To test this hypothesis, we transfected C2C12 cells, a mouse myoblast cell line, with a β-gal reporter plasmid containing the *mef2c* promoter (*mef2c*-AUG/β-gal). The promoter exhibited minimal activity in these cells when transfected with empty pRK5 expression plasmid (Fig. 2A), thus providing us with a virtually silent background to test the ability of NFAT proteins to transactivate the *mef2c* promoter. As expected, the expression plasmid pRK5-MyoD was able to robustly transactivate the promoter by approximately 200 fold in these cells (Fig 2A). Unlike MyoD, NFATc1 and NFATc3, on their own, were not able to transactivate the *mef2c* promoter.

While NFAT proteins can function independently as transcriptional regulators, they typically require co-factors to activate or repress gene transcription due to their low affinity DNA binding (Hogan et al. 2003). Therefore, to test if NFATc1 or NFATc3 requires a co-factor for the activation of the *mef2c* promoter, we co-transfected MyoD and either NFATc1 or NFATc3 with our *mef2c* enhancer reporter plasmid (Fig. 2A). NFATc3 has no additional effect on the activation of the *mef2c* enhancer reporter when co-expressed with MyoD. However, to our surprise, we found a dramatic reduction of *mef2c* promoter activity from 200 fold to approximately 23 fold, when NFATc1 was co-expressed with MyoD (Fig. 2A). These data suggest that NFATc1, but not NFATc3, may potentially repress MyoD activation of the *mef2c* promoter *in vivo*.

There are two potential mechanisms to explain the finding that NFATc1 represses MyoD activation of the *mef2c* promoter *in vivo*. The first possibility is that NFATc1 acts

as a repressor through direct binding to *cis*-acting elements within the *mef2c* promoter. Alternatively, NFATc1 could be repressing MyoD activation of the *mef2c* promoter via MyoD protein itself, either through direct protein-protein interactions or through some indirect mechanism. To discriminate between these two possibilities, we cloned a *mef2c* promoter fragment containing only the 3' end of the conserved enhancer sequence (Fig 3A) into a β-gal reporter plasmid (*mef2c*-3'end-AUG/β-gal). This 3' region of the promoter does not contain any of the five putative NFAT binding sites we identified. However, it does still contain the essential E-box binding site that is required for MyoD transactivation of the *mef2c* enhancer (Wang et al. 2001; Dodou et al. 2003). C2C12 cells were transfected with the *mef2c*-3'end- AUG/β-gal reporter and with either MyoD alone or in combination with NFATc1 expression plasmids. As expected MyoD alone was able to robustly activate the *mef2c*-3'end- AUG/β-gal reporter (Fig. 3B). MyoD activation of the reporter was set at 100% activation. However, when co-transfected with NFATc1, promoter activity went from 100% activation to only 7.8% activation (Fig. 3B). These results suggest that NFATc1 inhibits MyoD activation of the *mef2c* promoter via a mechanism involving MyoD protein and not through NFATc1 binding to *cis*-acting elements within the promoter.

The *mef2c* promoter region has previously been cloned into the transgenic reporter plasmid HSP68-*lacZ* (Kothary et al. 1989), and the ability of this fragment to direct expression in transgenic mice has been analyzed throughout development (Wang et al. 2001; Dodou et al. 2003). This fragment directs *lacZ* expression beginning at E9.0 in rostral somites, corresponding with the first myotomal expression of endogenous *mef2c* (Edmondson et al. 1994), with expression becoming more robust by E9.5. Expression is

apparent in skeletal muscle throughout mouse development. Robust β-gal activity is observed in the myotomal compartment within the somites at E11.5 and can be seen in all skeletal muscles by E13.5 (Dodou et al. 2003). Importantly, no expression of β-gal is observed outside of the skeletal muscle lineage, indicating that this fragment of the *mef2c* gene represents a skeletal muscle specific promoter and enhancer only and does not contain elements sufficient to direct expression to other regions where endogenous *mef2c* is expressed. We used this *mef2c*-HSP68-*lacZ* reporter plasmid to further test whether NFAT *cis*-acting elements are required for regulation of the *mef2c* enhancer *in vivo*. We generated transgenic embryos harboring a mutation of the NFAT site 2 *cis*-acting element within the *mef2c* enhancer (Fig. 3C). This site was tested first, as it was the site that most robustly bound NFATc1 in EMSA (Fig. 1B). Transgenic embryos were collected on E11.5 and X-gal stained for *lacZ* expression. As shown previously (Wang et al. 2001; Dodou et al. 2003), the wild-type (WT) *mef2c* enhancer construct directed strong expression to the somites at E11.5 (5 blue/5 transgenic) (Fig. 3C). Mutation of NFAT site 2 (mNFAT(2)) appeared to have little affect on *lacZ* expression (3 blue/5 transgenic) (Fig. 3C).

Because we did not observe altered *mef2c* enhancer activity in the presence of the NFAT site 2 mutation in transgenic embryos, we did not proceed to test all NFAT sites we found to bind NFATc1 in EMSA experiments. However, it is possible that the other NFAT *cis*-acting elements might be required alone, or perhaps in combination, to affect *mef2c* enhancer activity. To test this possibility, we generated a *mef2c* enhancer construct that contains mutations for all NFAT sites within the *mef2c* enhancer that were bound by NFATc1 in EMSA (sites 2, 4, and 5). This mutated *mef2c* enhancer (*mef2c* mNFAT

(2,4,5)-AUG/β-gal) was used in transactivation assays in murine C3H10T1/2 fibroblast cells. MyoD alone was able to activate the wild-type *mef2c* enhancer approximately 35 fold over reporter alone, and this activation was unchanged with the *mef2c* mNFAT (2,4,5)-AUG/β-gal construct (Fig. 3D). Importantly, MyoD activation of the *mef2c* mNFAT (2,4,5)-AUG/β-gal reporter was still dramatically repressed by NFATc1, showing that these three sites are not required for NFATc1 inhibition of MyoD transactivation of the *mef2c* enhancer. Taken together, these results show that NFATc1 represses MyoD activation of the *mef2c* enhancer through either direct protein-protein interactions with MyoD or via an indirect mechanism effecting MyoD protein, and not through NFAT *cis*-acting elements.

Transactivation of the *MRF4* and *myogenin* promoters by MyoD is inhibited by NFATc1

To further test the hypothesis that NFATc1 is inhibiting MyoD activity through protein-protein interaction and not through *cis*-acting elements, we examined the activation of two other MyoD-dependent target enhancers from the *myogenin* and *Mrf4* genes. These two enhancers do not contain any evolutionarily conserved NFAT consensus sites (sequences not shown). C2C12 myoblasts were transfected with reporter plasmids *myogenin*-luciferase or *MRF4*-βgal and with a MyoD expression plasmid, alone or in combination with NFAT expression plasmids (Fig. 4A and 4B). As expected, MyoD strongly transactivated each of the reporter plasmids. Strikingly, MyoD-dependent transactivation was strongly repressed by NFATc1 but not NFATc3 or NFATc4 (data not

shown for NFATc4), suggesting a role specifically for NFATc1 in the inhibition of MyoD activity.

NFATc1 inhibits MyoD-mediated conversion of fibroblasts into myotubes

When expressed in primary fibroblasts or in a wide variety of other cell types, such as pigment, nerve, fat and liver, MyoD has the remarkable ability to convert these cells to skeletal muscle (Weintraub et al. 1989). Transfection of MyoD into the C3H10T1/2 mouse fibroblast cell line can also convert these cells into myotubes when cultured under low serum conditions (Weintraub et al. 1991). We took advantage of this *in vitro* MyoD-mediated myogenic conversion assay as a way to further test NFATc1 inhibition of MyoD function. We examined whether NFATc1 could influence MyoD-mediated myogenic conversion of multipotential C3H10T1/2 fibroblast cells into myotubes (Fig. 5). As expected, C3H10T1/2 cells transfected with empty vector only did not express fast myosin heavy chain (MY32) and they did not form multinucleated myotubes (Fig. 5A). Similarly, transfection of an NFATc1 expression vector alone did not result in myotube formation or fast myosin heavy chain expression (Fig. 5B). By contrast, transfection of MyoD expression vector into C3H10T1/2 cells, resulted in robust myogenic conversion as shown by the formation of fast myosin heavy chain-positive (MY32) myotubes (Fig. 5C). Strikingly, co-expression of NFATc1 in combination with MyoD resulted in a nearly complete inhibition of myotube formation and fast myosin heavy chain expression (Fig. 5D). Inhibition of MyoD-induced myogenic conversion by NFATc1 was further examined by western blot for fast myosin heavy chain (Fig. 5E). This assay showed nearly identical results to the immunofluorescence and myotube

formation assay: control and NFATc1 only transfected C3H10T1/2 cells had no expression of fast myosin heavy chain; MyoD induced robust myosin heavy chain expression, and this induction was profoundly inhibited by co-expression of NFATc1 (Fig. 5E). Notably, previous studies suggest that NFATc3 helps promote myogenesis (Weintraub et al. 1991; Delling et al. 2000; Kegley et al. 2001), but in our experiments MyoD-mediated conversion of C3H10T1/2 cells was not affected by co-expression of NFATc3 (data not shown). These results demonstrate that NFATc1 specifically inhibits MyoD-mediated myogenic conversion and MyoD-induced expression of fast myosin heavy chain.

NFATc1 physically interacts with MyoD

Given that NFATc1 represses MyoD activity, and that this repression is not acting through NFAT *cis*-acting elements, we wanted to gain insight into the biochemical mechanism through which NFATc1 represses MyoD activity. To this end, we tested whether NFATc1 physically interacts with MyoD (Fig. 6). NFATc1 and MyoD were co-expressed in C3H10T1/2 fibroblasts and co-immunoprecipitation experiments were performed. An antibody against MyoD was used for co-immunoprecipitation, followed by immunoblotting using an NFATc1 specific antibody (Fig. 6A). Indeed, MyoD co-immunoprecipitated NFATc1 protein. NFATc1 binding with MyoD was specific, as NFATc1 was not seen in lanes corresponding to an IgG antibody control or a beads only control (Fig. 6A).

To identify the domain(s) of NFATc1 required for interaction with MyoD, we tested the ability of several flag-tagged NFATc1 truncation mutants to co-

immunoprecipitate with MyoD. NFATc1 was divided into 3 main domains: the N-terminal domain, the CAT domain, and the Rel/DBD domain. An antibody against MyoD was used for co-immunoprecipitation, followed by immunoblotting using a flag antibody. Among the domains tested, only the Rel/DBD domain, which encodes the DNA binding domain of NFATc1, was necessary and sufficient for the physical interaction with MyoD (Fig. 6B). In addition, we tested the ability of several NFATc1 truncation mutants to repress MyoD-dependent activation of the *mef2c*-73K βgal reporter. We found that the Rel/DBD domain of NFATc1 was sufficient to repress MyoD activation of the reporter (Fig. 6C). These results clearly show that NFATc1 interacts with MyoD via the NFATc1 Rel/DBD domain, which is also sufficient for functional repression of MyoD on target promoters.

To identify the domain(s) of MyoD required for interaction with NFATc1, we tested the ability of flag-tagged MyoD truncation mutants to co-immunoprecipitate with NFATc1. Two MyoD truncation mutants were made: the first had a deletion of the N-terminal MyoD transactivation domain (MyoD dTAD pRK5 flag) and the second had a deletion of the C-terminal domain (MyoD dCterm pRK5 flag). Both of these constructs still contained the bHLH domain. An antibody against NFATc1 was used for co-immunoprecipitation, followed by immunoblotting using a flag antibody to detect the MyoD truncation mutants. Among the domains tested, only MyoD dTAD physically interacted with MyoD (Fig. 6D). This suggests that only the N-terminal TAD of MyoD can interact with NFATc1. If the bHLH domain of MyoD was able to interact with NFATc1 we would have observed pull-down of the MyoD-dCterm truncation mutant as well. To test whether the N-terminal domain of MyoD was sufficient to interact with

NFATc1, we used a myc-tagged N-terminal MyoD construct and tested its ability to interact with NFATc1 in co-immunoprecipitation experiments. As expected from our MyoD truncation mutant Co-IP experiments, the N-terminal region of MyoD was sufficient to for interaction with NFATc1 (Fig. 6E).

NFATc1 does not affect MyoD nuclear localization

MyoD is localized to the cell nucleus in growing myoblasts where it can subsequently activate gene transcription (Tapscott et al. 1988). One possible mechanism by which NFATc1 could be inhibiting MyoD function is through preventing MyoD nuclear localization. To test this, we performed immunofluorescence on C3H10T1/2 cells that were transfected with MyoD alone (Fig. 7A-C) or together with NFATc1 (Fig. 7D-F) and then cellular localization of MyoD was determined using a MyoD antibody. MyoD expression was found to be restricted to the nucleus in cells examined 24 hours after the initiation of differentiation (Fig. 7B-C). Nuclear localization was determined by DAPI co-staining. In co-transfected cells, the cellular localization of MyoD did not change in the presence of NFATc1 (Fig. 7E), which was largely expressed in the nuclei of differentiating cells as well (Fig. 7D). We also co-transfected MyoD with a constitutively active NFATc1 mutant and found that in this case as well, MyoD nuclear localization was unaffected (Fig. 7H). These results show that NFATc1 does not inhibit MyoD through a mechanism involving MyoD exclusion for the nucleus.

NFATc1 does not inhibit MyoD DNA binding or dimerization with E-proteins

In order to determine the mechanism by which NFATc1 inhibits MyoD activity we sought to determine if NFATc1 might be inhibiting MyoD DNA binding or dimerization with E-proteins. First, we utilized a mammalian two-hybrid system to test whether NFATc1 could inhibit activation of a pG5-E1b-Luc reporter (Heidt et al. 2007) by E12 and MyoD. This reporter contains 5 upstream activator sequence (UAS) binding sites that are recognized by the yeast Gal4 DNA binding domain (Gal4 DBD) (Fig. 8A schematic). We have fused the E12 bHLH domain to the Gal4 DBD. Two steps are required for the activation of the pG5-E1b-Luc reporter. The first is the interaction of the E12 bHLH domain with the bHLH domain of MyoD. Once these two proteins interact, the N-terminal transactivation domain of MyoD is required for reporter activation. C3H10T1/2 cells transfected with Gal4-E12bHLH alone failed to activate the reporter since this protein lacks a transcriptional activation domain of its own (Fig. 8A). By contrast, co-transfection of Gal4-E12bHLH with MyoD, which contains a transactivation domain, resulted in potent activation of the reporter via dimerization between the E12 and MyoD bHLH domains. Data are expressed as percent activation, where Gal4-E12bHLH + MyoD activation of the reporter is set to 100%. Activation of the reporter was reduced from 100% to 20% in the presence of NFATc1, and was unchanged in the presence of NFATc3 (Fig. 8A). These results suggest that NFATc1 is either inhibiting MyoD/E protein dimerization or inhibiting the MyoD transactivation domain. To further understand how NFATc1 inhibits MyoD activity, we also tested the activation of the pG5-E1b-Luc reporter with the MyoD bHLH domain fused to the Gal4 DBD, and co-transfected E47-VP16, a plasmid that expresses the bHLH domain of E47 fused to the viral transcriptional activator protein VP16 (Fig. 8B). Gal4-MyoDbHLH did not activate

the reporter alone, since this protein lacks the N-terminal transcriptional activation domain. E47-VP16 failed to activate the reporter without MyoD, since E47-VP16 cannot bind to the upstream activator sequence. Co-transfection of Gal4-MyoDbHLH with E47-VP16, resulted in potent transactivation of the reporter due to dimerization via the MyoD and E47 bHLH domains. Interestingly, this activation was unaltered in the presence of NFATc1 and NFATc3. This result suggests that NFATc1 does not inhibit dimerization of MyoD with E-proteins. However, it is also likely that NFATc1 is unable to interact with Gal4-MyoDbHLH since this construct lacks the N-terminal region, which we have shown in co-immunoprecipation experiments, to be the domain necessary for MyoD interaction with NFATc1.

To further test whether NFATc1 inhibits MyoD/E-protein dimerization and DNA binding we performed an electromobility shift assay. Recombinant MyoD, E12, and NFATc1 proteins were transcribed and translated in vitro and used in EMSAs with a radiolabeled, double-stranded oligonucleotide probe representing an E-box binding site from the *mef2c* skeletal muscle promoter. Wild-type MyoD and E12 did not bind to the E-box on their own, however, when both are present, a robust shift is observed (Fig. 8C). Recombinant NFATc1 protein was added in increasing amounts, ranging from 0.3X to 10X the amount of E12 and MyoD, which were added in a 1:1 ratio as determined by ^{35}S-methionine incorporation (data not shown). Addition of NFATc1 had a negligible effect on MyoD/E12 binding to the E-box binding site (Fig. 8C). MyoD/E12 binding was specific, as it was efficiently competed by unlabeled wild-type (W) competitor oligonucleotide, but not with a mutant (M) competitor oligonucleotide of the *mef2c* E box site. As a further test of the ability of NFATc1 to inhibit MyoD binding to E-box

elements, we used a multimerized E-box reporter construct, which contains 4 tandem E-box sites (4R-TK-Luc). C3H10T1/2 cells were co-transfected with MyoD in the presence or absence of NFATc1. MyoD robustly activated the 4R-TK-Luc reporter, and this activation was not significantly altered in the presence of NFATc1 (Fig. 8D). Taken together, these data suggest that MyoD heterodimerization with E-proteins, and subsequent DNA binding to E-box sites, is not inhibited by NFATc1.

NFATc1 inhibits MyoD-mediated transactivation via the N-terminal activation domain

Since NFATc1 is not inhibiting MyoD DNA binding or heterodimerization with E-proteins, it is possible that NFATc1 is inhibiting the MyoD transactivation domain, which is one possible explanation for the results observed in Fig. 8A. To test this possibility we fused full length MyoD to the Gal4 DBD and tested its ability to activate a reporter construct in the presence or absence of NFATc1. This reporter contains two UAS binding sites for the Gal4-MyoD fusion protein (2X Gal4-E1b-Luc) (Fig. 9A schematic). In this assay, DNA binding is facilitated by the UAS/Gal4 DBD interaction, and not by the bHLH domain of MyoD. Therefore, only the transactivation ability of full length MyoD is being tested in this assay. C3H10T1/2 cells were transfected with reporter plasmid and MyoD in the presence or absence of NFATc1. Gal4-MyoD alone strongly activated the reporter, with activation being set at 100%, which is ~20 fold over background (Fig. 9A). In contrast, in the presence of NFATc1, reporter activation went from 100% activation to approximately 20% (Fig. 9A). We did not observe this decrease

in Gal4-MyoD activation of the reporter in the presence of NFATc3, showing that the inhibition of the MyoD transactivation domain is specific to NFATc1.

In order to determine if the N-terminal domain of MyoD is sufficient for inhibition by NFATc1, we fused the MyoD N-terminus or the MyoD bHLH domain only to the Gal4 DBD (Gal4 MyoD N-term and Gal4 MyoD bHLH). These constructs were co-transfected into C3H10T1/2 cells with the reporter plasmid 2X-Gal4-E1b-*luciferase* with or without NFATc1. Gal4-MyoD and Gal4 MyoD N-term strongly activated this reporter. Importantly, the activation by both Gal4-MyoD and Gal4 MyoD N-term was significantly reduced in the presence of NFATc1 ($p = 0.02$ and $p = 0.01$, respectively), whereas no significant difference is observed when NFATc1 was co-expressed with Gal4 MyoD bHLH. These results show that NFATc1 is negatively regulating MyoD-mediated transactivation, and that the MyoD N-terminal domain is sufficient for NFATc1 inhibition of MyoD transactivation function.

Generation of an *nfatc1* skeletal muscle specific knockout mouse

The role of NFATc1 in skeletal muscle is largely unknown because *nfatc1*-null mice exhibit embryonic lethality at mid-gestation due to abnormalities in cardiac valve development (de la Pompa et al. 1998; Ranger et al. 1998). To determine the function of NFATc1 in skeletal muscle and to validate NFATc1 inhibition of MyoD *in vivo*, we inactivated *nfatc1* specifically in skeletal muscle by crossing mice with a floxed *nfatc1* allele with mice harboring the skeletal muscle specific *Mef2c*-73k-Cre transgene (Heidt and Black 2005), according to the strategy outlined in Fig. 10A. To verify loss of *nfatc1* expression in skeletal muscle, we performed qRT-PCR on RNA isolated from the soleus

muscles of 7 week old adult male mice. We observed a greater than 80% reduction in *nfatc1* mRNA levels in *nfatc1*$^{SkM\text{-}KO}$ mice compared to control mice (*nfatc1*$^{flox/+}$) and ~30% reduction in *nfatc1* relative mRNA levels in *nfatc1*$^{SkM\text{-}KO}$ mice compared to *nfatc1*$^{flox/-}$ heterozygous mice (Fig. 10B). NFATc1 protein expression was also examined in *nfatc1*$^{SkM\text{-}KO}$ and control mice by western blot, which showed marked reduction in NFATc1 protein expression in the gastrocnemius muscles of *nfatc1*$^{SkM\text{-}KO}$ mice compared to controls (Fig. 10C). Residual *nfatc1* expression in skeletal muscles of *nfatc1*$^{SkM\text{-}KO}$ may be due to detection of *nfatc1* expression in other cell types within RNA and protein extracts collected from whole muscle tissue or may be due to incomplete excision of *nfatc1*^{flox} by *Mef2c*-73k-Cre. Overall, taken together, these data show highly significant knock down of *nfatc1* in skeletal muscle.

nfatc1$^{SkM\text{-}KO}$ mice do not have growth deficits

nfatc1$^{SkM\text{-}KO}$ mice were born at expected Mendelian ratios (Fig. 10D) and survived to adulthood with no overt phenotype (data not shown). Adult male mice at 49 days of age were weighed to determine if they had any alteration in body mass. We did not observe any significant differences in body mass between control and *nfatc1*$^{SkM\text{-}KO}$ mice (Fig. 11A). Therefore, we think it unlikely that these mice have any overall body growth deficits. We also weighed different hindlimb muscles from 49 day old male mice to determine if loss of *nfatc1* resulted in a defect in muscle growth specifically. We did not observe any significant differences in the size of the soleus, gastrocnemius, and tibialis anterior muscles when comparing control and *nfatc1*$^{SkM\text{-}KO}$ mice (Fig. 11B). These results suggest that skeletal muscle growth is largely normal in *nfatc1*$^{SkM\text{-}KO}$ mice.

NFATc1 is required for proper fiber type balance

Fiber type composition is important for skeletal muscle function and the proportion of slow and fast fibers plays a pivotal role in whole body metabolism (Zurlo et al. 1994; Schiaffino and Reggiani 2011). NFAT proteins have been shown to play a role in the transcriptional regulation of fiber type genes (Chin et al. 1998; Wu et al. 2000; Calabria et al. 2009), and overexpression of a constitutively active form of NFATc1 in skeletal muscle *in vivo* induces expression of slow myosin in regenerating, denervated soleus muscle (McCullagh et al. 2004). Therefore, we hypothesized that mice lacking NFATc1 in skeletal muscle might have altered fiber type composition. To test this hypothesis, metachromatic ATPase staining was used to quantify the number of Type I (slow) and Type II (fast) fibers in the soleus muscle of 7 week old mice. *nfatc1*$^{SkM\text{-}KO}$ mice had a significantly reduced percentage of Type I fibers compared to control mice (34.5% versus 44.5%, $p = 0.006$) (Fig. 12A and 12B, quantification Fig. 12E). These findings support a role for NFATc1 in establishing or maintaining the slow fiber phenotype and provide the first genetic evidence that NFATc1 is required for proper fiber type composition *in vivo*.

***nfatc1*$^{SkM\text{-}KO}$ mice do not have exercise deficits**

Type I (slow) myofibers utilize oxidative metabolism for energy production, and therefore are best suited for endurance type activities, such as running a marathon. Since *nfatc1*$^{SkM\text{-}KO}$ have a decrease in the number of Type I (slow) myofibers, we wanted to challenge *nfatc1*$^{SkM\text{-}KO}$ muscle by having mice undergo endurance exercise, and determine

if they were capable of running as much as wild-type mice. To test this, we used adult male mice in a voluntarily running wheel assay to test their exercise capabilities. Starting on post-natal day 39, mice underwent a 3-day training period to become acclimated to the running wheel. Mice were then allowed to voluntarily run for 7 consecutive days. Measurements were taken each day for distance run and time run, and then averaged. Despite the finding that *nfatc1*$^{SkM\text{-}KO}$ mice have a deficit in Type I (slow) myofibers, no significant difference between control mice (*nfatc1*$^{flox/+}$) and *nfatc1*$^{SkM\text{-}KO}$ mice was observed for time run (Fig. 13A) or distance run (Fig. 13B). These results show that *nfatc1*$^{SkM\text{-}KO}$ do not have exercise deficits.

NFATc1 controls the fast-to-slow fiber type switch in response to endurance exercise training

Type I (slow) muscle fibers are important for endurance exercise and the conversion of fast fibers to slow fibers can be induced in mice in response to a continuous period of voluntary exercise (Wernig et al. 1990; Pette and Staron 2001; Potthoff et al. 2007; Flynn et al. 2010). The importance of NFATc1 in the regulation of fast-to-slow fiber type switching has been highlighted in several studies using electrostimulation to promote fiber type switching (McCullagh et al. 2004; Mu et al. 2007; Calabria et al. 2009). Therefore, despite our finding that *nfatc1*$^{SkM\text{-}KO}$ mice did not have impairments in voluntary exercise capability (Fig. 13), we hypothesized that they may have an impairment in fast-to-slow fiber type switching in response to exercise. To test this hypothesis, we examined the fiber type composition of the soleus muscle in control and *nfatc1*$^{SkM\text{-}KO}$ mice following a 7-day period of voluntary exercise as described above.

Control mice showed a modest, but significant, increase in the percentage of Type I slow-twitch fibers in response to exercise, going from approximately 45% to 50% (Compare Fig. 12A and Fig. 12C, quantification Fig. 13E). In contrast, *nfatc1*$^{SkM\text{-}KO}$ mice did not undergo fiber type switching in response to exercise (Compare Fig. 12B and Fig. 12D, quantification Fig. 12E). These results provide the first physiological and genetic evidence that NFATc1 is required for fast-to-slow fiber type switching in response to exercise.

Metachromatic ATPase staining is an enzymatic stain that detects the amount of ATP in each myofiber (Ogilvie and Feeback 1990). Since slow fibers contain higher levels of ATP, they stain a dark blue, whereas fast fibers that contain lower levels of ATP stain light blue. We wanted to verify the results from the enzymatic metachromatic ATPase staining by an alternative method, so we used immunofluorescence to detect myosin slow protein within the soleus muscle. Myosin slow immunofluorescence staining was not used for quantification, but as an additional qualitative method for observing the difference in fiber type composition. Nearby transverse sections of the same pre-exercise and post-exercise soleus muscles used for metachromatic ATPase staining were used for myosin slow immunofluorescence. Red fibers indicate Type I (slow) fibers and black fibers indicate Type II (fast) fibers (Fig. 13 C-F). We found that this method showed similar results to our metachromatic ATPase staining, and that fibers that stained dark blue in that assay indeed corresponded with myosin slow expression.

nfatc1$^{SkM\text{-}KO}$ muscle may have an increase in muscle regeneration in post-exercised muscle

Skeletal muscle has remarkable regenerative capacity. Regenerating fibers are morphologically identified by the presence of centrally located nuclei within individual muscle fibers. Histological observation of the soleus muscle from post-exercised *nfatc1*$^{SkM\text{-}KO}$ mice showed a large number of regenerating fibers as identified by the presence of centrally located nuclei within individual fibers (Fig. 14B). In contrast, soleus muscles from control mice showed little to no regenerating fibers following the voluntary running assay (Fig. 14A). This suggests that NFATc1 may play a role in the regulation of satellite cells in response to exercise.

NFATc1 is expressed in fast and slow skeletal muscle fibers and is co-expressed with MyoD

To gain further insight into specific roles for NFATc1 in skeletal muscle, we examined NFATc1 protein expression by immunohistochemistry within the soleus muscle of adult mice. NFATc1 expression was detected in the nuclei within several fibers of the soleus muscle (Fig. 15A and 15B). Because the soleus muscle is composed of both fast and slow twitch fiber types (Wigston and English 1992), we wanted to determine whether NFATc1 localized to slow or fast fibers, so we performed immunofluorescence on serial sections using antibodies against fast and slow myosin isoforms. Importantly, we observed NFATc1 expression within the nuclei of both slow (Fig. 15C and 15D) and fast myofibers (Fig. 15E and 15F) within the soleus muscle.

NFATc1 and MyoD co-localize in skeletal muscle nuclei

Our co-immunoprecipitation experiments described earlier show that MyoD and NFATc1 physically interact. To determine if MyoD and NFATc1 are co-localized *in vivo* in skeletal muscle, we compared the expression of NFATc1 to the expression of MyoD. Serial sections from the soleus muscle were used for immunohistochemistry. (Several attempts were made using MyoD and NFATc1 antibodies for co-immunofluorescence on the same section, however mouse antibodies on mouse muscle tissue gave very high background, especially along the periphery of the muscle fiber where nuclei are present, and made it impossible to detect real signal over background. Other available NFATc1 antibodies produced in rabbit only worked in IHC, and not in IF). Interestingly, we found that MyoD and NFATc1 were co-expressed in the adult soleus as shown by positive staining in the same nuclei within a particular muscle fiber (Fig. 16A and 16B). This result, in combination with our previous Co-IP experiments, suggests that NFATc1 and MyoD likely interact in muscle *in vivo*. However, *in vivo* Co-IP experiments from muscle tissue would be needed to be certain of this conclusion.

nfatc1$^{SkM\text{-}KO}$ muscle has a defect in fast fiber gene expression at baseline

To further examine the role of NFATc1 in fiber type regulation, we examined the expression of several established fast and slow fiber genes in *nfatc1*$^{SkM\text{-}KO}$ and control mice by qRT-PCR. We found a significant increase in the expression of several fast fiber genes, including *MyHC-IIa, MyHCII-d/x, MyHC-IIb*, and *Tnni2,* in *nfatc1*$^{SkM\text{-}KO}$ soleus muscle compared to control (Fig. 17). We did not observe any significant changes in slow fiber gene expression (Fig. 17). Together, these results suggest that NFATc1 might

function in skeletal muscle fiber type control by repressing expression of fast muscle genes.

NFATc1 is required for proper expression of several MyoD target genes in skeletal muscle

MyoD plays a central role in transcriptional activation of numerous muscle genes during development and has been shown to promote the fast fiber phenotype in mice (Hughes et al. 1997; Macharia et al. 2010). Given the observation that NFATc1 represses fast muscle genes and that NFATc1 and MyoD are co-expressed within muscle (Fig. 16), we reasoned that NFATc1 might be repressing fast muscle genes and promoting the slow fiber phenotype through inhibition of MyoD function. Therefore, we decided to examine additional genes known to be transcriptionally activated by MyoD in *nfatc1*$^{SkM\text{-}KO}$ mice to determine if their expression was changed in the absence of NFATc1 (Fig. 18). Importantly, the majority of established MyoD target genes (Li and Capetanaki 1993; Bergstrom et al. 2002; Blais et al. 2005) that we examined had increased relative mRNA expression in *nfatc1*$^{SkM\text{-}KO}$ mice compared to controls, including *desmin, ckm (muscle creatine kinase),* and *nestin* (Fig. 18A).

MyoD also regulates the expression of several transcription factor genes through direct transcriptional activation to control muscle development, regeneration, and function, including the control of fiber type specification (Tapscott 2005; Schiaffino and Reggiani 2011). These critical transcription factor gene targets of MyoD include *myod* itself, *myogenin, MRF4, and mef2c* (Thayer et al. 1989; Black et al. 1995; Wang et al. 2001; Bergstrom et al. 2002; Dodou et al. 2003). Because several other known MyoD

targets were upregulated in skeletal muscle in *nfatc1*$^{SkM\text{-}KO}$ mice and to gain possible insights into how NFATc1 might be controlling fiber type phenotype and fast-to-slow switching, we examined the expression of these transcription factor genes in *nfatc1*$^{SkM\text{-}KO}$ mice. Interestingly, we found a significant increase in the expression of *mef2c*, *myod*, *myogenin*, and *MRF4* (Fig. 18B) in the soleus muscles of *nfatc1*$^{SkM\text{-}KO}$ mice compared to controls. Taken together, these data support the notion that NFATc1 inhibits the expression of known MyoD-activated genes and suggests that NFATc1 may achieve this repression through inhibition of MyoD function.

Figure Legends

Figure 1: The *mef2c* skeletal muscle specific promoter contains multiple NFAT sites

(A) The evolutionarily conserved skeletal muscle promoter resides upstream of exon 1 in mouse *mef2c* (Dodou et al. 2003) (Genbank accession #AY321453). Sequence alignment of the mouse, human, and chicken *mef2c* loci shows an evolutionarily conserved 429bp region upstream of the first transcribed exon. Nucleotides indicated in white have been conserved; those indicated in black are divergent. Red boxes indicate the evolutionarily conserved, candidate *cis*-acting NFAT consensus sites. The arrow indicates the transcriptional start site obtained from Genbank (accession #AK009139).

(B) Recombinant NFATc1 protein was used in EMSA with a radiolabeled double-stranded oligonucleotide encompassing each of the *mef2c* skeletal muscle promoter putative NFAT sites, named *mef2*-N1 through *mef2*-N5. For each oligo used, a control lane containing reticulocyte lysate without recombinant NFATc1 (represented by a minus (-) sign) is included. NFATc1 efficiently bound to the *mef2c* NFAT sites 2, 4, and 5, with the most robust binding occurring on NFAT site 2. For each of these sites, NFATc1 binding was competed by an excess of unlabeled wild type (W) *mef2c* NFAT probe, but not by an excess of unlabeled mutant (M) *mef2c* NFAT probe.

Figure 2: Transactivation of the *mef2c* promoter by MyoD is inhibited by NFATc1

(A) C2C12 cells were transfected with expression plasmids for either MyoD, NFATc1, or NFATc3. In samples where only one cDNA expression plasmid was transfected, an equal amount of the parental expression vector was transfected. The parental reporter plasmid AUG/βgal, or the wild-type *mef2c*-AUG/βgal reporter plasmid were co-transfected.

Results are reported as fold activation of βgal reporter over the empty vectors (AUG/βgal + parental vector). The data shown represent the mean values obtained in 4 independent transfections. Error bars represent the standard errors of the means. Fold activation for MyoD compared to MyoD + NFATc1 showed a significant decrease, $p < 0.001$, while the fold activation for MyoD compared to MyoD + NFATc3 showed no significant difference.

Figure 3: NFATc1 inhibition of MyoD transactivation does not require NFAT sites
(A) The 3' end (starting at nucleotide -106 relative to transcriptional start site) of the evolutionarily conserved skeletal muscle promoter of *mef2c* contains an E box, previously shown to be necessary for activation of the promoter by MyoD (Dodou et al. 2003). This region of the promoter contains none of the 5 putative NFAT sites. The black arrow indicates the transcriptional start site. The red arrow indicates nucleotide -106. (B) C2C12 cells were transfected with expression plasmids for either MyoD or NFATc1. In samples where a cDNA expression plasmid was not transfected, an equal amount of the parental expression vector was transfected. A reporter plasmid containing only the 3' end of the skeletal muscle promoter of *mef2c (mef2c* 3' end AUG/βgal) was co-transfected. Results are reported as percent activation, where MyoD activation of the reporter was set as 100% activation. The data shown represent the mean values obtained in 3 independent transfections. Error bars represent the standard errors of the means. (C) The wild-type *mef2c* skeletal muscle promoter fragment and a NFAT site 2 mutant fragment (mNFAT(2)) were fused to the HSP68-*lacZ* reporter and used to generate transgenic mice. Representative transgenic embryos for the wild-type *mef2c* promoter construct and

the mutant at 11.5 dpc are shown. The wild-type fragment directed strong expression to the myotomal compartment of the somites (5 blue/5 transgenic), and this expression was largely unaffected in the mNFAT(2) transgenic embryos (3 blue/5 transgenic). NFAT site 2 is the site corresponding to the NFAT site that bound most robustly in gel shift experiments. (D) C3H10T1/2 cells were transfected with expression plasmids for either MyoD, NFATc1, or NFATc3. In samples where only one cDNA expression plasmid was transfected, an equal amount of the parental expression vector was transfected. The wild-type *mef2c*-AUG/βgal reporter plasmid or a mutant reporter plasmid *mef2c* mNFAT (2,4,5)-AUG/βgal was co-transfected. Results are reported as fold activation of βgal reporter over the empty vector. The data shown represent the mean values obtained in 3 independent transfections. Error bars represent the standard errors of the means.

Figure 4: MyoD transactivation of the *MRF4* and *myogenin* promoters is also inhibited by NFATc1

(A) C2C12 cells were transfected with expression plasmids for either MyoD, NFATc1, or NFATc3. In samples where a cDNA expression plasmid was not transfected, an equal amount of the parental expression vector was transfected. A reporter plasmid containing the -184 *myogenin* promoter, which extends from nucleotides −184 to +11, relative to the transcriptional start site (MyoG-pGL3-Luc), was co-transfected. Results are reported as fold activation of luciferase reporter over empty vector alone. The data shown represent the mean values obtained in 3 independent transfections. Error bars represent the standard errors of the means. Fold activation for MyoD compared to MyoD + NFATc1 shows a significant decrease, $p = 0.002$, while the fold activation for MyoD compared to MyoD +

NFATc3 shows no significant difference. (B) C2C12 cells were transfected with expression plasmids for either MyoD, NFATc1, or NFATc3. In samples where a cDNA expression plasmid was not transfected, an equal amount of the parental expression vector was transfected. A reporter plasmid containing the *MRF4* promoter (MRF4-AUG/βgal) was co-transfected. Results are reported as fold activation of MRF4-AUG/βgal over empty vector. The data shown represent the mean values obtained in 3 independent transfections. Error bars represent the standard errors of the means. Fold activation for MyoD compared to MyoD + NFATc1 shows a significant decrease, $p = 0.004$, while the fold activation for MyoD compared to MyoD + NFATc3 shows no significant difference.

Figure 5: NFATc1 inhibits MyoD-mediated conversion of fibroblasts into myotubes (A) C3H10T1/2 fibroblasts were transiently transfected with expression plasmids for empty vector (B) NFATc1 alone (C) MyoD alone (D) or MyoD and NFATc1. In transfections where only one cDNA was transfected, empty expression plasmid was co-transfected so that all samples had the same total amount of plasmid transfected. Cells were allowed to differentiate in 2% horse serum (DM) for 5 days, beginning 24 hours post-transfection. Subsequently, differentiated cells were immunostained for MyHC fast protein (MY32 antibody). (A) No MyHC fast was detected after 5 days in DM with empty vector. (B) No MyHC fast was detected after 5 days in DM with transfection of NFATc1 alone. (C) Transient transfection of MyoD alone induced the conversion of fibroblasts into MyHC-expressing myotubes (green staining). (D) Co-transfection of MyoD and NFATc1 resulted in a dramatic reduction in MyHC fast immunostaining and

very few myotubes were observed. (E) Western blot quantitation revealed a dramatic increase in the amount of total MyHC fast protein between MyoD and MyoD + NFATc1 differentiated cells. Anti-tubulin was used as a loading control on the same cell lysates to demonstrate comparable protein levels for all conditions. Identical results were obtained in at least 6 independent experiments.

Figure 6: MyoD and NFATc1 physically interact

(A) C3H10T1/2 cells were co-transfected with MyoD and NFATc1. Immunoprecipitation on protein extracts was performed using a rabbit anti-MyoD antibody and protein G sepharose beads. Eluates were analyzed by western blotting using an anti-NFATc1 antibody. A rabbit IgG control and beads only control are included. (B) Protein extracts from C3H10T1/2 cells were co-transfected with MyoD and Flag-tagged NFATc1 truncation mutants. Immunoprecipitation was performed using a rabbit anti-MyoD antibody and protein G sepharose beads. Eluates were subjected to western blotting using a mouse anti-Flag antibody. (C) C2C12 cells were transfected with expression plasmids for either MyoD, full length (FL) NFATc1, or various NFATc1 truncation and deletion mutants. In samples where only one cDNA expression plasmid was transfected, an equal amount of the parental expression vector was transfected. The parental reporter plasmid AUG/βgal, or the wild-type *mef2c*-AUG/βgal reporter plasmid were co-transfected. Results are reported as fold activation of the *mef2c*-AUG/βgal reporter over the empty vector. The data shown represent the mean values obtained in 3 independent transfections. Error bars represent the standard errors of the means. Fold activation for MyoD compared to MyoD + NFATc1, MyoD + NFATc1 (425-694), MyoD + NFATc1

(107-694) and MyoD + NFATc1 (1-694)dCAT all show a significant decrease ($p \leq 0.01$) in fold activation. (D) Protein extracts from C3H10T1/2 cells were co-transfected with NFATc1 and Flag-tagged MyoD truncation mutants. Immunoprecipitation was performed using a rabbit anti-NFATc1 antibody and protein G Dynabeads. Eluates were analyzed by western blotting using a mouse anti-flag antibody. (E) Protein extracts from C3H10T1/2 cells were co-transfected with NFATc1 and a myc-tagged N-terminus MyoD truncation mutant. Immunoprecipitation was performed using a rabbit anti-NFATc1 antibody and protein G Dynabeads. Eluates were analyzed by western blotting using a mouse anti-myc antibody.

Figure 7: NFATc1 does not affect MyoD nuclear localization

(A) DAPI staining showing cell nuclei of C3H10T1/2 cells transfected with MyoD only. (B) MyoD immunofluorescence of MyoD transfected C3H10T1/2 cells showing nuclear localization of MyoD protein after 24 hours in low serum differentiation media. (C) Merged image of MyoD and DAPI. (D) NFATc1 immunofluorescence of C3H10T1/2 cells transfected with MyoD and NFATc1 after 24 hours in low serum differentiation media. (E) MyoD expression remains restricted to the nucleus in the presence of NFATc1. (F) Merged image of NFATc1 and MyoD showing co-localization of these two factors within several nuclei. (G) NFATc1 staining of C3H10T1/2 cells co-transfected with MyoD and a constitutively active NFATc1 mutant. (H) MyoD staining of C3H10T1/2 cells co-transfected with MyoD and a constitutively active NFATc1 mutant. (I) Merged image of constitutively active NFATc1 and MyoD showing co-localization of these two factors within several nuclei.

Figure 8: NFATc1 does not inhibit MyoD DNA binding or dimerization with E-proteins

(A) Plasmids expressing a fusion of the bHLH domain of E12 and the Gal4 DBD (Gal4-E12 bHLH), full length MyoD, NFATc1 and NFATc3 were co-transfected into C3H10T1/2 cells with the reporter plasmid pG5E1b-*luciferase*. Gal4-E12bHLH failed to activate the reporter alone, since this protein lacks a transcriptional activation domain on its own. By contrast, co-transfection of Gal4-E12bHLH with MyoD, which does contain an activation domain, resulted in potent transactivation of the reporter via dimerization between the E12 and MyoD bHLH domains. This activation was reduced from 100% to 20% in the presence of NFATc1, but was unchanged in the presence of NFATc3. Data are expressed as percent activation, where Gal4-E12bHLH + MyoD activation of the reporter is set to 100%. Results are from 4 independent experiments. Error bars represent the standard errors of the means. (B) Plasmids expressing a fusion of the bHLH domain of MyoD and the Gal4 DBD (Gal4-MyoDbHLH) were co-transfected into C3H10T1/2 cells with the reporter plasmid pG5E1b-*luciferase*. Gal4-MyoDbHLH does not activate the reporter alone, since this protein lacks the N-terminal transcriptional activation domain. E47-VP16 failed to activate the reporter without MyoD, since E47-VP16 cannot bind to the upstream activator sequence. Co-transfection of Gal4-MyoDbHLH with E47-VP16, a plasmid that expresses the bHLH domain of E47 fused to the viral transcriptional activator protein VP16, resulted in potent transactivation of the reporter due to dimerization via the MyoD and E47 bHLH domains. This activation was unaltered in the presence of NFATc1 and NFATc3. Data are expressed as percent activation, where Gal4-

MyoDbHLH + E47-VP16 activation of the reporter is set to 100%. Results are from 3 independent experiments. Error bars represent the standard errors of the means. (C) Recombinant MyoD, E12, and NFATc1 proteins were transcribed and translated in vitro and used in EMSAs with a radiolabeled, double-stranded oligonucleotide probe representing an E-box binding site from the *mef2c* skeletal muscle promoter. Wild-type MyoD and E12 did not bind to the E-box on their own, but, when both were present, a robust shift was observed. The addition of NFATc1 in increasing amounts had a negligible effect on MyoD/E12 binding to the E-box binding site. MyoD/E12 binding was specific, as it was efficiently competed by wild type unlabeled competitor oligonucleotide, but not with a mutant version of the *mef2c* E box. (D) Plasmids expressing MyoD or NFATc1 were co-transfected into C3H10T1/2 cells with the reporter plasmid 4R-TK-*luciferase,* which contains four multimerized copies of an E box driving luciferase expression. MyoD activated this reporter plasmid approximately 50-fold. Co-transfection of MyoD and NFATc1 exhibited no significant reduction in activation of the reporter at around 40 fold. Data are shown as the mean *n*-fold activation over the activation of 4R-TK-*luciferase* by pRK5 alone from 3 independent transfections. Error bars represent the standard errors of the means.

Figure 9: NFATc1 inhibits MyoD-mediated transactivation via the N-terminal activation domain

(A) Plasmids expressing a fusion of full length MyoD and the Gal4 DBD (MyoD-Gal4) were co-transfected into C3H10T1/2 cells with the reporter plasmid 2X-Gal4-E1b-*luciferase*, a reporter plasmid dependent on two Gal4 binding sites. Gal4-MyoD strongly

activated this reporter, and this activation was significantly reduced in the presence of NFATc1 ($p = 0.01$), but not in the presence of NFATc3 (not significant). Data are expressed as percent activation of the reporter when co-transfected with MyoD-Gal4 alone. Results are from 4 independent experiments. Error bars represent the standard errors of the means. (B) Plasmids expressing full length MyoD, MyoD N-terminus only, or MyoD bHLH only fused to the Gal4 DBD (MyoD-Gal4) were co-transfected into C3H10T1/2 cells with the reporter plasmid 2X-Gal4-E1b-*luciferase*. Gal4-MyoD and Gal4 MyoD N-term strongly activated this reporter, and the activation of both was significantly reduced in the presence of NFATc1 ($p = 0.02$ and $p = 0.01$, respectively), but no repression was observed in the presence of NFATc3 (not significant). No significant difference was observed when NFATc1 was co-expressed with Gal4 MyoD bHLH. Data are expressed as fold activation of the reporter over empty vectors. Results are from 4 independent experiments. Error bars represent the standard errors of the means.

Figure 10: Generation of a skeletal muscle-specific knockout of *nfatc1*

(A) Schematic showing the strategy used to generate a skeletal muscle-specific knockout of NFATc1. *nfatc1* was inactivated specifically in skeletal muscle by crossing mice with a floxed *nfatc1* allele with mice harboring the skeletal muscle specific *Mef2c*-73k-Cre transgene (Heidt and Black 2005). (B) Quantitative RT-PCR on RNA isolated from the soleus muscles of 6 week old adult male mice. A greater than 80% reduction was observed for *nfatc1* mRNA levels in $nfatc1^{SkM\text{-}KO}$ mice compared to control mice ($nfatc1^{flox/+}$) and ~30% reduction in *nfatc1* mRNA levels in $nfatc1^{SkM\text{-}KO}$ compared to

nfatc1$^{flox/-}$ mice. Results are from 3 animals for each genotype. Error bars represent the standard errors of the means. (C) Comparison of NFATc1 protein expression in *nfatc1*$^{SkM\text{-}KO}$ and control mice shown by western blot. There is a marked reduction in NFATc1 protein expression in the gastrocnemius muscles of *nfatc1*$^{SkM\text{-}KO}$ mice compared to controls. This experiment was repeated on 3 animals for each genotype with similar results. (D) Table showing expected and observed Mendelian numbers for *nfatc1*$^{SkM\text{-}KO}$ mice. Mice were born at expected Mendelian ratios and survived to adulthood with no overt phenotype (data not shown).

Figure 11: *nfatc1*$^{SkM\text{-}KO}$ mice do not have growth deficits

(A) Measurements of body weight of 49 day old male mice. *nfatc1*$^{SkM\text{-}KO}$ mice did not show any significant difference in body weight compared to control mice (*nfatc1*$^{flox/+}$) or heterozygotes (*nfatc1*$^{flox/-}$). The data shown represent the mean values obtained from 5-11 mice of each genotype. Error bars represent the standard errors of the means.

(B) The weight of individual muscles was compared between control mice (*nfatc1*$^{flox/+}$), heterozygotes (*nfatc1*$^{flox/-}$), and conditional knockout mice (*nfatc1*$^{SkM\text{-}KO}$). Weights were measured for the soleus (black), gastrocnemius (blue), and tibialis anterior (red) taken from the hindlimbs of 49 day old male mice. The data shown represent the mean values obtained from 5-11 mice of each genotype. Error bars represent the standard errors of the means.

Figure 12: NFATc1 is required for proper fiber type balance and fiber type switching in response to exercise

Soleus muscles from male mice at 49 days of age were used for fiber type analysis by Metachromatic ATPase staining. Type I (slow) fibers stain dark blue. Type II (fast) fibers stain light blue. (A, E) Metachromatic ATPase staining results and fiber type quantification for *nfatc1*$^{flox/+}$ mice prior to the voluntary running assay (pre-exercise) showed approximately 45% of Type I (slow) fibers. At least three 10X fields were counted for 7 mice. (B, E) Metachromatic ATPase staining results and fiber type quantification for *nfatc1*$^{SkM\text{-}KO}$ mice prior to the voluntary running assay (pre-exercise) showed a significant decrease in the number of Type I (slow) fibers at approximately 35% ($p = 0.006$, control versus CKO, pre-exercise). At least three 10X fields were counted for 6 mice. (C, E) Metachromatic ATPase staining results and fiber type quantification for *nfatc1*$^{flox/+}$ mice after the voluntary running assay (post-exercise) showed approximately a 5% increase in the number of Type I (slow) fibers. At least three 10X fields were counted for 9 mice. ($p = 0.01$, control pre-exercise versus control post-exercise). (D, E) Metachromatic ATPase staining and fiber type quantification results for *nfatc1*$^{SkM\text{-}KO}$ mice after the voluntary running assay (post-exercise) showed no change in the number of Type I (slow) fibers. At least three 10X fields were counted for 7 mice. (E) The data shown represent the mean values. Error bars represent the standard errors of the means.

Figure 13: *nfatc1*$^{SkM\text{-}KO}$ mice do not have exercise deficits

Adult male mice were used in a voluntarily running wheel assay to test their exercise abilities. Starting on post-natal day 39, mice underwent a 3-day training period to become acclimated to the running wheel. Mice were then allowed to voluntarily run for 7

consecutive days. Measurements for distance run (A) and time run (B) were taken each day and then averaged. No significant difference between control mice (*nfatc1*$^{flox/+}$, n = 10) and *nfatc1*$^{SkM\text{-}KO}$ mice (n = 12) was observed for distance run (A) or time run (B). The data shown represent the mean values. Error bars represent the standard errors of the means. (C-F) Myosin slow immunofluorescent staining for fiber type identification from soleus muscle sections of males at 49 days of age at 10x magnification. Red fibers indicate Type I (slow) fibers and black fibers indicated Type II (fast) fibers.

Figure 14: *nfatc1*$^{SkM\text{-}KO}$ muscle may have an increase in muscle regeneration in post-exercised muscle

(A) Transverse sections of the soleus muscle of adult control mice showing little to no regenerating fibers following a 7 day voluntary running assay. (B) Soleus muscle sections of adult *nfatc1*$^{SkM\text{-}KO}$ mice showing a large number of regenerating fibers following a 7 day voluntary running assay. Regenerating fibers are morphologically identified by the presence of centrally located nuclei within individual muscle fibers. Centrally located nuclei of some myofibers are shown with black arrows. Multiple sections from at least 6 mice of each genotype were analyzed.

Figure 15: NFATc1 is expressed in slow and fast myofiber nuclei

(A) Immunohistochemistry of the soleus muscle from 7 week old mice shows NFATc1 expression within the nuclei of several muscle fibers. Image taken at 10X magnification. (B) Zoomed in image taken at 60X magnification, corresponding to the black box in figure A. Some NFATc1 positive nuclei are shown with a black arrow. (C) Serial section

of the adult soleus muscle used in figure A showing immunofluorescence staining for myosin slow (red). The green fibers show autofluorescence and are merely included as an aid for visualization all the muscle fibers. Image taken at 10X magnification. (D) Zoomed in image taken at 60X magnification, corresponding to the white box in figure C. It is evident that NFATc1 positive nuclei in some myofibers shown in figure A correspond to Type I (slow) fibers, identified by to their expression of myosin slow (red). (E) Serial section of the adult soleus muscle used in figure A showing immunofluorescence staining for myosin fast (red). The green fibers show autofluorescence and are merely included as an aid for visualization all the muscle fibers. Image taken at 10X magnification. (F) Zoomed in image taken at 60X magnification, corresponding to the white box in figure E. NFATc1 positive nuclei in some myofibers shown in figure A correspond to Type II (fast) fibers, identified by their expression of myosin fast (red).

Figure 16: NFATc1 and MyoD co-localize in skeletal muscle nuclei

(A) Immunohistochemistry for MyoD in the soleus muscle of 7 week old mice. MyoD positive nuclei are shown with a black arrow. (B) Serial section of fibers shown in Figure A showing immunohistochemistry for NFATc1 in the soleus muscle of 7 week old mice. NFATc1 positive nuclei are shown with a black arrow, and correspond to the same nuclei in the same fiber as those of MyoD in figure A. Images were taken at 60X magnification.

Figure 17: *nfatc1*$^{SkM\text{-}KO}$ muscle has a defect in fast fiber gene expression at baseline

Quantitative RT-PCR on RNA isolated from the soleus muscles of 7 week old, unexercised, adult male mice. Several genes known to be expressed in Type II (fast)

fibers or Type I (slow) fibers were selected for gene expression analysis. The majority of the fast genes selected showed a significant increase in the relative mRNA expression of fast fiber genes, and no significant difference in the relative mRNA expression in slow fiber gene expression in *nfatc1*$^{SkM\text{-}KO}$ muscle (red bars) compared to control muscle (black bars). Quantitative RT-PCR was performed using whole soleus muscle from 6 mice of each genotype. For genes that were significantly increased, $p < 0.05$ (indicated by an asterisk).

Figure 18: NFATc1 is required for proper expression of several MyoD target genes in skeletal muscle

Quantitative RT-PCR on RNA isolated from the soleus muscles of 7 week old, unexercised, adult male mice. (A) Several genes known to be MyoD transcriptional targets were selected for gene expression analysis. The majority of MyoD target genes selected showed a significant increase in the relative mRNA expression in *nfatc1* $^{SkM\text{-}KO}$ muscle (red bars) compared to control muscle (black bars). Quantitative RT-PCR was performed using whole soleus muscle from 6 mice of each genotype. For genes that were significantly increased, $p < 0.05$ (indicated by an asterisk). (B) Several transcription factors known to be MyoD transcriptional targets were selected for gene expression analysis. All of the MyoD target genes selected showed a significant increase in the relative mRNA expression in *nfatc1*$^{SkM\text{-}KO}$ muscle (red bars) compared to control muscle (black bars). Quantitative RT-PCR was performed using whole soleus muscle from 6 mice of each genotype. For genes that were significantly increased, $p < 0.05$ (indicated by an asterisk).

Figure 19: Schematic model: NFATc1 inhibits MyoD in order to promote the slow fiber phenotype

A schematic showing a proposed model for NFATc1 inhibition of MyoD in the context of fiber type regulation. In response to exercise or contractile activity, NFATc1 acts to drive the fast-to-slow fiber type switch by promoting the transcription of slow fiber genes in addition to inhibiting fast fiber gene expression through inhibition of MyoD transcriptional activity.

Figure 1

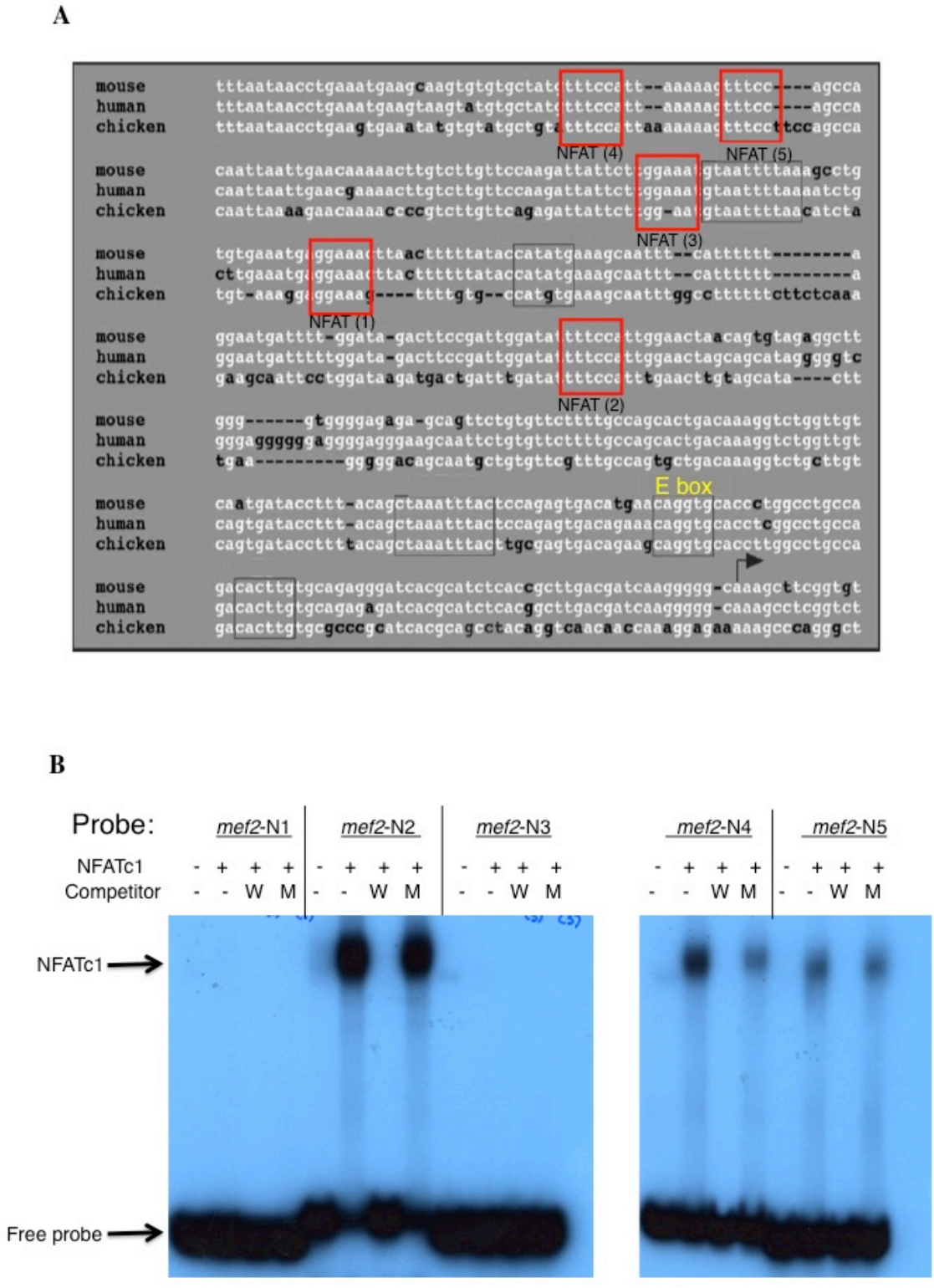
A
mouse
human
chicken
NFAT (4)
NFAT (5)
NFAT (3)
NFAT (1)
NFAT (2)
E box
B
Probe:
mef2-N1
mef2-N2
mef2-N3
mef2-N4
mef2-N5
NFATc1
Competitor
W
M
NFATc1
Free probe

Figure 2

A

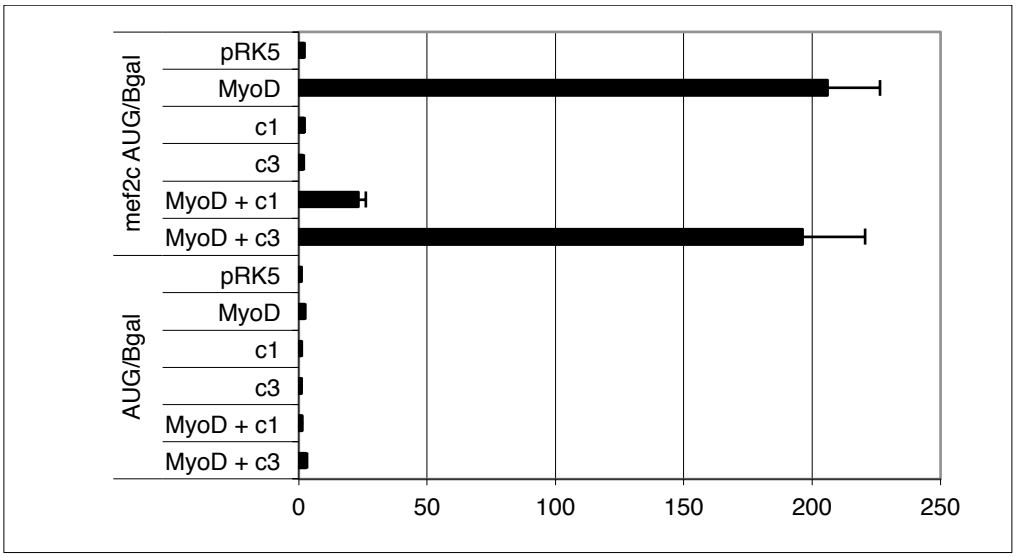
mef2c AUG/Bgal
pRK5
MyoD
c1
c3
MyoD + c1
MyoD + c3
AUG/Bgal
pRK5
MyoD
c1
c3
MyoD + c1
MyoD + c3
0
50
100
150
200
250
Fold Activation

Figure 3

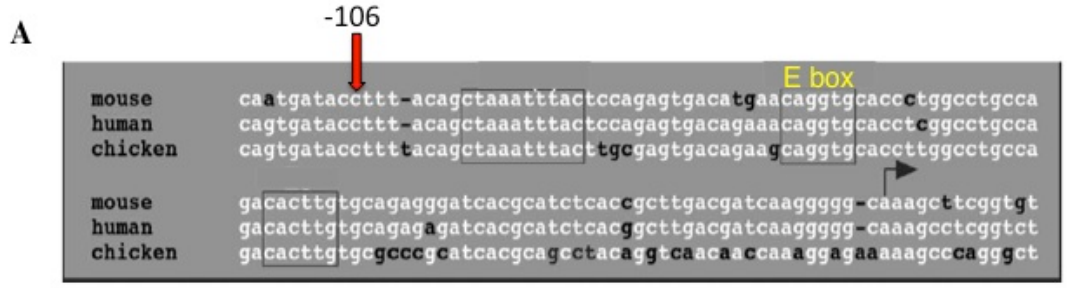

B

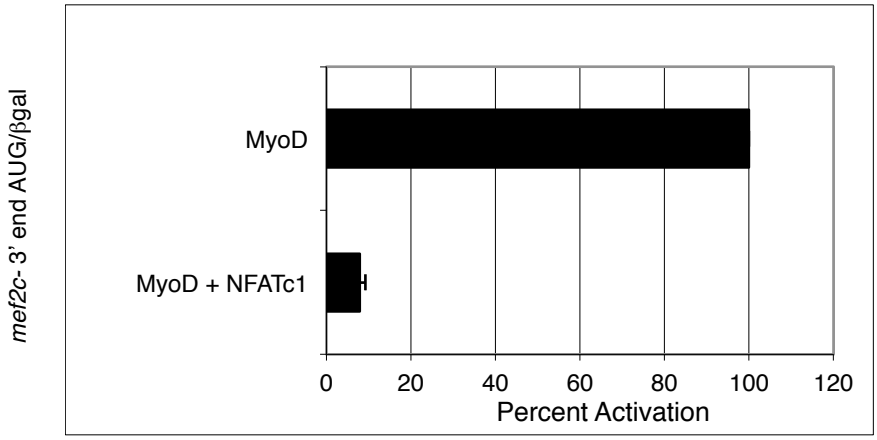

C

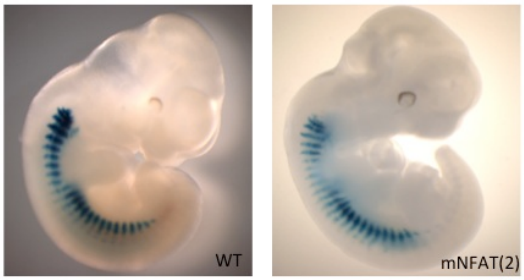

E11.5

Figure 3 continued

D

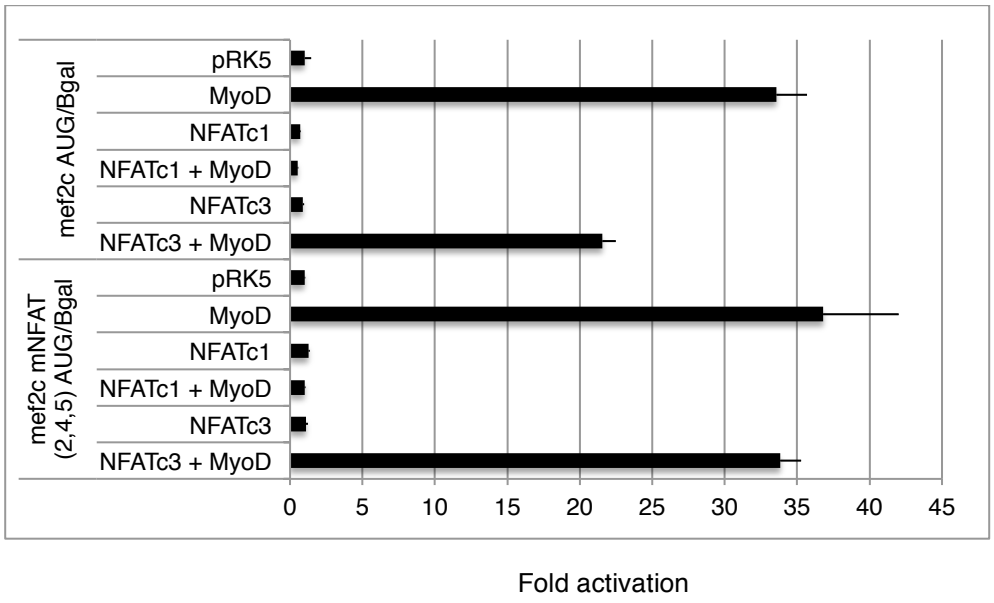

Figure 4

A

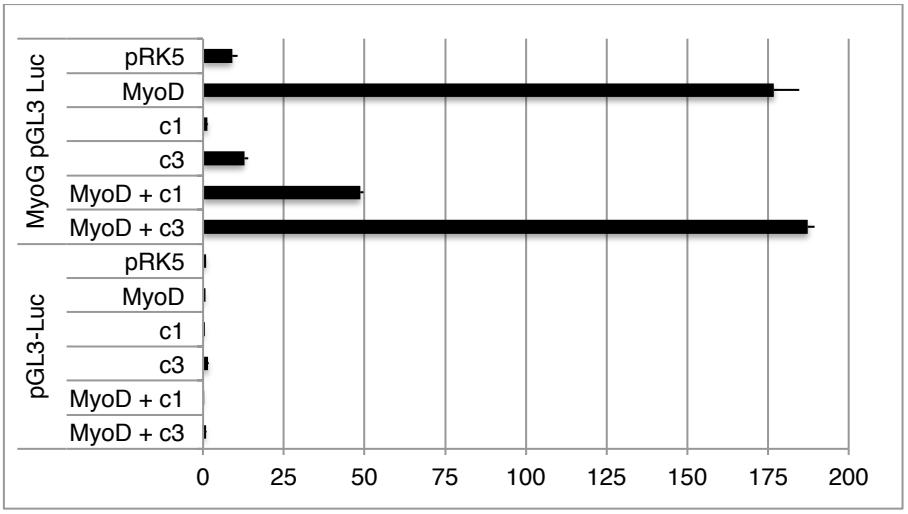
MyoG pGL3 Luc
pRK5
MyoD
c1
c3
MyoD + c1
MyoD + c3
pGL3-Luc
pRK5
MyoD
c1
c3
MyoD + c1
MyoD + c3
0
25
50
75
100
125
150
175
200

B

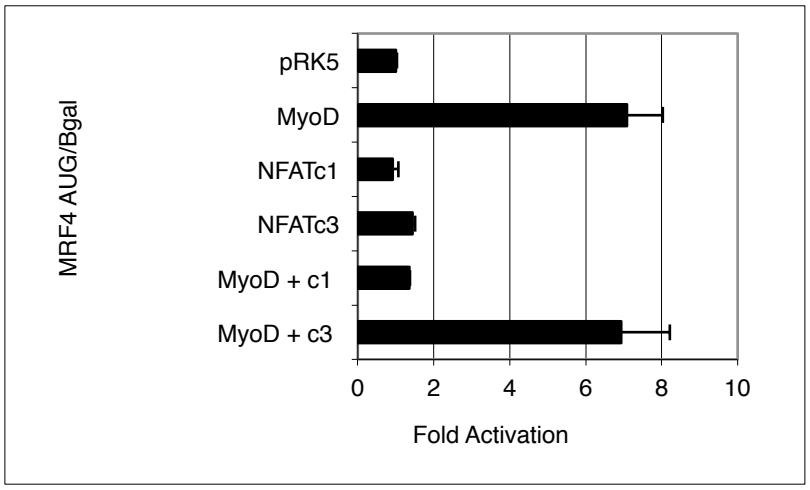
MRF4 AUG/Bgal
pRK5
MyoD
NFATc1
NFATc3
MyoD + c1
MyoD + c3
0
2
4
6
8
10
Fold Activation

Figure 5

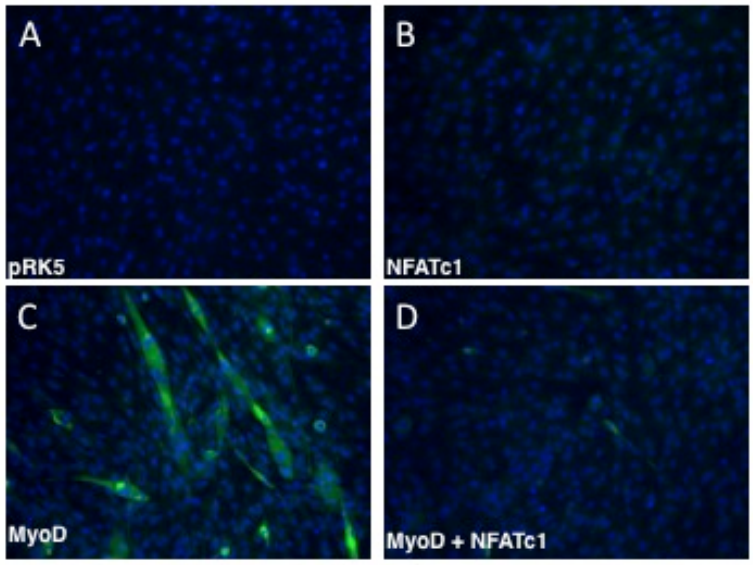
A
pRK5
B
NFATc1
C
MyoD
D
MyoD + NFATc1

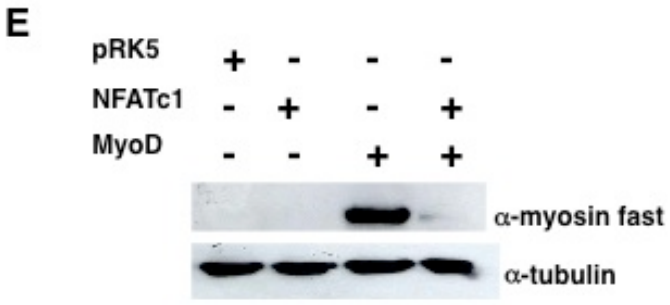
E
pRK5 + - - -
NFATc1 - + - +
MyoD - - + +
α-myosin fast
α-tubulin

Figure 6

A

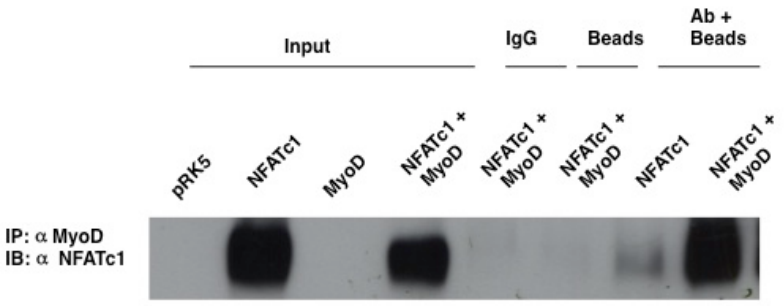
Input
IgG
Beads
Ab + Beads
pRK5
NFATc1
MyoD
NFATc1 + MyoD
NFATc1 + MyoD
NFATc1 + MyoD
NFATc1
NFATc1 + MyoD
IP: α MyoD
IB: α NFATc1

B

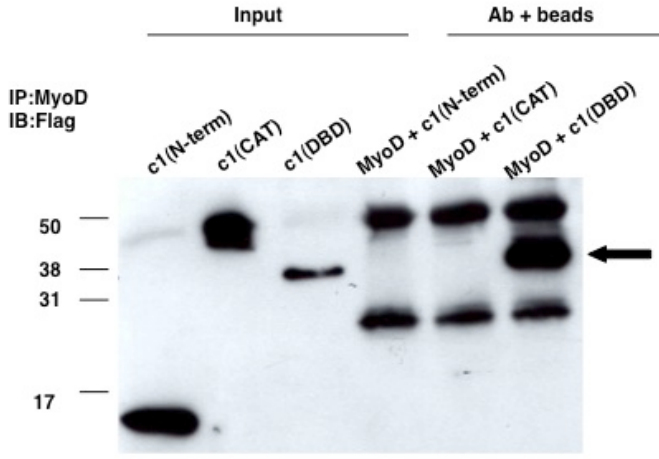
Input
Ab + beads
IP:MyoD
IB:Flag
c1(N-term)
c1(CAT)
c1(DBD)
MyoD + c1(N-term)
MyoD + c1(CAT)
MyoD + c1(DBD)
50
38
31
17

C

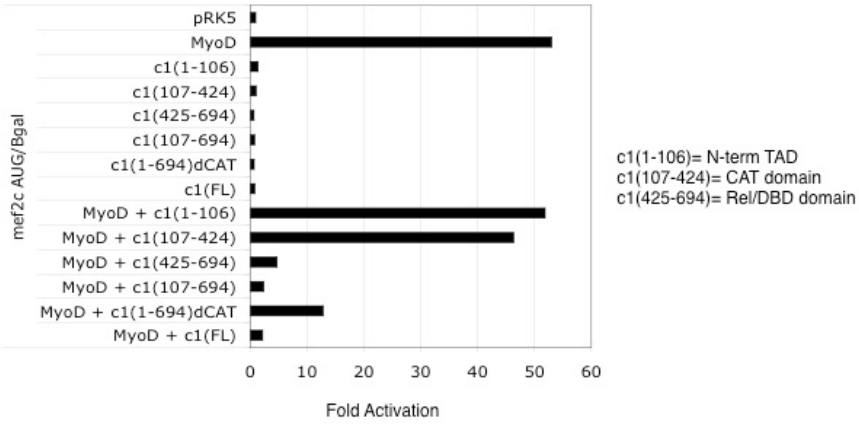
pRK5
MyoD
c1(1-106)
c1(107-424)
c1(425-694)
c1(107-694)
c1(1-694)dCAT
c1(FL)
MyoD + c1(1-106)
MyoD + c1(107-424)
MyoD + c1(425-694)
MyoD + c1(107-694)
MyoD + c1(1-694)dCAT
MyoD + c1(FL)
mef2c AUG/Bgal
0
10
20
30
40
50
60
Fold Activation
c1(1-106)= N-term TAD
c1(107-424)= CAT domain
c1(425-694)= Rel/DBD domain

Figure 6 continued

D

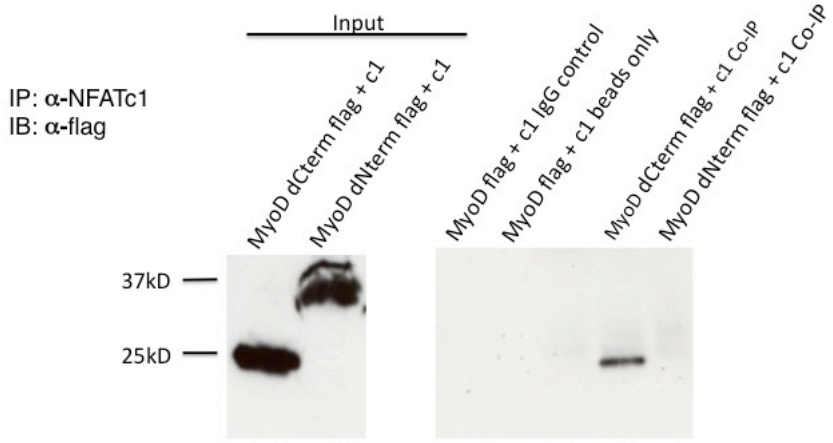

E

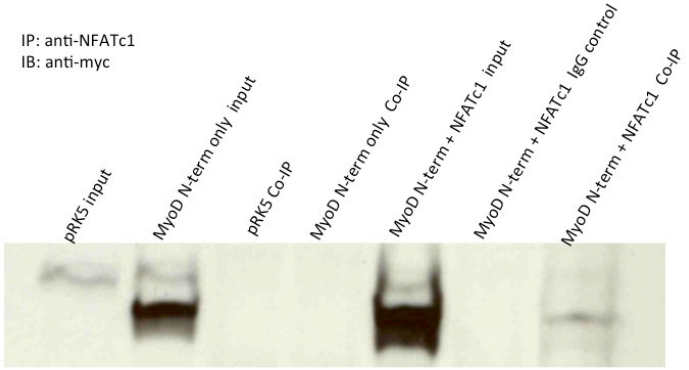

Figure 7

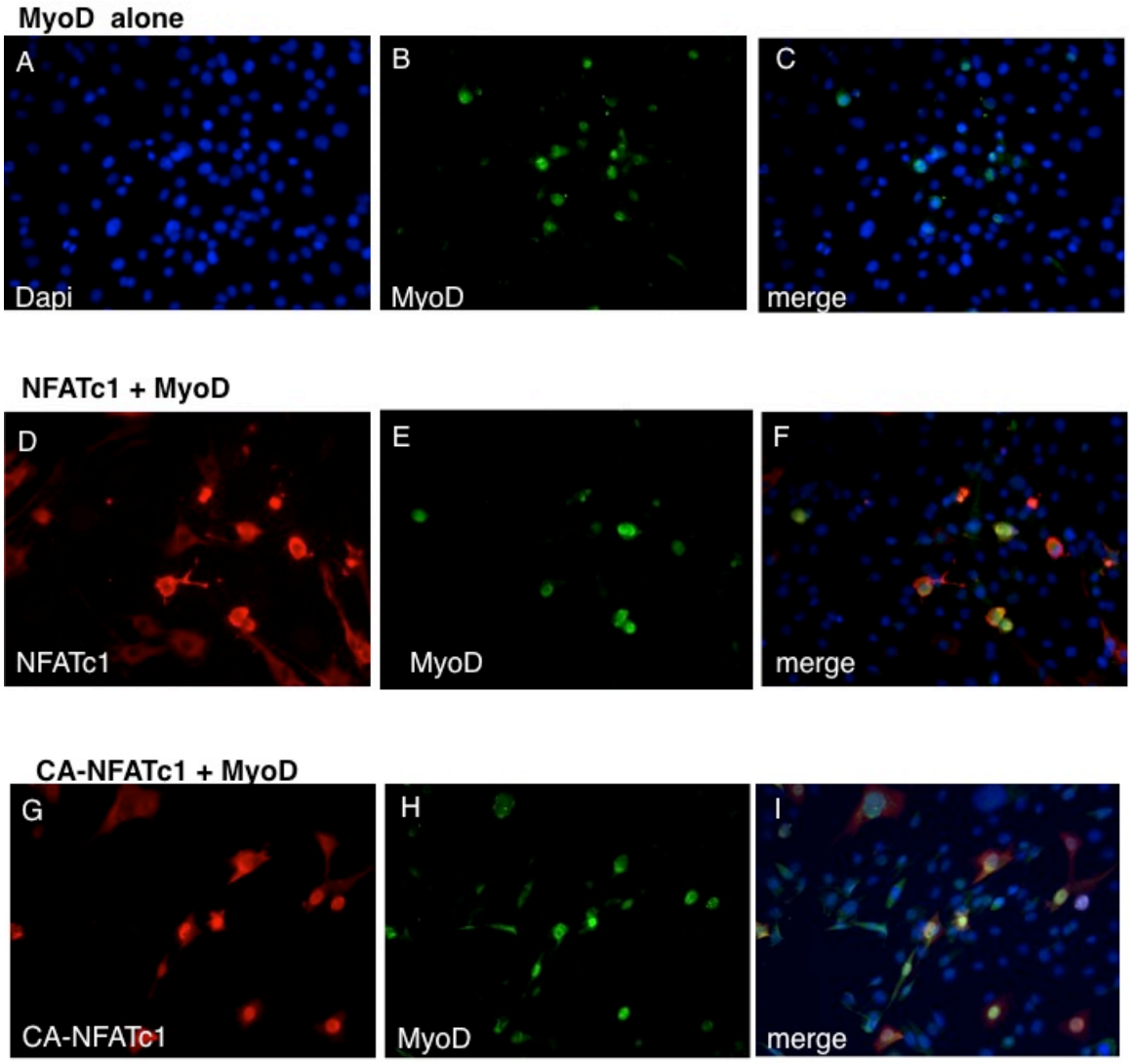
MyoD alone
A
Dapi
B
MyoD
C
merge
NFATc1 + MyoD
D
NFATc1
E
MyoD
F
merge
CA-NFATc1 + MyoD
G
CA-NFATc1
H
MyoD
I
merge

Figure 8

A

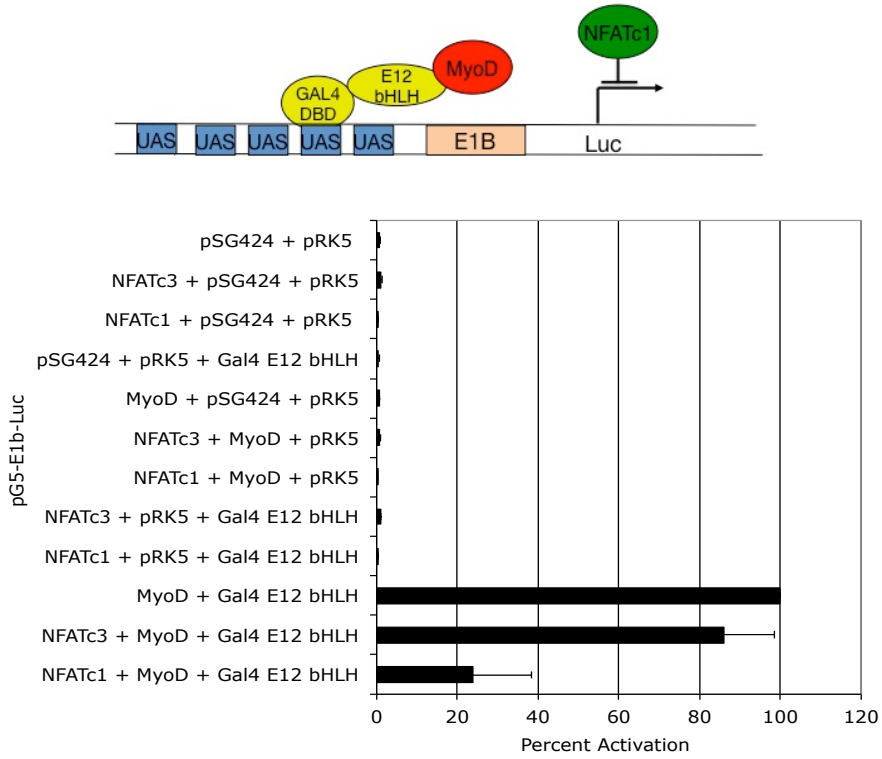
NFATc1
MyoD
E12 bHLH
GAL4 DBD
UAS
UAS
UAS
UAS
UAS
E1B
Luc
pG5-E1b-Luc
pSG424 + pRK5
NFATc3 + pSG424 + pRK5
NFATc1 + pSG424 + pRK5
pSG424 + pRK5 + Gal4 E12 bHLH
MyoD + pSG424 + pRK5
NFATc3 + MyoD + pRK5
NFATc1 + MyoD + pRK5
NFATc3 + pRK5 + Gal4 E12 bHLH
NFATc1 + pRK5 + Gal4 E12 bHLH
MyoD + Gal4 E12 bHLH
NFATc3 + MyoD + Gal4 E12 bHLH
NFATc1 + MyoD + Gal4 E12 bHLH
0
20
40
60
80
100
120
Percent Activation

B

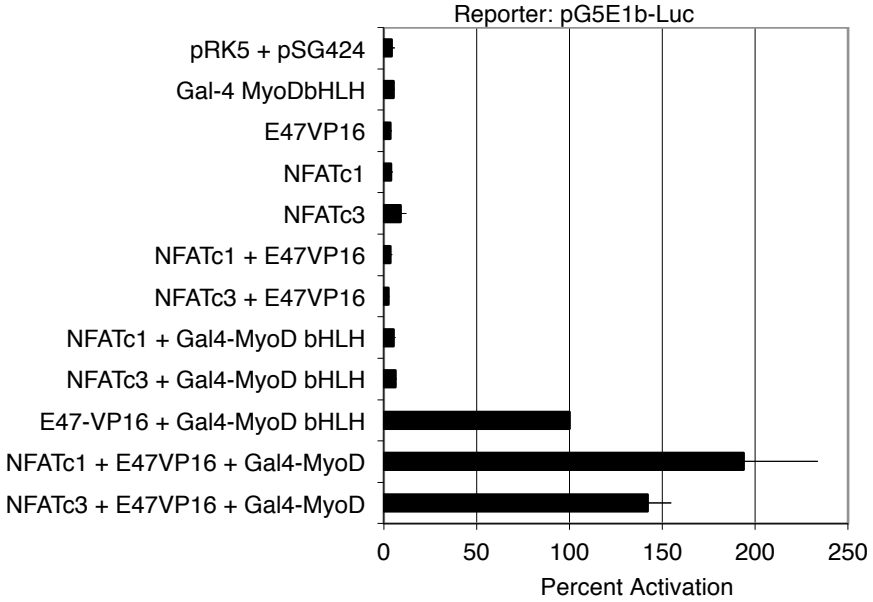
Reporter: pG5E1b-Luc
pRK5 + pSG424
Gal-4 MyoDbHLH
E47VP16
NFATc1
NFATc3
NFATc1 + E47VP16
NFATc3 + E47VP16
NFATc1 + Gal4-MyoD bHLH
NFATc3 + Gal4-MyoD bHLH
E47-VP16 + Gal4-MyoD bHLH
NFATc1 + E47VP16 + Gal4-MyoD
NFATc3 + E47VP16 + Gal4-MyoD
0
50
100
150
200
250
Percent Activation

Figure 8 continued

C

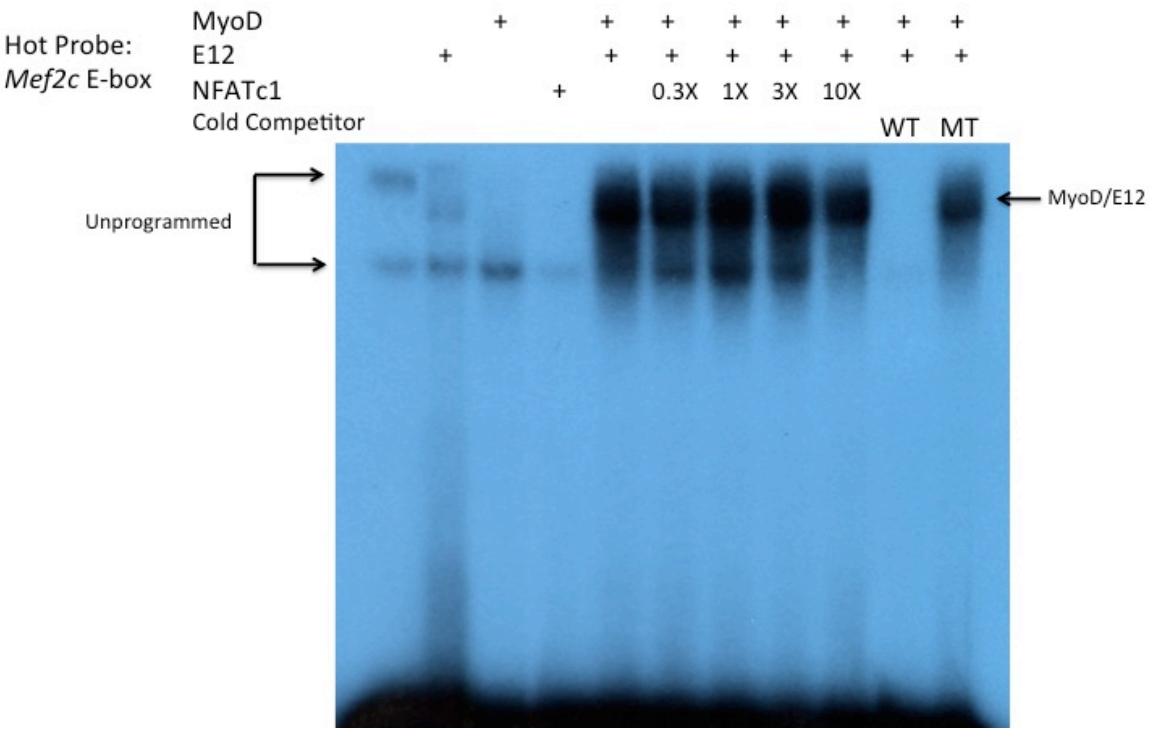

D

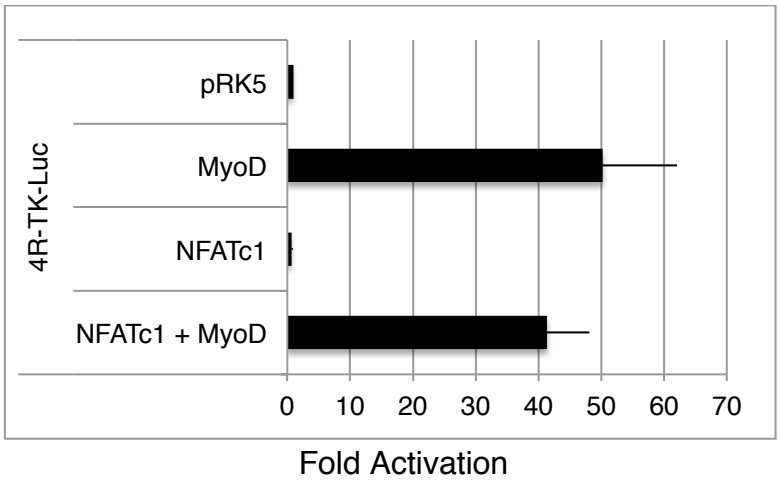

Figure 9

A

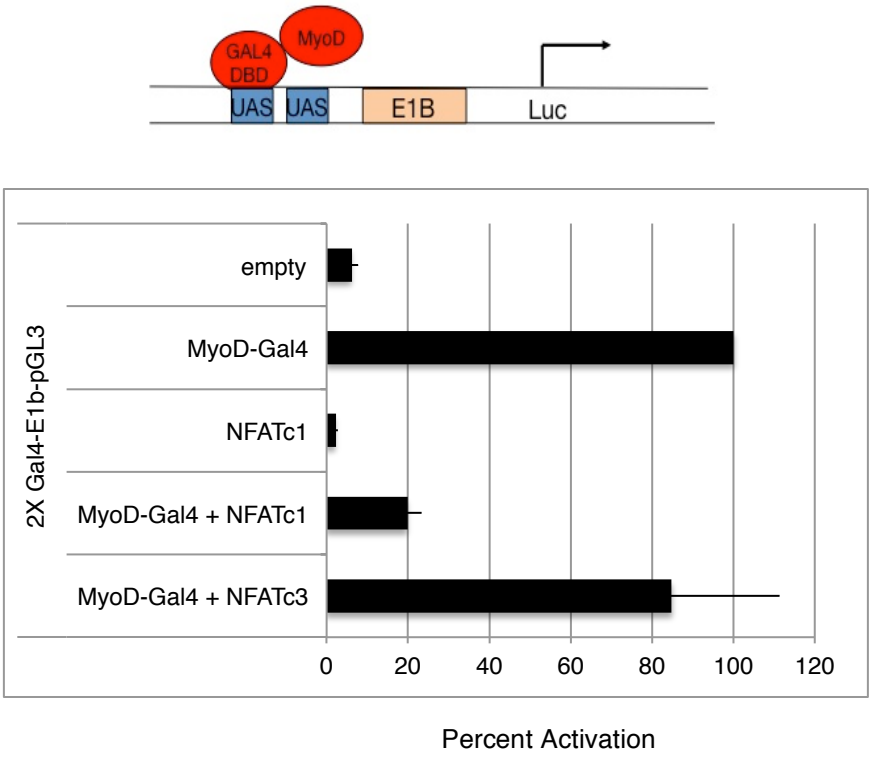
GAL4 DBD
MyoD
UAS
UAS
E1B
Luc
2X Gal4-E1b-pGL3
empty
MyoD-Gal4
NFATc1
MyoD-Gal4 + NFATc1
MyoD-Gal4 + NFATc3
0
20
40
60
80
100
120
Percent Activation

B

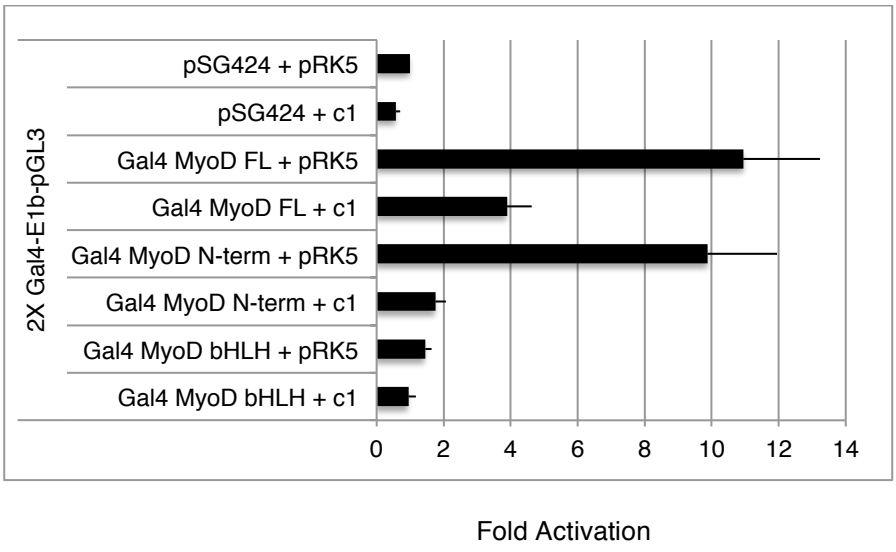
2X Gal4-E1b-pGL3
pSG424 + pRK5
pSG424 + c1
Gal4 MyoD FL + pRK5
Gal4 MyoD FL + c1
Gal4 MyoD N-term + pRK5
Gal4 MyoD N-term + c1
Gal4 MyoD bHLH + pRK5
Gal4 MyoD bHLH + c1
0
2
4
6
8
10
12
14
Fold Activation

Figure 10

A

nfatc1 $^{flox/flox}$ X *mef2c*-AHF-Cre$^{Tg/0}$

nfatc1 $^{+/\Delta}$ X *mef2c-73K*-Cre$^{Tg/0}$

mef2c-73K-Cre$^{Tg/0}$; *nfatc1* $^{+/\Delta}$ X *nfatc1* $^{flox/flox}$

25% CKO: *mef2c-73K*-Cre$^{Tg/0}$; *nfatc1* $^{flox/\Delta}$

B

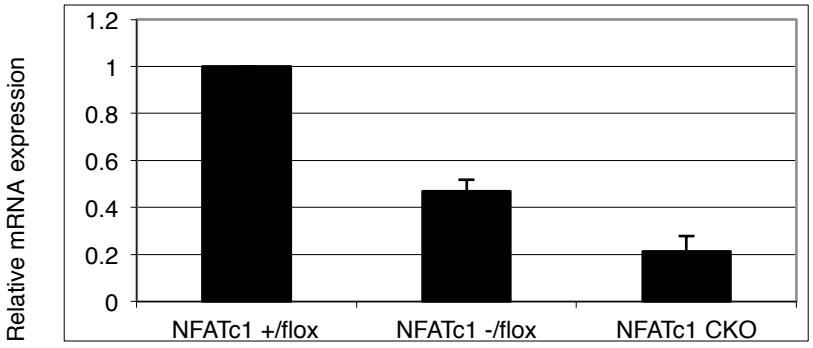

C

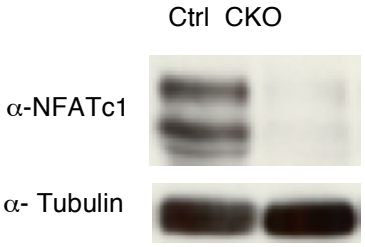

D

Genotype	Expected	Observed
NFATc1 +/flox	43.5 (25%)	48 (~28%)
NFATc1 Δ/flox	43.5 (25%)	49 (~28%)
NFATc1 +/flox; *mef2c* cre	43.5 (25%)	33 (~19%)
NFATc1 Δ/flox; *mef2c* cre	43.5 (25%)	44 (~25%)

Figure 11

A

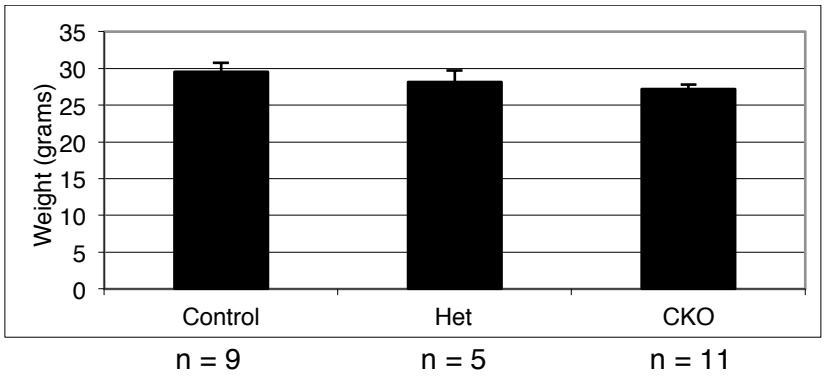
Weight (grams)
35
30
25
20
15
10
5
0
Control
Het
CKO
n = 9
n = 5
n = 11

B

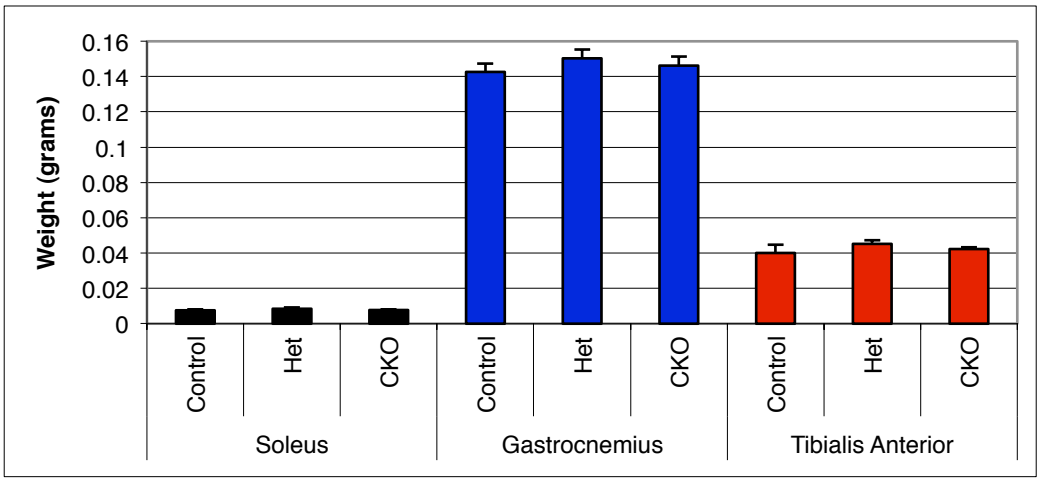
Weight (grams)
0.16
0.14
0.12
0.1
0.08
0.06
0.04
0.02
0
Control
Het
CKO
Soleus
Gastrocnemius
Tibialis Anterior

Figure 12

A

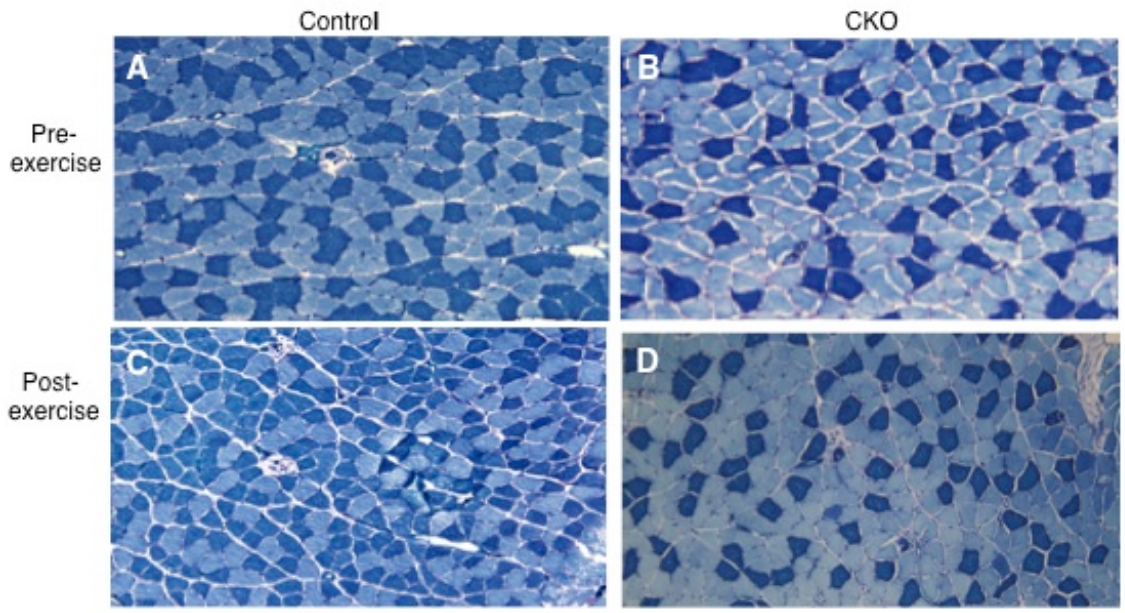
Control
CKO
A
B
C
D
Pre-exercise
Post-exercise

E

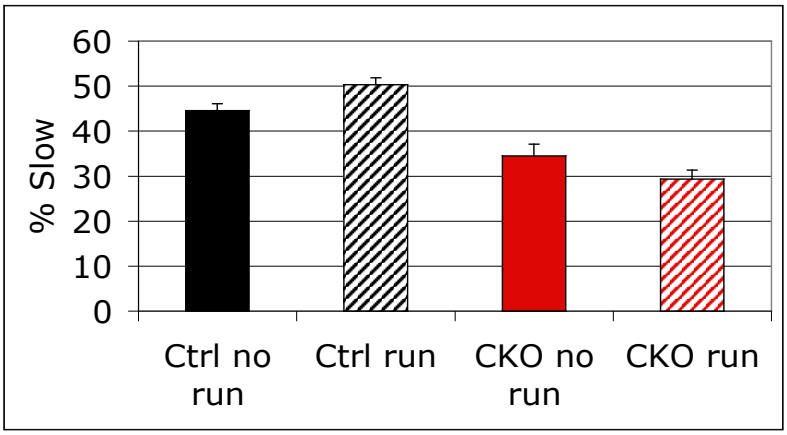
% Slow
60
50
40
30
20
10
0
Ctrl no run
Ctrl run
CKO no run
CKO run

Figure 13

A

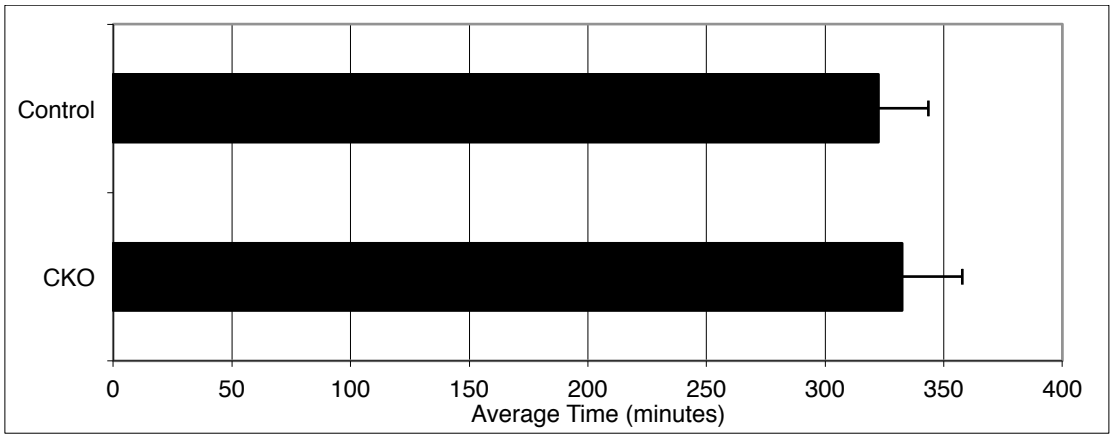
Control
CKO
0
50
100
150
200
250
300
350
400
Average Time (minutes)

B

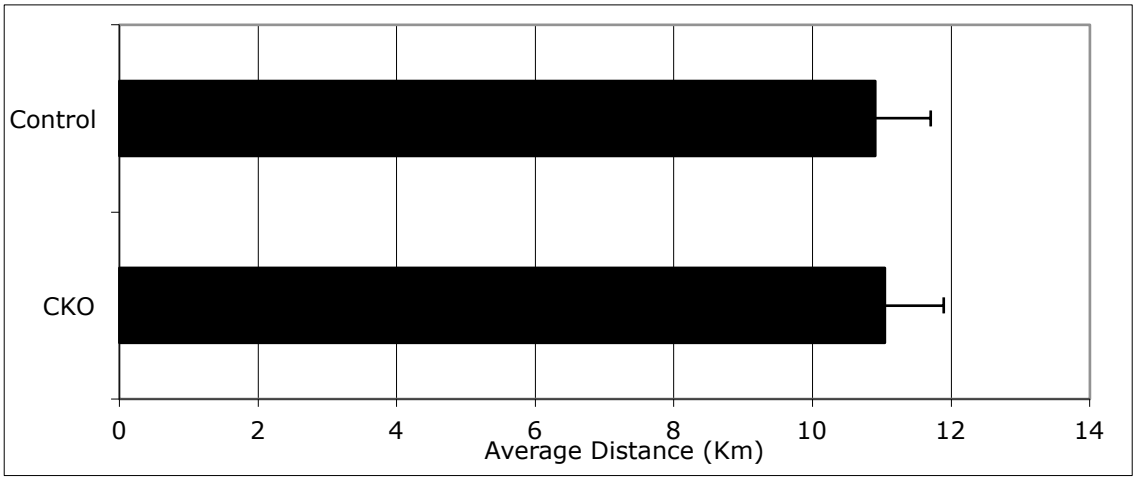
Control
CKO
0
2
4
6
8
10
12
14
Average Distance (Km)

Figure 13 continued

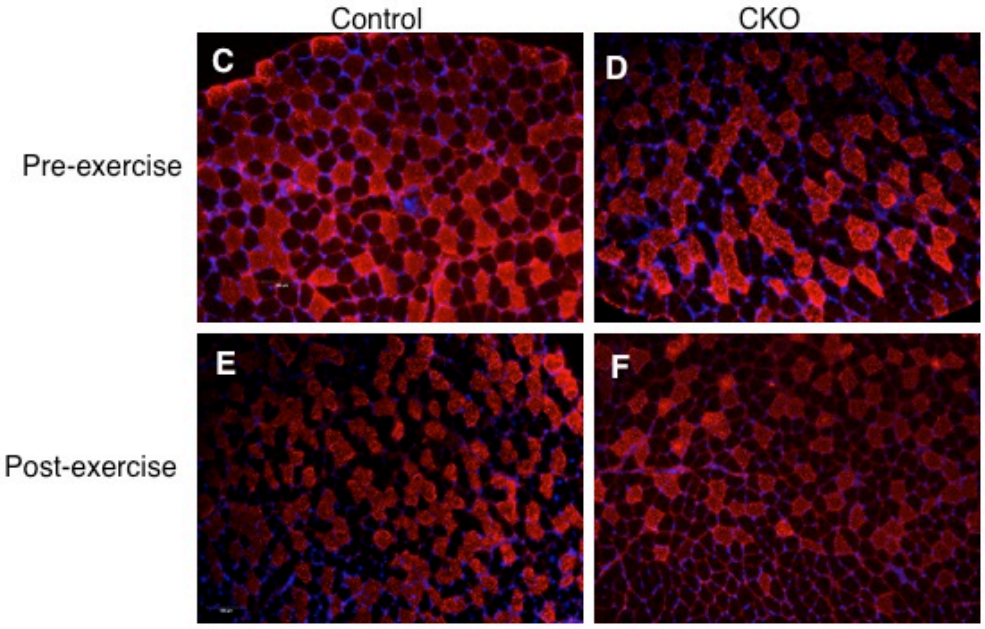

Figure 14

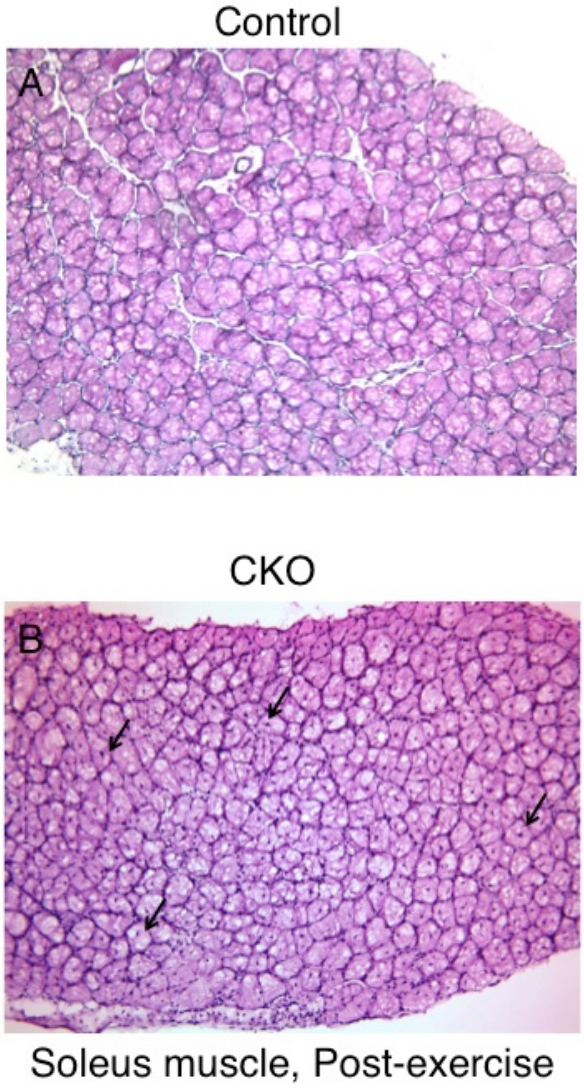

Soleus muscle, Post-exercise

Figure 15

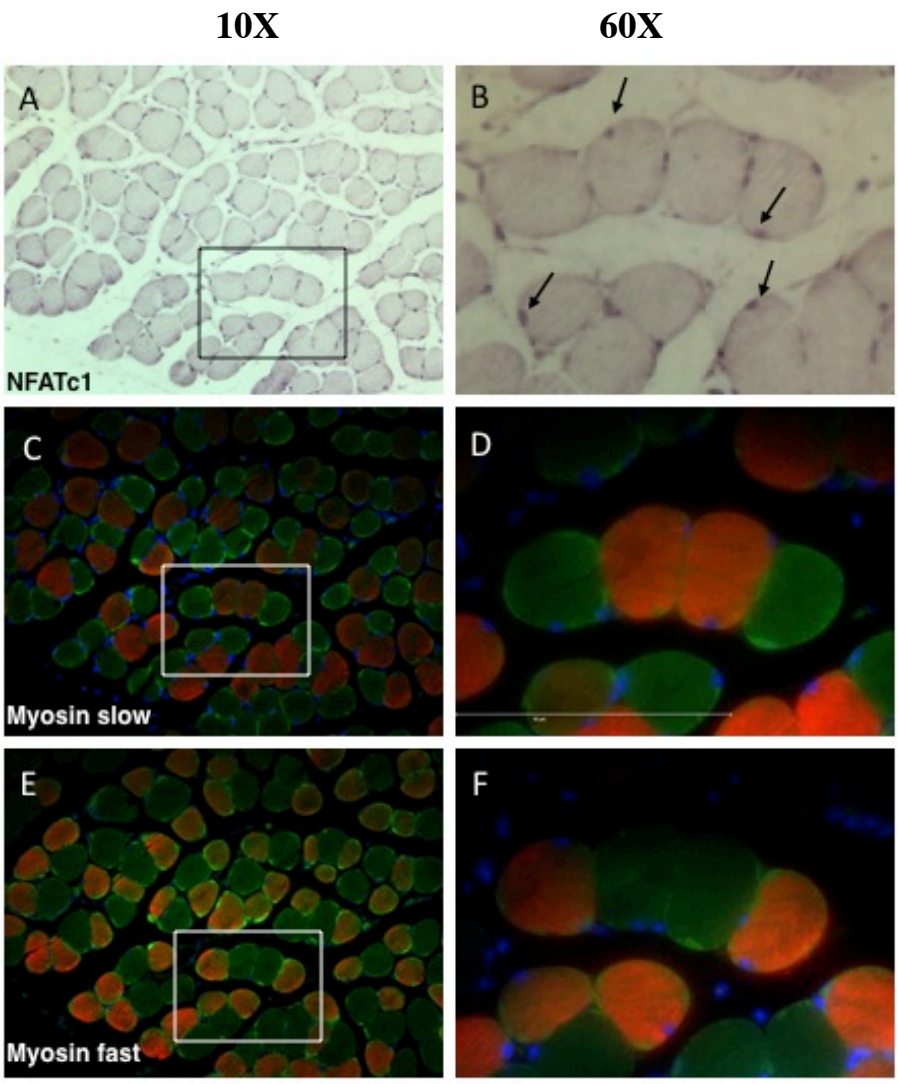

Figure 16

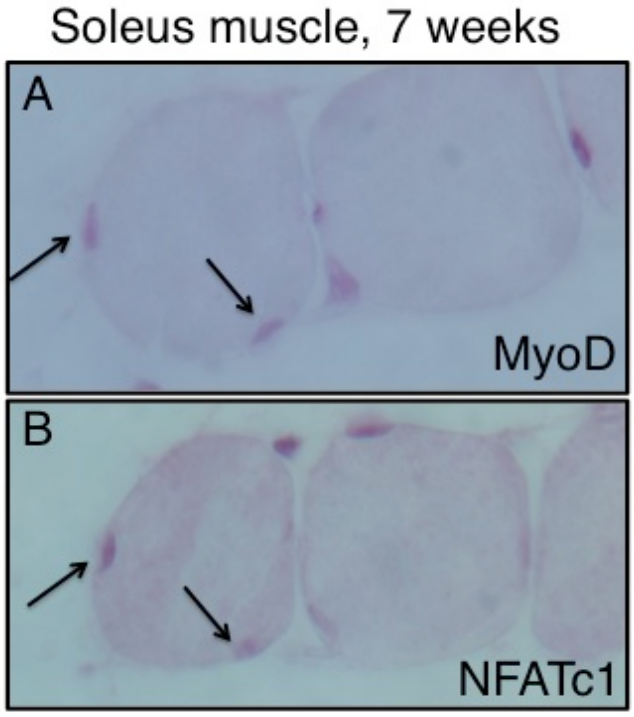

Figure 17

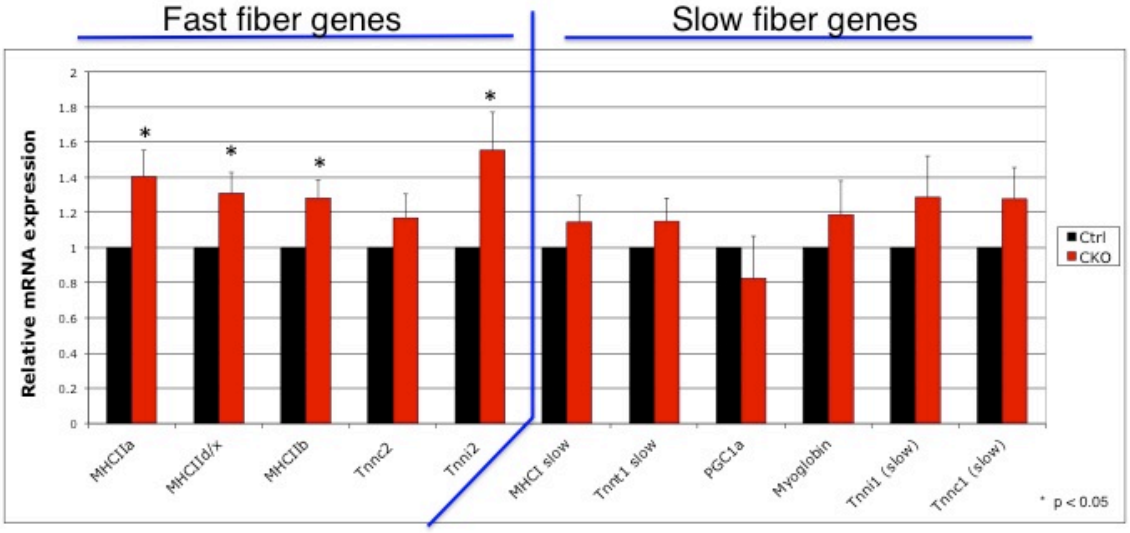
Fast fiber genes
Slow fiber genes
Relative mRNA expression
2
1.8
1.6
1.4
1.2
1
0.8
0.6
0.4
0.2
0
MHCIIa
MHCIId/x
MHCIIb
Tnnc2
Tnni2
MHCI slow
Tnnt1 slow
PGC1a
Myoglobin
Tnni1 (slow)
Tnnc1 (slow)
Ctrl
CKO
* p < 0.05

Figure 18

A

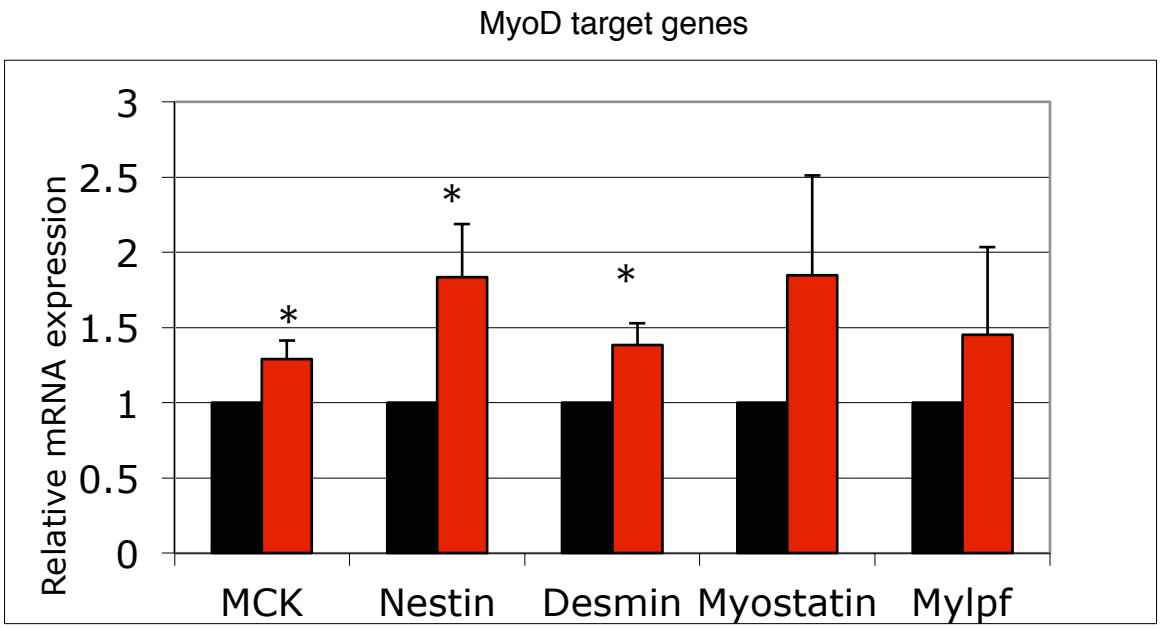
MyoD target genes
Relative mRNA expression
3
2.5
2
1.5
1
0.5
0
*
*
*
MCK
Nestin
Desmin
Myostatin
Mylpf
* p < 0.05

B

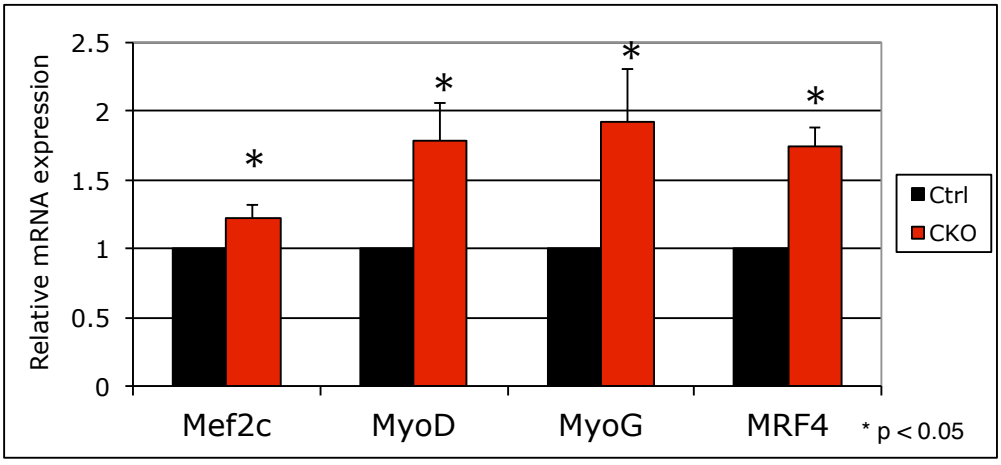
Relative mRNA expression
2.5
2
1.5
1
0.5
0
*
*
*
*
Ctrl
CKO
Mef2c
MyoD
MyoG
MRF4
* p < 0.05

Figure 19

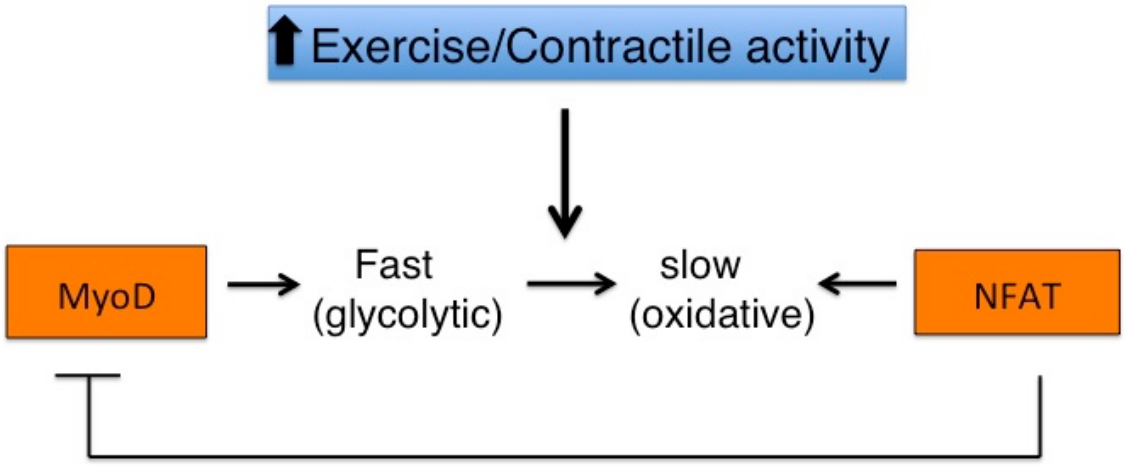
Exercise/Contractile activity
MyoD
Fast
(glycolytic)
slow
(oxidative)
NFAT

Chapter 3: Conclusions and Implications

MyoD and NFATc1 in the control of fiber type

Fiber type is first established during late embryonic development (Condon et al. 1990). During late embryogenesis and early postnatal growth, slow fiber gene expression is under the control of a genetically-encoded developmental program that appears to be independent of physiological stimulation (Calabria et al. 2009; Schiaffino and Reggiani 2011). Following the early postnatal period, the balance of slow and fast fibers is controlled in part by physiological conditions, including exercise and the patterns of electrical activity from innervating motor neurons (Schiaffino and Reggiani 2011). This has been demonstrated by delivering a slow pattern of electrical activity, mimicking endurance exercise, to fast muscle fibers that resulted in a fast-to-slow fiber type switch (Termin et al. 1989; Ausoni et al. 1990; Liu and Schneider 1998; Bozzo et al. 2005). Interestingly, this also results in the inactivation of MyoD through phosphorylation of T115 by protein kinase C (Liu et al. 1998; Ekmark et al. 2007). A prolonged slow electrical pattern delivered to fast fibers also results in a reduction of MyoD mRNA and protein expression (Ekmark et al. 2007). Furthermore, expression of endogenous *myoD* is increased in denervated fibers, suggesting activity-dependent suppression of *myoD* (Charge et al. 2008). Taken together, these studies strongly support the notion that MyoD regulates fast fiber genes and suggest that MyoD functions as a link between electrical activity and expression of fast muscle genes (Ekmark et al. 2007).

Consistent with the idea that MyoD is an important regulator of the fast fiber type, MyoD is expressed more highly in fast fibers than in slow fibers (Hughes et al. 1997), and *myoD*-null mice have an increase in the number of slow fibers (Macharia et al. 2010).

Moreover, over-expression of an active form of MyoD in muscle results in a slow-to-fast fiber type conversion, supporting a role for MyoD in promoting the fast fiber phenotype (Ekmark et al. 2007). Given the opposing functions of MyoD and NFAT in the control of fast versus slow fiber gene expression in response to electrical stimulation, and our findings that NFATc1 represses MyoD function, it is possible that NFATc1 regulates MyoD in response to motor neuron activity to promote the slow fiber phenotype through repression of MyoD activity, which normally acts to promote a fast fiber phenotype.

Given the role of MyoD in nearly every aspect of muscle development and function, it is perhaps not surprising that there are many positive and negative regulators of MyoD activity that act through a variety of mechanisms (Berkes and Tapscott 2005; Tapscott 2005). For example, Id is a well-established repressor of MyoD function. Id forms a heterodimer with the E protein partners of MyoD, thereby sequestering them from MyoD and inhibiting DNA binding (Benezra et al. 1990). Another negative regulator is TGF-beta, which inhibits muscle differentiation through Smad-3 mediated functional repression of MyoD-E protein heterodimerization (Liu et al. 2001). In the work presented here, we show that NFATc1 negatively regulates MyoD activity, which occurs, at least in part, by blocking the function of the MyoD N-terminal transactivation domain. This study is the first to show a mechanism of MyoD inhibition involving the function of the N-terminal transactivation domain. Here, we propose a model for NFATc1 regulation of the slow fiber phenotype whereby NFATc1 inhibits fast fiber gene expression initiated by MyoD through prevention of MyoD transcriptional activity, thereby driving myofibers towards a slow fiber phenotype (Figure 19).

The phosphatase calcineurin is thought to initiate skeletal muscle differentiation in part by activating MEF2 and MyoD, and calcineurin-dependent transcriptional pathways are involved in skeletal muscle fiber type control (Chin et al. 1998; Naya et al. 2000; Friday et al. 2003; Parsons et al. 2003; Parsons et al. 2004). Calcineurin activity is also important for the maintenance of the slow-fiber phenotype in adult muscle (Naya et al. 2000; Oh et al. 2005; Schiaffino and Reggiani 2011). NFAT proteins are major effectors of calcineurin signaling (Crabtree and Olson 2002), and NFAT proteins act as nerve activity sensors in skeletal muscle to control activity-dependent myosin switching in the fast-to-slow direction (McCullagh et al. 2004; Calabria et al. 2009). Several studies have supported the transcriptional role of NFAT proteins as a group in the activation of slow fiber genes and repression of fast fiber genes. These studies focused on the identification of NFAT *cis*-acting elements within slow and fast fiber genes, and used promoter reporter assays and *in vivo* electroporation to study gain of function of NFAT (McCullagh et al. 2004; Rana et al. 2008; Calabria et al. 2009). However, no direct genetic evidence for the role of NFAT proteins in the control of fiber type has been provided previously. Several studies have used the small peptide VIVIT, which specifically inhibits calcineurin-mediated activation of NFAT by preventing the interaction of calcineurin with NFAT (Aramburu et al. 1999), or calcineurin inhibitors to infer NFAT protein function downstream of calcineurin (Torgan and Daniels 2001; McCullagh et al. 2004; Miyazaki et al. 2004; Armand et al. 2008). Importantly, VIVIT and calcineurin inhibitors block the activity of all NFAT isoforms (Aramburu et al. 1999), which makes it difficult to define isoform specific functions to NFAT proteins. Furthermore, pharmacologic or genetic inhibition of calcineurin can affect several other

factors in addition to NFAT, such as MEF2 and MyoD (Friday et al. 2003), as well as exert possible off target effects, which are always of concern in pharmacologic approaches. In the present study, we have taken a genetic approach to determine the specific role of NFATc1 in skeletal muscle. We clearly show that *nfatc1*$^{SkM\text{-}KO}$ mice have a defect in fiber type composition, displaying fewer slow fibers in unexercised muscle and a blunted fast-to-slow transition following endurance exercise training, providing the first physiological evidence for the role of any NFAT protein in fiber type switching. Thus, these studies suggest that NFATc1 is likely the primary NFAT isoform downstream of calcineurin responsible for regulating fiber type *in vivo*.

NFATc1 mechanism of repression of MyoD activity

One outstanding question raised by this work is whether NFATc1 inhibits MyoD transactivation ability through merely direct binding to the N-terminal transactivation domain, or if other factors are involved in the mechanism of NFATc1 repression. Alternatively, NFATc1 could be facilitating recruitment of a co-repressor or preventing interaction of MyoD with a co-activator in order to inhibit MyoD function. NFAT proteins have been shown to act as repressors in other tissues through recruitment of HDACs. One study reported that NFATc2 represses *cdk4* promoter activity by reducing acetylation of histone H3 through recruitment of an HDAC to the *cdk4* promoter, and showed that NFATc2 physically interacted with HDAC1 (Baksh et al. 2002). A more recent study used a constitutively active NFATc1 mutant and showed that it forms a repressor complex with HDAC3 on the *osteocalcin* regulatory region, resulting in the repression of *osteocalcin* gene expression (Choo et al. 2009). Both HDAC1 and HDAC3

are class I HDACs, so it is possible that NFATc1 might be recruiting a class I HDAC to MyoD to form a repressor complex. Furthermore, MyoD itself can interact with class I HDACs in myoblasts (Mal et al. 2001; Puri et al. 2001). We did some preliminary experiments to test whether HDAC activity might be involved in NFATc1 repression of MyoD-mediated myogenic conversion and found that even in the presence of 100nM trichostatin A (TSA), an inhibitor of Class I and II HDACs, NFATc1 was still able to repress MyoD-mediated conversion of C3H10T1/2 cells into myotubes. Although further investigation would be needed to completely rule out HDAC involvement, given this result, we think it more likely that NFATc1 might be preventing interaction of MyoD with a co-activator.

One possible co-activator candidate is the histone acetyltransferase p300/CBP, which interacts with the N-terminal domain of MyoD, and then recruits p300/CREB-binding protein-associated factor (PCAF) to form a ternary multimeric complex (Eckner et al. 1996; Puri et al. 1997; Puri et al. 1997; Sartorelli et al. 1997). p300 stimulates MyoD-dependent transcription by acetylating nucleosomal histones surrounding E-boxes, in addition to acetylating MyoD itself, resulting in its increased DNA binding and transcriptional activity (Sartorelli et al 1997, Polesskaya et al 2001). In addition, PCAF-mediated acetylation of MyoD has been suggested to cause a conformational change and increase MyoD DNA affinity (Sartorelli et al. 1999; Polesskaya et al. 2001). Lysine 99, 102, and 104 of MyoD have been shown to be acetylated (Polesskaya et al. 2000), and a mutant form of MyoD that cannot be acetylated at these residues is impaired in its transcriptional and myogenic conversion abilities (Sartorelli et al. 1999), which is the same effect on MyoD that we have observed by NFATc1. Interestingly, lysines 99, 102,

104 are all within, or immediately adjacent to, the N-terminal TAD of MyoD which includes amino acids 1-101. Therefore, it is possible that NFATc1 might be competing with p300/CBP for binding to MyoD, or sterically blocking these critical lysine residues, thereby preventing MyoD acetylation. In preliminary co-immunoprecipitation experiments using transfected C3H10T1/2 cells, we found that the physical interaction of MyoD and p300/CBP does not occur in the presence of NFATc1. These results suggest that NFATc1 may be competing with p300/CBP for binding to MyoD. This result supports our finding that NFATc1 inhibits MyoD transcriptional activity and provides further mechanistic detail for how inhibition might occur. It may also be of interest to determine whether MyoD protein itself is hypoacetylated in the presence of NFATc1, given our finding that NFATc1 may prevent interaction of MyoD with p300/CBP. Lastly, it might be interesting to examine histone modifications of MyoD target genes in the presence of NFATc1 and see if they are hypoacetylated.

The differential roles of NFAT proteins in skeletal muscle

During late embryogenesis and early postnatal growth, slow fiber expression is under the control of a developmental program that is independent of calcineurin (Swoap et al. 2000; Oh et al. 2005). We have shown that *nfatc1*$^{SkM\text{-}KO}$ mice have fewer slow twitch fibers both before and after exercise. However, we find it unlikely that NFATc1 plays a developmental role in fiber type specification. One study demonstrated that NFATc1, but not NFATc3, shuttles between the cytoplasm and nuclei in resting, unstimulated muscle fibers. This nucleocytoplasmic shuttling was not altered by either calcineurin or the kinases GSK, PKA, and CK1, which strongly influence NFATc1 nuclear translocation in response to electrical stimulation (Shen et al. 2006). This raised the possibility that even

though calcineurin does not appear to be involved in the development of fiber type (Swoap et al. 2000; Oh et al. 2005), NFATc1 may still be able to translocate to the nucleus in unstimulated developing fibers and play a role in establishing fiber type. Therefore, we looked for NFATc1 expression in the developing mouse embryo. However, we did not observe NFATc1 protein expression in skeletal muscle at any developmental stages examined, including E12.5, E14.5, E16.5, and E18.5 (data not shown). This suggests that signaling pathways besides calcineurin/NFAT likely act to first establish fiber type during embryonic development. The role of NFATc1 may be more important for fiber type maintenance in the adult muscle, and regulating fiber type plasticity in response to both nerve activity and physical demand. In addition, NFATc1 negative regulation of MyoD is perhaps functioning only in adult muscle fibers that are already specified as either fast or slow, in order to maintain the slow fiber phenotype or regulate fast to slow fiber type switching. This could be examined in more detail in future studies. Perhaps examining muscle from control and *nfatc1*$^{SkM\text{-}KO}$ mice at an early postnatal timepoint during the initial establishment of fiber type when innervation is beginning might reveal an initially normal balance of fast and slow fibers, and that over time, slow fibers may not maintained due to loss of NFATc1. Alternatively, if there are fewer slow fibers in *nfatc1*$^{SkM\text{-}KO}$ mice after the first few post-natal weeks, this would suggest NFATc1 plays a role in the early establishment of muscle fibers in response to the first differential patterns of motor neuron activity that differ between fast and slow muscle fibers. In preliminary immunofluorescence experiments, NFATc1 expression was observed at P0 in skeletal muscles of the hindlimb and forelimb of wild type mice,

suggesting it may indeed play a role in establishing fiber type at these critical early timepoints.

Our studies, taken together with studies of other *nfat* gene knockout mice seem to suggest that different NFAT isoforms have unique functions in skeletal muscle (Horsley et al. 2001; Kegley et al. 2001). Here, we show that NFATc1 potently inhibits MyoD activity. In contrast to our observations with NFATc1, previous studies have suggested that NFATc3 promotes myogenesis via positive regulation of MyoD activity (Aramburu et al. 1999; Delling et al. 2000; Kegley et al. 2001). Delling et al reported that NFATc3 promotes the differentiation of C3H10T1/2 fibroblasts into myotubes *in vitro* when co-transfected with MyoD (Delling et al. 2000), and NFATc3 was shown to synergize with MyoD to cooperatively activate the *myogenin* promoter (Armand et al. 2008). Interestingly, both NFATc3 (Armand et al. 2008) and NFATc1 physically interact with MyoD, but only NFATc1 represses MyoD activity. Although we did not observe repression of MyoD activity on the *myogenin* promoter by NFATc3, we also did not observe any cooperative activation of the *myogenin* promoter by NFATc3 and MyoD in transactivation assays. Taken together, these observations suggest the possibility that physical interaction of MyoD with NFATc1 versus NFATc3 results in the recruitment of distinct co-activators and co-repressors that determine the effect on MyoD activity and the pattern of muscle-specific gene expression. Additionally, NFAT proteins contain several phosphorylation sites within the highly conserved CAT domain, and different kinases phosphorylate various NFAT family members, allowing for an added layer of isoform specific regulation of NFAT proteins. In addition to regulation by kinases, NFATc1, but not NFATc3, displays activity and calcineurin-independent nuclear

shuttling in adult skeletal muscle fibers (Shen et al. 2006). Post-translational modifications are another important layer of NFAT protein regulation and can affect nuclear/cytoplasmic shuttling or interactions with other proteins. It would be of interest to see what nuclear shuttling mechanisms, post-translational modifications, and co-factor interactions may result in differential regulation of these two NFAT isoforms in order to positive or negatively MyoD activity.

NFATc1 and muscle regeneration

While we highlight the importance of NFATc1 repression of MyoD in the context of fiber type in this study, there are several other functions of MyoD that may be regulated by NFATc1, which may be of interest in future studies. One interesting observation that was not thoroughly followed up on in this study is the effect of exercise on muscle from *nfatc1*$^{SkM\text{-}KO}$ mice. There is a low level of muscle regeneration that occurs in response to exercise in wild type mice. However, from histological analysis of exercised muscle from *nfatc1*$^{SkM\text{-}KO}$ mice, there appears to be a much higher prevalence of muscle regeneration as identified by centrally located nuclei within individual muscle fibers (Fig. 15). Although the number of regenerating fibers was never quantified, it was common to identify muscle from conditional knockout mice merely based on the vast number of regenerating fibers. Regeneration was not seen throughout the entire length of the muscle, but was still quite extensive in *nfatc1*$^{SkM\text{-}KO}$ mice. It would be interesting to see if NFATc1 is expressed in adult satellite cells, and whether it co-localizes with MyoD in

this cell population. MyoD is expressed in activated satellite cells prior to the onset of cell cycle withdrawal and terminal differentiation (Charge and Rudnicki 2004; Zammit et al. 2006). It may be possible that NFATc1 represses MyoD following activation of satellite cells in order to prevent precocious differentiation by fine-tuning the timing of MyoD-mediated cell cycle withdrawal. Indeed, several groups have demonstrated that satellite cell-derived primary myoblasts isolated from adult *MyoD*-null mice display an accelerated growth rate and delayed terminal differentiation (Sabourin et al. 1999; Yablonka-Reuveni et al. 1999; Cornelison et al. 2000; Huijbregts et al. 2001; Asakura et al. 2007). Therefore, *MyoD*-null myoblasts have been suggested to display characteristics that are more primitive than wild-type myoblasts and may represent an intermediate stage between stem and myogenic precursor cells.

Alternatively, it is possible that the apparent increase in regenerating fibers in $nfatc1^{SkM\text{-}KO}$ mice is due to a functional or structural defect in the fibers themselves, causing them to be more prone to damage or injury. Therefore, it might be interesting to determine if the muscle from $nfatc1^{SkM\text{-}KO}$ mice is damaged following exercise by performing immunohistochemistry for fibrosis, such as the Masson's Trichrome stain.

Fiber type and Disease

There are several diseases that have been suggested to involve skeletal muscle fiber type composition. Sarcopenia is the age-related gradual loss of muscle mass, strength and function (Waters et al. 2000; Vandervoot and Symons 2001; Evans 2010; Verdijk et al. 2010), and is characterized by a reduction in the number and size of muscle fibers (Porter et al. 1995). Slow Type I fiber size remains relatively constant with age,

whereas fast Type II muscle fiber size diminishes (Houmard et al. 1998; Short et al. 2005; Koopman et al. 2006; Stellingwerff et al. 2007; Verdijk et al. 2007). The reduction in muscle mass, also known as atrophy, that occurs in fast Type II muscle fibers during sarcopenia is believed to play a major role in the pathogenesis of frailty and functional impairment that occurs with old age or extended bedrest (Morley et al. 2001; Kim et al. 2005; Evans 2010). Interestingly, basal MRF mRNA expression increases in proportion to the degress of sarcopenia in senescent muscle (Hameed et al. 2003; Luquet et al. 2003; Edstrom and Ulfhake 2005; Kim et al. 2005; Kosek et al. 2006; Raue et al. 2006). These findings, in combination with our results that NFATc1 promotes the slow fiber phenotype and that *nfatc1*$^{SkM\text{-}KO}$ mice have increased MRF mRNA expression, suggest that NFATc1 might play a role in regulating fiber type and MyoD in aging muscle. Due to its role as a repressor of MyoD activity, and a regulator of fast-to-slow fiber type switching, NFATc1 and its upstream and downstream regulatory pathways might represent interesting therapeutic targets for afflictions that differentially affect slow Type I versus fast Type II fibers such as muscle atrophy and sarcopenia.

Given that *nfatc1*$^{SkM\text{-}KO}$ mice have a reduced number of Type I muscle fibers, it would be of interest to examine these mice in more phenotypic and physiological detail. For instance, rats put on high-fat diets that gained the most weight were found to possess fewer type I fibers (Abou Mrad et al. 1992), and skeletal muscle from obese or type 2 diabetic humans, has been observed to have reduced oxidative capacity and fewer type I fibers (Lillioja et al. 1987; Hickey et al. 1995; Tanner et al. 2002). It would be interesting to see if *nfatc1*$^{SkM\text{-}KO}$ mice gain more weight with age, and whether the muscle has a reduced oxidative capacity. Furthermore, a predominance of Type I fibers has been

shown to enhance insulin-mediated glucose uptake, protect against glucose intolerance, and reduce adipocyte size (Luquet et al. 2003; Ryder et al. 2003; Oberbach et al. 2006). Given these observations, it is possible that insulin-mediated glucose uptake, glucose intolerance, and adipocyte size might also be altered in *nfatc1*$^{SkM\text{-}KO}$ mice.

In conclusion, these studies reveal a novel role for NFATc1 as an inhibitor of MyoD activity and establish NFATc1 as an important factor in controlling the balance between fast and slow fibers in adult skeletal muscle. Understanding the regulatory pathways that control fiber type specialization and conversion of these myofiber types is of potential benefit to both healthy individuals engaged in exercise training and patients challenged by various myopathies or physical inactivity.

Chapter 4: Materials and Methods

Knockout and transgenic mice

Mef2c-73k-Cre and *nfatc1*$^{flox/flox}$ mice have been described previously (Heidt and Black 2005; Aliprantis et al. 2008). Briefly, a targeting vector containing exon 3 of *nfatc1* and a neomycin resistance cassette, both flanked by loxP sites, was generated using standard gene targeting approaches (Aliprantis et al. 2008). Exon 3 encodes the regulatory domain of NFATc1. Cre-mediated recombination of the loxP sites results in the delta allele (Δ). To generate *nfatc1*$^{+/\Delta}$ mice, male *nfatc1*$^{flox/flox}$ mice were crossed to *Mef2c*-AHF-Cre (Verzi et al. 2005) female mice to convert the *nfatc1*^{flox} allele to the *nfatc1*$^{\Delta}$ allele. When crossed from the female, *Mef2c*-AHF-Cre functions as a universal deleter line, resulting in Cre-dependent recombination in all cells, including the germline, in all offspring (data not shown). To generate *nfatc1*$^{SkM\text{-}KO}$ mice, male *Mef2c*-73k-Cre; *nfatc1*$^{+/\Delta}$ mice were crossed to female *nfatc1*$^{flox/flox}$ mice.

For transgenic mice, transgenic reporter constructs were digested away from the HSP68-*lacZ* plasmid backbone, gel purified, and resuspended in 5mM Tris-HCl, 0.2mM EDTA (pH 7.4) at a concentration of 2ng/ml for pronuclear injection. Injected embryos were implanted into pseudopregnant CD-1 females, and embryos were collected at indicated developmental stages for transient analyses. The presence of the *lacZ* transgene was detected by Southern blot or PCR as described below. β-galactosidase expression from *lacZ* transgenic embryos was detected by X-gal staining. In brief, embryos were fixed in 2% paraformaldehyde, 0.2% glutaraldehyde in 1X phosphate buffered saline (PBS) at 4°C for 30 min to 2 hours, depending on the age of the embryo. Embryos were

rinsed twice in 1X PBS and stained for β-galactosidase overnight in the dark at room temperature in PBS containing 5mM $K_4Fe(CN)_6$, 5mM $K_3Fe(CN)_6$, 2mM MgCl2, 1mg/ml 5-bromo-4-chloro-3-indolyl β-D-galactopyranoside (X-gal). Following staining, embryos were rinsed twice in 1X PBS and post-fixed in 4% paraformaldehyde overnight at 4°C.

Genotyping

Genotyping was performed on tail biopsies digested in 500µl of tail prep buffer (100mM NaCl, 25mM EDTA pH8.0, 1% SDS, 10mM Tris-HCl pH 8.0, and 15µl of 20mg/ml stock of proteinase K). Genomic DNA was recovered by phenol-chloroform extraction and ethanol precipitation. Genotyping was performed by Southern blot using standard methods, or by PCR on genomic tail DNA. Mice containing a *Cre* transgene were identified by digestion of purified genomic DNA with EcoRV at 37°C overnight, and then Southern blotting using a radiolabeled *Cre* probe. The *Cre* probe was generated by purifying an NcoI-BamHI fragment from the plasmid pBS-*Cre*. *LacZ* transgenes were identified by digestion of genomic DNA with EcoRV overnight at 37°C, and then Southern blotting with a radiolabeled *lacZ* probe. The *lacZ* probe was generated by purifying an EcoRI fragment from pCR2.1-TOPO-*lacZ*. In cases where PCR genotyping was utilized, the following primers, reactions, and PCR programs were used:

***nfatc1* allele** (3 primer PCR reaction detects wild-type allele at 375bp, floxed allele at 425bp, and delta allele at ~500bp.)

INT2-S5-(A) 5'- AAGGAATTACTGGGAAGCCTGGCA- 3'

INT3-S2-(B) 5'- AGGGACTATCATTTGGCAGGGACA- 3'

INT3-AS2-(C) 5'- ACAGGAAACAGCTCTGTTCCACAC- 3'

The PCR reaction used for *nfatc1* allele genotyping is 1µl genomic tail DNA, 5µl 10X standard Taq buffer (NEB), 2µl 10mM dNTPs, 2µl 25mM $MgCl_2$, 1µl each of 25ng/µl primers INT2-S5-(A), INT3-S2-(B), INT3-AS2-(C), 36µl ddH_2O, 1µl Taq DNA polymerase (All Star). The PCR program used for *nfatc1* allele genotyping is 94°C 5 minutes, followed by 30 cycles of 94°C 1min, 66°C 1min, 72°C 1min, followed by 72°C 10 minutes.

***Cre* allele**

Cre1(JH)-geno 5'- CCTGTTTTGCACGTTCACCG- 3'

Cre3(JH)-geno 5'- ATGCTTCTGTCCGTTTGCCG- 3'

The PCR reaction used for *Cre* allele genotyping was performed using reagents from the Taq PCR Core Kit (Qiagen). The reaction used is 1µl genomic tail DNA, 2µl 10X Taq buffer, 1 µl 2.5mM dNTPs, 0.5µl each of 40µM stock primers Cre1(JH)-geno and Cre3(JH)-geno, 4µl Q solution, 11µl ddH_2O, 0.1µl Taq DNA polymerase (Qiagen). The PCR program used for *Cre* allele genotyping is 95°C 5 minutes, followed by 30 cycles of 95°C 30 seconds, 60°C 30 seconds, 72°C 30 seconds, followed by 72°C 7 minutes. PCR product size is approximately 275bp.

***LacZ* allele**

LacZTag1 5'- TTTAACGCCGTGCGCTGTTCG- 3'

LacZTag2 5'- ATCCAGCGATACAGCGCGTCG- 3'

The PCR reaction used for *LacZ* allele genotyping was done using reagents from the Taq PCR Core Kit (Qiagen). The reaction used is 1µl genomic tail DNA, 2µl 10X Taq buffer, 1 µl 2.5mM dNTPs, 0.5µl each of 40µM stock primers LacZTag1 and LacZTag2, 4µl Q

solution, 11µl ddH_2O, 0.1µl Taq DNA polymerase (Qiagen). The PCR program used for *LacZ* allele genotyping is 94°C 3 minutes, followed by 10 cycles of 94°C 30 seconds, 67°C 45 seconds, 57°C for 45 seconds, 72°C 45 seconds, followed by 26 cycles of 94°C 30 seconds, 57°C 45 seconds, 72°C 45 seconds, followed by 72°C 5 minutes. PCR product size is approximately 200bp. The 73K-*LacZ* allele was the only *lacZ* allele genotyped using this method. Southern blotting was usually used for 73K-*LacZ* genotyping. NFAT site mutants were genotyped by Southern blotting as well.

Plasmids and mutagenesis

The following plasmids were used in transfection, and were previously described as indicated: *Mef2c*-73K AUG/Bgal (Dodou et al. 2003), *Myogenin*184 pGL3-Luc (Heidt et al. 2007), MRF4 promoter (Black et al. 1995) and subcloned into vector AUG/Bgal, pG5-E1b-Luc (Heidt et al. 2007), MyoD pRK5 (Heidt et al. 2007), E12-bHLH-pSG424 (Verzi et al. 2002), MyoD-bHLH-VP16 pRK5 (Verzi et al. 2002). NFATc1 and NFATc3 cDNA were kindly provided by JD Molkentein and subcloned into pRK5. PCR amplification of NFATc1-pRK5 human cDNA or MyoD-pRK5 mouse cDNA was used to make all truncation mutants using primer sets as listed with specific plasmid descriptions below. All PCR cloning was performed with the High Fidelity PCR System (Roche) according to manufacturer's instructions.

Plasmids

pRK5 flag

Oligos pRK5 flag-S 5'- CGATATGGACTACAAAGACGATGACGATAAAATCG

ATGGATCCGAATTCTGCAGATATCCATGGCGGCCGCTCGAGCATGCAT-3' and pRK5 flag-AS 5'- CTAGATGCATGCTCGAGCGGCCGCCATGGATATCTGCAGA ATTCGGATCCATCGATTTTATCGTCATCGTCTTTGTAGTCCATAT-3' were annealed and ligated into pRK5 cut with ClaI/XbaI.

2X Gal4 E1b-pGL3 basic

Plasmid pGL3 basic, which contains no SV40 promoter or SV40 enhancer, was digested with NheI and XhoI, then ligated with the annealed oligos 2×GAL4-F 5′-ctagccggagtactgtcctccgcggagtactgtcctccgagggtatataatgc-3′ and 2×GAL4-R 5′-tcgagcattatataccctcggaggacagtactccgcggaggacagtactccgg-3′. Oligos were annealed by adding 10µl of each oligo to 20µl of annealing buffer (100mM Tris pH 8, 100mM NaCl), and heating in a heat block at 95°C for 10 min and then turning off the heat block and allowing the reaction cool to RT.

1X Gal4 E1b-pGL3 basic

Plasmid pGL3 basic was digested with NheI and XhoI, then ligated with the annealed oligos 1×GAL4-F 5′-ctagccggagtactgtcctccgagggtatataatgc-3′ and 1×GAL4-R 5′-tcgagcattatataccctcggaggacagtactccgg-3′. Oligos were annealed as described for the plasmid 2X Gal4 E1b-pGL3 basic.

73K 3' end AUG/ß-gal

A 216bp fragment, starting at nucleotide -106 relative to the transcriptional start site of the 73K *mef2c* enhancer, was amplified by PCR from plasmid template 73K pBluescript

using a 5' primer containing a BamHI site. The amplicon was digested with BamHI and ligated into the BamHI site of the AUG/ß-gal vector. Primers used were 73K BamHI-F 5'-GGTCTGGTTGTCAAGGATCCCTTTACAG- 3' and T7.

NFATc1 (1-106) PCS2+MT

Residues 1-106 of human NFATc1 cDNA were amplified as a XhoI/XbaI PCR fragment and ligated into vector pCS2+MT (contains a 6X-myc tag) cut with XhoI/XbaI. The 6X myc tag is at the N-terminus. An in-frame stop codon is within the 3' XbaI cloning site. The PCR primers used were c1(1-106)F 5'-GCCATACTCGAGATGCCAAGCACCAGC- 3' and c1(1-106)R 5'- GCAATCTAGACGTGGCCGGAGGAGAGG- 3'.

NFATc1 (1-106) pRK5 Flag

A 318bp fragment corresponding to amino acids 1-106 of human NFATc1 was cut from construct NFATc1 (1-106) pCS2+MT with XhoI/XbaI and subcloned into pRK5 Flag cut with XhoI/XbaI.

NFATc1 (107-424) PCS2+MT

Residues 107-424 (CAT domain) of human NFATc1 cDNA were amplified as a XhoI/XbaI PCR fragment and ligated into vector pCS2+MT (contains a 6X-myc tag) cut with XhoI/XbaI. These residues encode the NFATc1 CAT domain. The 6X myc tag is at the N-terminus. An ATG was included before amino acid 107 and an in-frame stop codon is within the 3' XbaI cloning site. The PCR primers used were: c1(107-424)F 5'-

GCCATACTCGAGATGACCAGGCCTGATGG- 3' and c1(107-424)R 5'-GCAATCTAGACCGGGCCTGAGTGGGAC- 3'.

NFATc1 (107-424) pRK5 Flag

A 951bp fragment corresponding to amino acids 107-424 of human NFATc1 was cut from construct NFATc1 (107-424) pCS2+MT with XhoI/XbaI and subcloned into pRK5 Flag cut with XhoI/XbaI.

NFATc1 (425-694) PCS2+MT

Residues 425-694 (Rel/DBD domain) of human NFATc1 cDNA were amplified as a XhoI/XbaI PCR fragment and ligated into vector pCS2+MT (contains a 6X-myc tag) cut with XhoI/XbaI. These residues encode the NFATc1 Rel/DBD domain. The 6X myc tag is at the N-terminus. An ATG was included before amino acid 425 and an in-frame stop codon is within the 3' XbaI cloning site. The PCR primers used were c1(425-694)F 5'- CGGTTACTCGAGATGTATGAGCTTCGGATTG- 3' and c1(425-694)R 5'-GGCAATCTAGACGGGAAGGTAGGTGAAAC- 3'.

NFATc1 (425-694) pRK5 Flag

Construct NFATc1 pRK5 was used as a PCR template with primers c1(425-694)F and c1(425-694)R. An 807bp PCR fragment corresponding to amino acids 425-694 of human NFATc1 was cut with XhoI and XbaI (sites engineered within PCR primers) and the corresponding insert was cloned into XhoI/XbaI cut pRK5 Flag. See NFATc1 (425-694) PCS2+MT details for PCR primer sequences.

NFATc1 (FL) PCS2+MT

Full length human NFATc1 cDNA was cloned as a XhoI/XbaI PCR fragment and ligated into vector pCS2+MT (contains a 6X-myc tag) cut with XhoI/XbaI. The 6X myc tag is at the N-terminus. An in-frame stop codon is within the 3' XbaI cloning site. PCR primers used were c1(1-106)F (see above for sequence) and c1(FL)R
5'- GCAATCTAGACGAAAAAGCACCCCACGCG- 3'.

NFATc1 (FL) pRK5 Flag

A 2400bp fragment corresponding to full length human NFATc1 was cut from construct NFATc1 (FL) pCS2+MT with XhoI/XbaI and subcloned into pRK5 Flag cut with XhoI/XbaI.

NFATc1 pRK5

A 2400bp fragment corresponding to full length human NFATc1 cDNA (kindly provided by JD Molkentein) was generated as an EcoRI/HindIII partial digest and subcloned into pRK5 cut with EcoRI/HindIII. This clone was made by Dr. Analeah Heidt.

MyoD (1-101) pRK5 flag

A 316bp fragment corresponding to amino acids 1-101 of mouse MyoD was amplified from construct MyoD pRK5 and the PCR product was digested with XhoI/XbaI, then subcloned into pRK5 Flag cut with XhoI/XbaI. Primers used for amplification of this fragment were MyoD (1-101)F-Xho, 5'- gcgcttctcgagatggagcttctatcgccg -3' and MyoD

(1-101)R-Xba, 5'- gcaatctagacgcacgccttgcaggccc -3'. An in-frame stop codon is embedded within the 3' XbaI cloning site.

MyoD (1-101) PCS2+MT

Plasmid MyoD (1-101) pRK5 Flag was cut with XhoI/XbaI to release 316bp fragment containing the first 101 amino acids of mouse MyoD cDNA. Vector PCS2+MT (contains 6X myc tag) was digested with XhoI/XbaI and ligated with the MyoD (1-101) fragment.

MyoD (N-term) pSG424

The plasmid MyoD (1-101) pRK5 flag was used as a PCR template with the primers myoDNtermMfeI_for, 5'- gcaattgatggagcttctatcgccgcc- 3' and myoDNtermEcoRI_rev, 5'- ggaattcgcacgccttgcaggcc-3'. The PCR product was digested with MfeI/EcoRI and ligated into the vector pSG424 that was digested with EcoRI. This construct was cloned by Dr. Barbara Celona.

MyoD ΔTAD pRK5 Flag

This construct is mouse MyoD cDNA with a deletion of amino acids 1-101, which correspond to the N-terminal transactivation domain (TAD) of MyoD. The start codon comes from the Flag tag. Plasmid MyoD pRK5 was used as a PCR template with the primers MyoD dTAD-5', 5'-gcaagaattcaagcgcaagaccacc-3' and MyoD dTAD-3', 5'-gcaagaattctcaaagcacctgata-3'. The 650bp PCR product was digested with EcoRI and then ligated into the plasmid pRK5 Flag digested with EcoRI.

MyoD ΔCterm pRK5 Flag

This construct is mouse MyoD cDNA with a deletion of amino acids 167-318, which correspond to the C-terminal domain of MyoD. Plasmid MyoD pRK5 was used as a PCR template with the primers MyoD dCterm-5', 5'- gcaagaattcgagcttctatcgccg-3' and MyoD ΔCterm-3', 5'- gcaagaattctcagtcgcgcagcagag-3'. The 498bp PCR product was digested with EcoRI and then ligated into the plasmid pRK5 Flag digested with EcoRI. An in-frame stop codon was included in the MyoD ΔCterm-3' primer.

MyoD ΔC/H pRK5 Flag

The plasmid MyoD (FL) pRK5 Flag was used as a PCR template for the deletion of C/H region of MyoD, corresponding to amino acids 63-99. The primers used were MyoDdC/H-1 5'- ccggaggagcacgcgggtcgctgc-3' and MyoDdC/H-2 5'- gcagcgacccgcgtgctcctccgg-3'. Mutation was made using the Quik Change Mutagenesis kit (Agilent Technologies).

NFATc3 pRK5

Plasmid NFATc3 pME (obtained from J. Molkentin) was used as a PCR template to subclone human NFATc3 into pRK5. The primers used were c3EcoRI-5', 5'- gctctaaaagctgcggaattcgcgg-3' and c3HindIII-3', 5' ggctgcagtaagctttgttagagcc-3'. The 3.2kB PCR product was digested with EcoRI/HindIII and subcloned into pRK5 digested with EcoRI/HindIII.

CA-NFATc1 pRK5

This construct contains a 2100bp fragment of constitutively active (CA), full length NFATc1 from the mouse, containing multiple serine to alanine mutations in the SRR and SPXX repeat motifs in the NFATc1 regulatory domain. The plasmid CA-NFAT2 pRV (which is NFATc1) was obtained from Addgene (made in the lab of Anjana Rao). This plasmid was digested with XhoI, then ligated into pRK5 Flag cut with XhoI. Next, CA-NFATc1 pRK5 Flag was cut with EcoRI and HindIII and cloned into pRK5 cut with EcoRI/HindIII.

***Mef2c*-73K mNFAT (2,4,5) AUG/ß-gal**

To clone the *mef2c*-73K mutant constructs for the generation of transgenic mice and for use in *in vitro* assays, the *mef2c*-73K pBluescript II SK construct was used as the original template in SOEing PCR reactions (Horton) with T7, T3, the mutagenic primers listed below and their reverse complements. The PCR products were digested with NotI/SpeI and the mutated fragment was subcloned into AUG/ß-gal digested with NotI/SpeI. Once one mutation was verified by sequencing, this construct was used as the template for subsequent mutations. Primers used were 73K-NFAT(2)mA: (made by Analeah Heidt) 5'- GGGCCGATTGGATATTAAGGATTGGA-3', mNFAT(4)Arm2-F: 5'-gctatgcccccattaaaaagtttccagcc- 3', mNFAT (5)Arm2F: 5'-cattaaaaagccccagccacaattaattg-3'.

Electrophoretic mobility shift assays

To radioactively label probes encompassing potential binding sites,

oligonucleotides were designed to include a consensus-binding site flanked by 10-15 base pairs and 5'-gg-3' nucleotides at the 5' end on the positive and negative strands. Oligonucleotides were annealed by mixing 5µg of each strand with 2X annealing buffer (100mM Tris pH 7.6, 10mM DTT, 20mM MgCl2, 2mM Spermidine), incubating at 95°C for 10 minutes, and then allowing the reaction to cool to room temperature. 2µg of double-stranded oligonucleotides were labeled with ^{32}P-dCTP using Klenow to fill in overhanging 5' ends and purified on a non-denaturing polyacrylamide-TBE gel. Labeled probe was purified from the gel and resuspended in 40mM KCl and incubated in a 37°C water bath overnight. Recombinant protein was generated using an expression vector containing cDNA, which was transcribed and translated using the TNT QuickCoupled Transcription/Translation System (Promega).

For EMSA experiments used to test MyoD/E12 heterodimerization and E box binding, addition of protein to each EMSA was normalized by quantitation of [^{35}S]methionine-labeled proteins generated in parallel reactions. Quantitation was conducted by phosphorimager analysis using ImageQuant v. 1.2 software (Molecular Dynamics). After protein quantification, recombinant NFATc1 protein made from NFATc1 (Rel) pCITE2B was added in increasing amounts, ranging from 0.3X to 10X the amount of E12 and MyoD, which were added in a 1:1 ratio as determined by ^{35}S-methionine incorporation. The vectors used for generating protein are listed below (Table 1) with references and the specific polymerase used in TNT reactions. Also listed are the control and mutant probes. The control probes for MyoD and E12 are an E-box element from the *mef2c* skeletal muscle enhancer (Dodou et al. 2003), and the NFAT control probe is from an IL4 enhancer.

Table 1: Expression vectors and control probes for EMSA

Expression Vector	Enzyme	Control Probes
MyoD pRK5 Flag	SP6	Control: 5'-gggagtgacatgaacaggtgcaccctggcctg-3' Mutant: 5'-gggagtgacatgaattcgtgcaccctggcctg-3' (Dodou et al 2003)
E12 pCITE2A	T7	Control: 5'-gggagtgacatgaacaggtgcaccctggcctg-3' Mutant: 5'-gagtgacatgaattcgtgcaccctggcctg-3' (Dodou et al 2003)
NFATc1 (Rel) pCITE2B	T7	IL4 Control: 5'-gggtacattggaaaattttattacac-3' IL4 Mutant: 5'- gggtacattccttattttattacac- 3'
NFATc1 pRK5	SP6	IL4 Control: 5'-gggtacattggaaaattttattacac-3' IL4 Mutant: 5'- gggtacattccttattttattacac- 3'

DNA binding reactions were preincubated at room temperature for 10 min prior to probe addition in 1X binding buffer (40 mM KCl, 15 mM HEPES pH 7.9, 1 mM EDTA, 0.5 mM DTT, 5% glycerol) containing 2-5µl of recombinant protein lysate (NFATc1) or unprogrammed lysate, 1 mg of poly dI–dC, and 1-2µg of competitor DNA (100 fold excess). For dimerization shifts, a total of 6µl of lysate was used per reaction, with unprogrammed lysate used to make up the 6µl total volume of lysate as needed for each reaction. Radioactively labeled probe was added to each reaction, which were then incubated an additional 20 min at room temperature. Reactions were electrophoresed on a 6% non-denaturing polyacrylamide gel at 150V for 2-3 hours at room temperature. Gels were then vacuum-dried and exposed to film. The sense strand sequences of the oligonucleotides used for EMSA of the putative NFAT sites in the *mef2c* skeletal muscle enhancer are shown in Table 2.

Table 2: List of *mef2c* enhancer probes

(Name is listed as it appears on the oligo tube; sense strand only is shown.)

WT-NFAT(1)-F	5'- gggtgaaatgaggaaacttaac- 3'
73K-NFAT(2)-A	5'- gggccgattggatattttccattgga- 3'
WT-NFAT(3)-F	5'- gggattattcttggaaatgtaatt- 3'
WT-NFAT(4)-F	5'- gggtgtgctatgtttccattaaa- 3'
WT-NFAT(5)-F	5'- ggttaaaaagtttccagccac- 3'

Cell culture and transfections

C2C12 cells were maintained in Dulbecco modified Eagle medium (DMEM) supplemented with 1% L-glutamine, 1% penicillin-streptomycin and 15% fetal bovine serum. The day prior to transfection, cells were split into 12-well cell culture plates at a density of (4×10^4) cells/well. The following day, C2C12 were transfected. Transfection reactions contained 1.6µg of total plasmid DNA, 50µl of DMEM serum free media, and 4µl of Fugene 6 transfection reagent (Roche) per well.

C3H10T1/2 cells were maintained in Dulbecco modified Eagle medium (DMEM) supplemented with 1% L-glutamine, 1% penicillin-streptomycin and 10% fetal bovine serum. The day prior to transfection, cells were split into 12-well cell culture plates at a density of (4×10^4) cells/well. The following day, C3H10T1/2 were transfected. Transfection reactions contained 1.6µg of total plasmid DNA, 300µl of Opti-MEM, and 4µl of Lipofectamine LTX reagent (Invitrogen) per well. For all transfections, reactions were incubated at room temperature for 30 min and then added to cells with fresh media. For all transfection experiments involving reporter constructs, cells were switched to DMEM with 2% horse serum (differentiation media) 16 h post-transfection and allowed to differentiate for an additional 24-36 h prior to harvesting. All transfections lacking an

expression plasmid contained an equal amount of parental expression vector such that each transfection had an equivalent amount of plasmid DNA.

Transactivation and reporter assays

For transactivation and reporter assays, transfected cells were harvested 24-36 hours after transfection. First, cells were washed 2X in cold PBS, and collected by scraping in 1ml of 1X PBS. Lysates were centrifuged at full speed for 2 minutes to pellet cells. Cell pellets were resuspended in 50µl of 0.1M $NaPO_4$. Cells were lysed by freeze/thaw, alternating 3 times between a 37°C water bath and liquid nitrogen, each for 1 minute. After 3 freeze/thaw cycles, cells were pelleted by centrifugation. 25µl of cellular extract was assayed for β-galactosidase using the Luminescent β-gal kit (Clontech) or for luciferase activity using the Luciferase Assay Reagent (Promega). For β-galactosidase assays, 2µl of substrate was mixed with 98µl of buffer from the Luminescent β-gal kit (Clontech), and added to 25µl of cellular lysate from each sample. Reactions were incubated in the dark for 1 h at room temperature in an opaque 96-well plate, and then relative light units were detected using a GloMax MultiDetection microplate luminometer (Promega). For luciferase assays, 25µl of cell lysate was mixed with 75µl of luciferase reagent from the Luciferase Assay Reagent (Promega), in an opaque 96-well plate, and relative light units were detected immediately using a GloMax MultiDetection microplate luminometer (Promega). Samples were normalized by total protein concentration using the Bradford assay with protein assay dye reagent (Bio-Rad).

Myogenic conversion assays

For myotube conversion assays, C3H10T1/2 cells were split the day before transfection at a density of 10^5 cells per well in 6-well cell culture plates. The following day, cells were transfected with either empty expression plasmid, MyoD-pRK5 only, or MyoD-pRK5 and NFATc1-pRK5. Transfections were done using 3µg of total plasmid DNA per well in 600µl of Opti-MEM and 7µl of Lipofectamine LTX reagent (Invitrogen). For the MyoD only transfection, 1.5µg of MyoD-pRK5 and 1.5µg of empty pRK5 expression plasmid were used. For the MyoD and NFATc1 co-transfection, 1.5µg of MyoD-pRK5 and 1.5µg of NFATc1-pRK5 expression plasmids were used. Transfection reactions were incubated at room temperature for 30 minutes and then added to cells in a dropwise fashion, with each well containing 2ml of fresh growth media (10% FBS, 1% P/S, 1% L-glutamine). The following morning, cells were switched to differentiation media (2% horse serum, 1% P/S in DMEM), and incubated for an additional 5 days prior to harvesting. Everyday for the 5 days the cells were in differentiation media, 1ml of media was removed from each well and replaced with 1ml of fresh differentiation media. After 5 days in differentiation medium, transfected C3H10T1/2 were washed in ice cold PBS, and lysed in 300µl cracking lysis buffer (835 mM sucrose, 1.7% SDS, 170 mM Tris [pH 8.8]), including protease inhibitor cocktail (Complete, Roche) and 10mM DTT, both added right before use. Cells were scraped from the wells and collected in Eppendorf tubes. Lysates were then sheared extensively through an 18g needle and then heated for 10 min at 95°C. Next, lysates were centrifuged at full speed for 5 minutes at 4°C to pellet cellular debris and then transferred to a fresh Eppendorf tube. Lysates were used in subsequent western blotting experiments.

Co-immunoprecipitation assays and western blots

Cellular lysates from cultured cells were collected for western blotting as described above. For tissue lysates, soleus or gastrocnemius muscles were homogenized in RIPA buffer (50mM Tris [pH 7.4], 150mM NaCl, 2mM EDTA, 1% NP-40, 0.1% SDS, protease inhibitor cocktail [Complete, Roche]) and then incubated at 4°C with gentle agitation for 1.5 hours. Lysates were then centrifuged at 14,000 × g for 10-20 min at 4°C to remove cellular debris. SDS sample buffer [50mM Tris [pH 6.8], 2% SDS, 10% glycerol, 0.016% Bromophenol Blue, 100 mM DTT] was added and samples were boiled for 5 min at 95°C and spun down again. Lysates were then subjected to SDS-PAGE and western blotting using standard procedures. Briefly, membranes were incubated in 5% milk in 1X TBST for 1 hour at room temperature to block non-specific antibody binding. Primary antibodies were diluted in 1% milk in 1X TBST, then incubated with membranes for 2 hours at room temperature, or overnight at 4°C. After incubation in primary antibody, membranes were washed 3 times for 5-10 minutes/wash with 1% milk in 1X TBST. Next, secondary antibodies were diluted in 1% milk in 1X TBST, then incubated with membranes for 1 hour at room temperature, followed by 3 washes in 1% milk in 1X TBST, for 5-10 minutes/wash. Signal was detected using an ECL Plus kit according to manufacturer's instructions (Pierce). The following antibodies were used in western blots: mouse anti-myosin fast (MY-32, Sigma, 1:1000), mouse anti-NFATc1 (BD Biosciences 1:250), and mouse anti-β-actin (Sigma, 1:1000) or mouse anti-tubulin (DSHB, 1:500) antibodies were used as loading controls.

For co-immunoprecipitation assays for full length MyoD and NFATc1, C3H10T1/2 cells were transfected with MyoD-pRK5 and NFATc1-pRK5 as described above in 6-well plates. After 36 hours in differentiation media, cells were harvested in 1ml of RIPA buffer/well and lysed in a water bath sonicator for 5 min. Lysates were centrifuged at 14,000 × g for 10 min at 4°C to remove debris, and were then incubated overnight at 4°C with 2µg of rabbit α-MyoD antibody (sc-760, Santa Cruz), or rabbit IgG isotype control. Samples were then incubated with gentle agitation at 4°C for 2 h with 50-100µl of washed Protein G Sepharose bead slurry (Sigma). Bound beads were washed 4 times with RIPA buffer and then boiled for 5 min in SDS sample buffer at 95°C. Lysates were then subjected to SDS-PAGE and western blotting as described above. The antibodies used were mouse α-NFATc1 antibody (clone 7A6, BD Pharmingen, 1:1000) and α-mouse HRP conjugated secondary (A4416, Sigma, 1:5000). Signal was detected using an ECL Plus kit according to manufacturer's instructions (Pierce). For co-immunoprecipitation experiments using Flag tagged NFATc1 truncation mutants, 2µg of rabbit α-MyoD antibody (sc-760, Santa Cruz) was used for the IP and mouse α-Flag (M2, Sigma, 1:1000) antibody was used to detect Flag tagged NFATc1 truncation mutants by immunoblot. The secondary antibody used was α-mouse HRP conjugated secondary (A4416, Sigma, 1:5000).

For co-immunoprecipitation experiments using the MyoD truncation mutants (Flag or myc tagged), cells were transfected in 10cm^2 plates (18µg total DNA, 3600µl OPTI-MEM, 42µl lipofectamine LTX) and switched to differentiation media the following day. After 24 hours in differentiation media, cells were harvested in 1ml/plate of NP40 buffer (20mM Tris pH7.4, 150mM NaCl, 10mM $MgCl_2$, 2mM EDTA, 10%

glycerol, 1% NP40, 1mM DTT). The Immunoprecipitation Dynabeads Protein G kit (Invitrogen) was used for Co-IP. Briefly, 50µl of Protein G Dynabeads were resuspended in 200µl of Ab Binding & Washing Buffer containing 10µg of rabbit α-NFATc1 antibody (SCBT, H-110) and incubated at RT for 20 min. Tubes were placed on magnet and supernatant was removed. Dynabeads-Ab complex was washed by resuspending in 200µl of Ab Binding & Washing Buffer. Next, 1ml of antigen (Ag) containing cell lysate was added to the Dynabeads-Ab complex and incubated at RT for 1.5 hours. Tubes were placed on magnet and supernatant was removed and transferred to a clean tube. The Dynabeads-Ab-Ag complex was washed 3X in 200µl of Washing Buffer and then transferred to a clean tube. The Dynabeads-Ab-Ag complex was resuspended in 100µl of Washing Buffer and transferred to a clean tube. Tubes were placed on magnet and supernatant was removed. The Dynabeads-Ab-Ag complex was resuspended in 40µl of Laemmli buffer (62.5 mM Tris-HCl, pH 6.8, 25% glycerol, 2% SDS, 0.01% Bromophenol Blue) and boiled for 10 min at 90°C. Eluates were collected and loaded onto a 10% SDS-PAGE gel, followed by western blotting with a either a mouse α-Flag (M2, Sigma, 1:1000) or mouse α-myc (Sigma, clone 9E10, 1:1000) antibody.

Immunofluorescence for cell culture and muscle sections

For immunofluorescence of cultured cells, glass coverslips were coated with 0.2% gelatin A (diluted in 1X PBS) for 10-30 minutes, and then washed 2X in PBS prior to plating cells at a density of 10^5 cells/well in a 6 well-plate. For immunostaining, cells were washed twice in 1X PBS and then fixed in 4% paraformaldehyde (diluted in 1X PBS) for 20 minutes at room temperature. Cells were washed twice with 1X PBS and

permeabilized in 0.2% TritonX-100 (diluted in 1X PBS) for 20 minutes at room temperature. Cells were washed 1X in PBS and blocked for 1 hour at room temperature in 3% normal goat serum (NGS). Primary antibodies were diluted in 3% NGS, and incubated with cells overnight at 4°C. The following day, cells were washed 3X in PBS for 5 minutes per wash. Secondary antibody was diluted in 3% NGS and incubated with cells for 1 hour at room temperature, then cells were washed 3X in PBS for 10 minutes per wash. The cover slips containing the stained cells were then removed from the 6-well plate and inverted onto a slide containing 2 drops of Slow-Fade Gold antifade reagent with DAPI (Invitrogen), so that the cell coated side of the cover slip faced down onto the slide, and then cells were imaged on a fluorescence microscope. Antibodies used were mouse anti-myosin fast (MY-32, Sigma, 1:200) and goat anti-mouse Alexa 488 (Molecular Probes, 1:300).

For immunofluorescence of soleus muscle sections, skeletal muscle was dissected and fixed overnight in 0.4% PFA prior to embedding in paraffin. Muscles were sectioned, de-waxed, and boiled in antigen retrieval solution (Biogenex) for 2.5 minutes in a microwave, followed by a 30 second rest. Microwaving and rest step were repeated 2 additional times. Slides were incubated in antigen retrieval solution for 20 minutes at room temperature and then washed in tap water for 5 min. Slides were incubated in blocking solution (3% BSA in 1X PBTX) for 1 h at room temperature. Primary antibodies were diluted in 3%BSA/PBTX, and incubated with cells overnight at 4°C. The following day, cells were washed 3X in PBTX for 5 minutes per wash. Secondary antibody was diluted in 3%BSA/PBTX and incubated with cells for 1 hour at room temperature, then cells were washed 3X in PBTX for 5-10 minutes per wash. Sections were mounted using Slow-Fade Gold antifade reagent with DAPI (Invitrogen) and

imaged on a fluorescence microscope. Antibodies used were mouse anti-myosin fast (MY-32, Sigma, 1:250), mouse anti-myosin slow (Sigma, 1:250) and goat anti-mouse Alexa 594 (Molecular Probes, 1:300).

Immunohistochemistry

Immunoperoxidase staining was performed on sections from muscles fixed O/N in 0.4% PFA, which were then embedded in paraffin. Sections were de-waxed and antigen retrieval (Biogene) was performed as described above. Next, sections were incubated for 30 minutes in 0.3% H_2O_2 (diluted in ddH_2O) in order to block endogenous peroxidase activity. Next, sections were washed for 5 min in PBS and incubated in block solution (3% BSA/PBTX) for 20 min at RT. Sections were then incubated with the following antibodies O/N in a humid chamber at 4°C: rabbit anti-NFATc1 (ab25916, Abcam, 1:150) dilution, rabbit anti-MyoD (M-318, Santa Cruz, 1:50). The following day sections were washed in PBTX for 10 minutes, three times. Then, sections were incubated with biotin-conjugated goat anti-rabbit antibody (Molecular Probes, 1:300) in block solution for 30 min at RT. After incubation with biotinylated antibody and washing in PBTX, slides were incubated for 30 min with streptavidin-HRP by mixing 2 drops of reagent A and 2 drops of reagent B from the Vectastain Elite ABC kit (Vector Laboratories; PK-6102) in 5ml of PBS (This solution needs to be prepared 30 min prior to use, at room temperature). After washing 3 times for 5 min/wash, peroxidase activity was detected with the peroxidase substrate VIP kit (Vector Laboratories; SK-4600), according to the manufacturer's instructions, and then sections were dehydrated per standard procedures prior to mounting with Cytoseal-60 (Richard Allen Scientific).

Immunofluorescence on muscle tissue cryosections was performed as described previously (Heidt and Black 2005), using the following antibodies: mouse anti-slow myosin (M8421, Sigma, 1:250) and mouse anti-fast myosin (MY-32, Sigma, 1:250), followed by Alexa Fluor 594-labeled donkey anti-mouse secondary antibody at a 1:500 dilution. Following incubation with secondary antibody, slides were washed three times in phosphate-buffered saline, mounted using SlowFade antifade with DAPI (Molecular Probes) and photographed on a fluorescence microscope.

Exercise Assays

Voluntary exercise assays were conducted as described previously (Allen et al. 2001) with minor modifications. Briefly, 39-day old male control and male *nfatc1*$^{SkM\text{-}KO}$ mice were housed individually in microisolator rodent cages with a standard metal rodent wheel (11.5 cm in diameter) suspended from two wire arms containing hooks that allowed the wheel to be hung over the edge of the cage. Each running wheel had a magnet super-glued to the wheel, which passes by a bicycle computer attached to one of the wire arms. The bicycle computer (Sigma Sport model BC600 or BC800) was used to record the distance and time run on the wheels from 6:00 pm to 10:00 am for seven consecutive nights, after an initial 3-night training period. Therefore, training began on post-natal day 39, and data was only used from post-natal day 42 to day 49. The computers were calibrated for the diameter of the running wheel prior to use according to the manufacturer's instructions. Plastic dividers were placed between cages in order to eliminate competition between running mice. Twenty-four hours following the 7-night exercise period, mice were weighed and sacrificed, and the hindlimb muscles were

dissected and prepared for subsequent analyses (50 day old mice). The exercise assays were performed under standard light/dark conditions, and mice were provided unlimited access to food and water throughout the course of the experiment. Mice that were used for pre-exercise (no run) comparisons to running mice were housed in a cage containing no wheel for the duration of the experiment and sacrificed at the same age as exercised mice. All experiments using animals were reviewed and approved by the Institutional Animal Care and Use Committee and complied with institutional and federal guidelines.

Metachromatic ATPase fiber type staining

Fiber type determination by metachromatic ATPase staining was performed as previously described (Ogilvie and Feeback 1990). Briefly, soleus muscles from 50-day old male mice were isolated and immediately frozen in OCT embedding medium (Tissue Tek) in a liquid nitrogen cooled, isopentane bath and cryosectioned at a thickness of 10 μm and mounted onto slides. Muscle sections were treated in pre-incubation buffer (50 mM potassium acetate [pH 4.4], 17 mM $CaCl_2$) for 8 min at 25°C in glass Coplin jars, followed by 3 washes in Tris rinse buffer for 2 minutes per wash (300 mM Tris-HCl [pH 7.8], 53 mM $CaCl_2$). Sections were placed lying flat in a humidifying chamber, and then incubated for 25 min at 25°C in incubation buffer (53 mM glycine [pH 9.4], 28 mM $CaCl_2$, 65 mM NaCl, 47.5 mM NaOH, 4mM ATP) so that the incubation solution covered the entire slide. A piece of parafilm was gently placed over the slides to ensure that the sections did not dry out and remained covered in incubation buffer. Sections were then rinsed 3 times in 1% (w/v) $CaCl_2$ solution in glass Coplin jars, for 2 minutes per wash. Next, 0.1% toluidine blue was used to stain muscle fibers for 1 min in glass Coplin

jars. Sections were rinsed in water until the water was no longer stained blue from the dye. Sections were dehydrated, starting with 70% ethanol, then 95% ethanol, then 100% ethanol for 1 minute each, and then 2 washes in xylene, for 1 minute each. Sections were then mounted with Cytoseal 60 (Richard Allen Scientific), and brightfield images were taken. At least three fields at 10X magnification were taken from different regions of each soleus muscle, and were counted using Image J software. Dark blue staining represents Type I (slow) fibers, and light blue staining represents Type II (fast) fibers.

RNA extraction and real-time quantitative PCR (qRT-PCR)

Total RNA was prepared from soleus and gastrocnemius muscles of 50 day old male mice. Muscles were homogenized using a Power Gen 35 homogenizer (Fisher Scientific) in 600µl of buffer RLT with 6µl of β-mercaptoethanol, and RNA was isolated using the RNeasy Fibrous Tissue Mini Kit (Qiagen) following the manufacturer's instructions, including the on column DNaseI incubation step. Following RNA isolation, RNA was further treated for 1 h at 37°C with DNaseI (Roche), to ensure proper digestion of genomic DNA in the RNA samples. The DNaseI reaction was stopped by adding 2µl of 0.2M EDTA (pH8) to each sample, and heating the reaction to 75°C for 10 minutes. Next, up to 2µg of RNA was used for cDNA synthesis using the Omniscript RT kit (Qiagen) according to the manufacturer's instructions. cDNA synthesis reactions were carried out at 37°C for 1 hour. For qRT-PCR reactions, 10ng of cDNA was used per reaction using MAXIMA SYBR Green kit (Fermentas), according to the manufacturer's protocol. The final concentration of primer used for each reaction was 0.1µM. For primer sets used see Table 3. NFATc1 primers have been previously described (Aliprantis et al.

2008), but are included in Table 3. All reactions were performed in triplicate. The reaction mixtures were analyzed on an Applied Biosystems 7900HT Fast Real Time PCR System. Results were calculated using the ddCt method (Livak et al. 2001) and GADPH was used for normalization. The dissociation curve for each reaction was analyzed to ensure that a single product was made from the reaction and were initially run on an agarose gel to ensure the size of the product matched the expected size.

Table 3: List of primer sets used for qRT-PCR experiments

Gene	Forward primers	Reverse primers
MyHC-IIa	5'- GGACCCACTGAACGAGACC-3'	5'- TGGCAGCTCCACCACTACTT-3'
MyHC-IIb	5'- AGAGCCAAGAGGAAACTGGAGG-3'	5'- CTCGTCCTCAATCTTGCTCTGC-3'
MyHC-IId/x	5'- AGAGCCAAGAGGAAACTGGAGG-3'	5'- CTCGTCCTCAATCTTGCTCTGC-3'
Tnnc2	5'- AGCGAAGAGGAACTGGCTGAGT-3'	5'- CGATCTCCTCTTCTGTCACATGC-3'
Tnni2	5'- GGCTCTAAGCACAAGGTGTGCA-3'	5'- ATTCTTCCTCCAGTCACCCACG-3'
MyHC-1	5'- CCTTGGCACCAATGTCCCGGCTC-3'	5'- GAAGCGCAATGCAGAGTCGGTG-3'
Tnnt1	5'- GAGCAGAGGATGACGCCAAGAA-3'	5'- TTCATCTCCCGACCAGTCTGTC-3'
PGC1a	5'- GAATCAAGCCACTACAGACACCG-3'	5'- CATCCCTCTTGAGCCTTTCGTG-3'
Tnni1	5'- GGCTCTAAGCACAAGGTGTCCA-3'	5- GCCAGACATAGCCTCCACATTC-3'
Tnnc1	5'- GATGGTTCGGTGCATGAAGGAC-3'	5'- CTTCCGTAATGGTCTCACCTGTG-3'
MCK	5'- GGCTTCACTCTGGACGATGTCA-3'	5'- CCTTGAAGACCGTGTAGGACTC-3'
Desmin	5'- GCGGCTAAGAACATCTCTGAGG-3'	5'- ATCTCGCAGGTGTAGGACTGGA-3'
Nestin	5'- AGGAGAAGCAGGGTCTACAGAG-3'	5'- AGTTCTCAGCCTCCAGCAGAGT-3'
myostatin	5'-AACCTTCCCAGGACCAGGAGAA-3'	5'- GGCTTCAAAATCGACCGTGAGG-3'
Mylpf	5'- CGACGCTATGATGAAGGAAGCC-3'	5'- GGACCTTGAAGGCTCCAGTGAT-3'
Mef2c	5'-GGCCATGGTACACCGAGTACAACGA-3'	5'-GGGGATCCCTGTGTTACCTGCACTTG-3'
MyoD	5'- GACAGGGAGGAGGGGTAGAG-3'	5'- TGCTGTCTCAAAGGAGCAGA-3'
Myogenin	5-' CAGTACATTGAGCGCCTACAG-3'	5'- GGACCGAACTCCAGTGCAT-3'
MRF4	5'- ATCAGCTACATTGAGCGTCTACA-3'	5'- CCTGGAATGATCCGAAACACTTG-3'
GAPDH	5'- CATGACCACAGTCCATGC-3'	5'- AGTGAGCTTCCCGTTCAG-3'
NFATc1	5'- TGCCTTTTGCGAGCAGTATCT-3'	5'- CAGGCAAGGATGGGCTCATAT-3'

NFATc1 qRT-PCR primers used are named Nfatc1ex3-F and Nfatc1ex3-R (sequence shown above). Sequence reference is Aliprantis et al (the same paper that originally describes the NFATc1 PCR genotyping strategy, and NFATc1 floxed allele).

Chapter 5: References

Abou Mrad, J., F. Yakubu, D. Lin, J. C. Peters, J. B. Atkinson and J. O. Hill (1992). "Skeletal muscle composition in dietary obesity-susceptible and dietary obesity-resistant rats." Am J Physiol **262**(4 Pt 2): R684-688.

Aliprantis, A. O., Y. Ueki, R. Sulyanto, A. Park, K. S. Sigrist, S. M. Sharma, M. C. Ostrowski, B. R. Olsen and L. H. Glimcher (2008). "NFATc1 in mice represses osteoprotegerin during osteoclastogenesis and dissociates systemic osteopenia from inflammation in cherubism." J Clin Invest **118**(11): 3775-3789.

Allen, D. L., B. C. Harrison, C. Sartorius, W. C. Byrnes and L. A. Leinwand (2001). "Mutation of the IIB myosin heavy chain gene results in muscle fiber loss and compensatory hypertrophy." Am J Physiol Cell Physiol **280**(3): C637-645.

Aramburu, J., M. B. Yaffe, C. Lopez-Rodriguez, L. C. Cantley, P. G. Hogan and A. Rao (1999). "Affinity-driven peptide selection of an NFAT inhibitor more selective than cyclosporin A." Science **285**(5436): 2129-2133.

Armand, A. S., M. Bourajjaj, S. Martinez-Martinez, H. el Azzouzi, P. A. da Costa Martins, P. Hatzis, T. Seidler, J. M. Redondo and L. J. De Windt (2008). "Cooperative synergy between NFAT and MyoD regulates myogenin expression and myogenesis." J Biol Chem **283**(43): 29004-29010.

Asakura, A., H. Hirai, B. Kablar, S. Morita, J. Ishibashi, B. A. Piras, A. J. Christ, M. Verma, K. A. Vineretsky and M. A. Rudnicki (2007). "Increased survival of muscle stem cells lacking the MyoD gene after transplantation into regenerating skeletal muscle." Proc Natl Acad Sci U S A **104**(42): 16552-16557.

Ausoni, S., L. Gorza, S. Schiaffino, K. Gundersen and T. Lomo (1990). "Expression of myosin heavy chain isoforms in stimulated fast and slow rat muscles." J Neurosci **10**(1): 153-160.

Baksh, S., H. R. Widlund, A. A. Frazer-Abel, J. Du, S. Fosmire, D. E. Fisher, J. A. DeCaprio, J. F. Modiano and S. J. Burakoff (2002). "NFATc2-mediated repression of cyclin-dependent kinase 4 expression." Mol Cell **10**(5): 1071-1081.

Bassel-Duby, R. and E. N. Olson (2006). "Signaling pathways in skeletal muscle remodeling." Annu Rev Biochem **75**: 19-37.

Beals, C. R., N. A. Clipstone, S. N. Ho and G. R. Crabtree (1997). "Nuclear localization of NF-ATc by a calcineurin-dependent, cyclosporin-sensitive intramolecular interaction." Genes Dev **11**(7): 824-834.

Benezra, R., R. L. Davis, D. Lockshon, D. L. Turner and H. Weintraub (1990). "The protein Id: a negative regulator of helix-loop-helix DNA binding proteins." Cell **61**(1): 49-59.

Bergstrom, D. A., B. H. Penn, A. Strand, R. L. Perry, M. A. Rudnicki and S. J. Tapscott (2002). "Promoter-specific regulation of MyoD binding and signal transduction cooperate to pattern gene expression." Mol Cell **9**(3): 587-600.

Bergstrom, D. A. and S. J. Tapscott (2001). "Molecular distinction between specification and differentiation in the myogenic basic helix-loop-helix transcription factor family." Mol Cell Biol **21**(7): 2404-2412.

Berkes, C. A. and S. J. Tapscott (2005). "MyoD and the transcriptional control of myogenesis." Semin Cell Dev Biol **16**(4-5): 585-595.

Biressi, S. and T. A. Rando (2010). "Heterogeneity in the muscle satellite cell population." Semin Cell Dev Biol **21**(8): 845-854.
Black, B. L., J. F. Martin and E. N. Olson (1995). "The mouse MRF4 promoter is trans-activated directly and indirectly by muscle-specific transcription factors." J Biol Chem **270**(7): 2889-2892.
Black, B. L., J. D. Molkentin and E. N. Olson (1998). "Multiple roles for the MyoD basic region in transmission of transcriptional activation signals and interaction with MEF2." Mol Cell Biol **18**(1): 69-77.
Black, B. L. and E. N. Olson (1998). "Transcriptional control of muscle development by myocyte enhancer factor-2 (MEF2) proteins." Annu Rev Cell Dev Biol **14**: 167-196.
Blackwell, T. K. and H. Weintraub (1990). "Differences and similarities in DNA-binding preferences of MyoD and E2A protein complexes revealed by binding site selection." Science **250**(4984): 1104-1110.
Blais, A., M. Tsikitis, D. Acosta-Alvear, R. Sharan, Y. Kluger and B. D. Dynlacht (2005). "An initial blueprint for myogenic differentiation." Genes Dev **19**(5): 553-569.
Booth, F. W. and D. B. Thomason (1991). "Molecular and cellular adaptation of muscle in response to exercise: perspectives of various models." Physiol Rev **71**(2): 541-585.
Bozzo, C., B. Spolaore, L. Toniolo, L. Stevens, B. Bastide, C. Cieniewski-Bernard, A. Fontana, Y. Mounier and C. Reggiani (2005). "Nerve influence on myosin light chain phosphorylation in slow and fast skeletal muscles." FEBS J **272**(22): 5771-5785.
Braun, T., M. A. Rudnicki, H. H. Arnold and R. Jaenisch (1992). "Targeted inactivation of the muscle regulatory gene Myf-5 results in abnormal rib development and perinatal death." Cell **71**(3): 369-382.
Brent, A. E. and C. J. Tabin (2002). "Developmental regulation of somite derivatives: muscle, cartilage and tendon." Curr Opin Genet Dev **12**(5): 548-557.
Buckingham, M. (2001). "Skeletal muscle formation in vertebrates." Curr Opin Genet Dev **11**(4): 440-448.
Buckingham, M., L. Bajard, T. Chang, P. Daubas, J. Hadchouel, S. Meilhac, D. Montarras, D. Rocancourt and F. Relaix (2003). "The formation of skeletal muscle: from somite to limb." J Anat **202**(1): 59-68.
Buonanno, A. and N. Rosenthal (1996). "Molecular control of muscle diversity and plasticity." Dev Genet **19**(2): 95-107.
Calabria, E., S. Ciciliot, I. Moretti, M. Garcia, A. Picard, K. A. Dyar, G. Pallafacchina, J. Tothova, S. Schiaffino and M. Murgia (2009). "NFAT isoforms control activity-dependent muscle fiber type specification." Proc Natl Acad Sci U S A **106**(32): 13335-13340.
Charge, S. B., A. S. Brack, S. A. Bayol and S. M. Hughes (2008). "MyoD- and nerve-dependent maintenance of MyoD expression in mature muscle fibres acts through the DRR/PRR element." BMC Dev Biol **8**: 5.
Charge, S. B. and M. A. Rudnicki (2004). "Cellular and molecular regulation of muscle regeneration." Physiol Rev **84**(1): 209-238.

Cheng, T. C., T. A. Hanley, J. Mudd, J. P. Merlie and E. N. Olson (1992). "Mapping of myogenin transcription during embryogenesis using transgenes linked to the myogenin control region." J Cell Biol **119**(6): 1649-1656.

Chin, E. R., E. N. Olson, J. A. Richardson, Q. Yang, C. Humphries, J. M. Shelton, H. Wu, W. Zhu, R. Bassel-Duby and R. S. Williams (1998). "A calcineurin-dependent transcriptional pathway controls skeletal muscle fiber type." Genes Dev **12**(16): 2499-2509.

Choo, M. K., H. Yeo and M. Zayzafoon (2009). "NFATc1 mediates HDAC-dependent transcriptional repression of osteocalcin expression during osteoblast differentiation." Bone **45**(3): 579-589.

Chow, C. W., M. Rincon, J. Cavanagh, M. Dickens and R. J. Davis (1997). "Nuclear accumulation of NFAT4 opposed by the JNK signal transduction pathway." Science **278**(5343): 1638-1641.

Chytil, M. and G. L. Verdine (1996). "The Rel family of eukaryotic transcription factors." Curr Opin Struct Biol **6**(1): 91-100.

Condon, K., L. Silberstein, H. M. Blau and W. J. Thompson (1990). "Differentiation of fiber types in aneural musculature of the prenatal rat hindlimb." Dev Biol **138**(2): 275-295.

Cornelison, D. D., B. B. Olwin, M. A. Rudnicki and B. J. Wold (2000). "MyoD(-/-) satellite cells in single-fiber culture are differentiation defective and MRF4 deficient." Dev Biol **224**(2): 122-137.

Cornelison, D. D. and B. J. Wold (1997). "Single-cell analysis of regulatory gene expression in quiescent and activated mouse skeletal muscle satellite cells." Dev Biol **191**(2): 270-283.

Crabtree, G. R. (1999). "Generic signals and specific outcomes: signaling through Ca2+, calcineurin, and NF-AT." Cell **96**(5): 611-614.

Crabtree, G. R. and E. N. Olson (2002). "NFAT signaling: choreographing the social lives of cells." Cell **109 Suppl**: S67-79.

Crescenzi, M., T. P. Fleming, A. B. Lassar, H. Weintraub and S. A. Aaronson (1990). "MyoD induces growth arrest independent of differentiation in normal and transformed cells." Proc Natl Acad Sci U S A **87**(21): 8442-8446.

Cserjesi, P. and E. N. Olson (1991). "Myogenin induces the myocyte-specific enhancer binding factor MEF-2 independently of other muscle-specific gene products." Mol Cell Biol **11**(10): 4854-4862.

Davis, R. L., P. F. Cheng, A. B. Lassar and H. Weintraub (1990). "The MyoD DNA binding domain contains a recognition code for muscle-specific gene activation." Cell **60**(5): 733-746.

Davis, R. L., H. Weintraub and A. B. Lassar (1987). "Expression of a single transfected cDNA converts fibroblasts to myoblasts." Cell **51**(6): 987-1000.

de la Pompa, J. L., L. A. Timmerman, H. Takimoto, H. Yoshida, A. J. Elia, E. Samper, J. Potter, A. Wakeham, L. Marengere, B. L. Langille, G. R. Crabtree and T. W. Mak (1998). "Role of the NF-ATc transcription factor in morphogenesis of cardiac valves and septum." Nature **392**(6672): 182-186.

de la Serna, I. L., K. A. Carlson and A. N. Imbalzano (2001). "Mammalian SWI/SNF complexes promote MyoD-mediated muscle differentiation." Nat Genet **27**(2): 187-190.

de la Serna, I. L., Y. Ohkawa, C. A. Berkes, D. A. Bergstrom, C. S. Dacwag, S. J. Tapscott and A. N. Imbalzano (2005). "MyoD targets chromatin remodeling complexes to the myogenin locus prior to forming a stable DNA-bound complex." Mol Cell Biol **25**(10): 3997-4009.

Delling, U., J. Tureckova, H. W. Lim, L. J. De Windt, P. Rotwein and J. D. Molkentin (2000). "A calcineurin-NFATc3-dependent pathway regulates skeletal muscle differentiation and slow myosin heavy-chain expression." Mol Cell Biol **20**(17): 6600-6611.

Dodou, E., S. M. Xu and B. L. Black (2003). "mef2c is activated directly by myogenic basic helix-loop-helix proteins during skeletal muscle development in vivo." Mech Dev **120**(9): 1021-1032.

Dreyer, H. C., C. E. Blanco, F. R. Sattler, E. T. Schroeder and R. A. Wiswell (2006). "Satellite cell numbers in young and older men 24 hours after eccentric exercise." Muscle Nerve **33**(2): 242-253.

Eckner, R., T. P. Yao, E. Oldread and D. M. Livingston (1996). "Interaction and functional collaboration of p300/CBP and bHLH proteins in muscle and B-cell differentiation." Genes Dev **10**(19): 2478-2490.

Edmondson, D. G., G. E. Lyons, J. F. Martin and E. N. Olson (1994). "Mef2 gene expression marks the cardiac and skeletal muscle lineages during mouse embryogenesis." Development **120**(5): 1251-1263.

Edstrom, E. and B. Ulfhake (2005). "Sarcopenia is not due to lack of regenerative drive in senescent skeletal muscle." Aging Cell **4**(2): 65-77.

Ekmark, M., Z. A. Rana, G. Stewart, D. G. Hardie and K. Gundersen (2007). "De-phosphorylation of MyoD is linking nerve-evoked activity to fast myosin heavy chain expression in rodent adult skeletal muscle." J Physiol **584**(Pt 2): 637-650.

Evans, W. J. (2010). "Skeletal muscle loss: cachexia, sarcopenia, and inactivity." Am J Clin Nutr **91**(4): 1123S-1127S.

Fladby, T. and J. K. Jansen (1990). "Development of homogeneous fast and slow motor units in the neonatal mouse soleus muscle." Development **109**(3): 723-732.

Flynn, J. M., E. Meadows, M. Fiorotto and W. H. Klein (2010). "Myogenin regulates exercise capacity and skeletal muscle metabolism in the adult mouse." PLoS One **5**(10): e13535.

Forcales, S. V. (2012). "The BAF60c-MyoD complex poises chromatin for rapid transcription." Bioarchitecture **2**(3): 104-109.

Friday, B. B., P. O. Mitchell, K. M. Kegley and G. K. Pavlath (2003). "Calcineurin initiates skeletal muscle differentiation by activating MEF2 and MyoD." Differentiation **71**(3): 217-227.

Gambke, B., G. E. Lyons, J. Haselgrove, A. M. Kelly and N. A. Rubinstein (1983). "Thyroidal and neural control of myosin transitions during development of rat fast and slow muscles." FEBS Lett **156**(2): 335-339.

Garry, D. J., R. S. Bassel-Duby, J. A. Richardson, J. Grayson, P. D. Neufer and R. S. Williams (1996). "Postnatal development and plasticity of specialized muscle fiber characteristics in the hindlimb." Dev Genet **19**(2): 146-156.

Gerber, A. N., T. R. Klesert, D. A. Bergstrom and S. J. Tapscott (1997). "Two domains of MyoD mediate transcriptional activation of genes in repressive chromatin: a

mechanism for lineage determination in myogenesis." Genes & development **11**(4): 436-450.
Gnocchi, V. F., R. B. White, Y. Ono, J. A. Ellis and P. S. Zammit (2009). "Further characterisation of the molecular signature of quiescent and activated mouse muscle satellite cells." PLoS One **4**(4): e5205.
Graef, I. A., J. M. Gastier, U. Francke and G. R. Crabtree (2001). "Evolutionary relationships among Rel domains indicate functional diversification by recombination." Proc Natl Acad Sci U S A **98**(10): 5740-5745.
Gundersen, K. (1998). "Determination of muscle contractile properties: the importance of the nerve." Acta Physiol Scand **162**(3): 333-341.
Guo, K., J. Wang, V. Andres, R. C. Smith and K. Walsh (1995). "MyoD-induced expression of p21 inhibits cyclin-dependent kinase activity upon myocyte terminal differentiation." Mol Cell Biol **15**(7): 3823-3829.
Hagiwara, N., B. Ma and A. Ly (2005). "Slow and fast fiber isoform gene expression is systematically altered in skeletal muscle of the Sox6 mutant, p100H." Dev Dyn **234**(2): 301-311.
Hagiwara, N., M. Yeh and A. Liu (2007). "Sox6 is required for normal fiber type differentiation of fetal skeletal muscle in mice." Dev Dyn **236**(8): 2062-2076.
Halevy, O., B. G. Novitch, D. B. Spicer, S. X. Skapek, J. Rhee, G. J. Hannon, D. Beach and A. B. Lassar (1995). "Correlation of terminal cell cycle arrest of skeletal muscle with induction of p21 by MyoD." Science **267**(5200): 1018-1021.
Hameed, M., R. W. Orrell, M. Cobbold, G. Goldspink and S. D. Harridge (2003). "Expression of IGF-I splice variants in young and old human skeletal muscle after high resistance exercise." J Physiol **547**(Pt 1): 247-254.
Hasty, P., A. Bradley, J. H. Morris, D. G. Edmondson, J. M. Venuti, E. N. Olson and W. H. Klein (1993). "Muscle deficiency and neonatal death in mice with a targeted mutation in the myogenin gene." Nature **364**(6437): 501-506.
Hawke, T. J. and D. J. Garry (2001). "Myogenic satellite cells: physiology to molecular biology." J Appl Physiol **91**(2): 534-551.
Heidt, A. B. and B. L. Black (2005). "Transgenic mice that express Cre recombinase under control of a skeletal muscle-specific promoter from mef2c." Genesis **42**(1): 28-32.
Heidt, A. B., A. Rojas, I. S. Harris and B. L. Black (2007). "Determinants of myogenic specificity within MyoD are required for noncanonical E box binding." Mol Cell Biol **27**(16): 5910-5920.
Hennig, R. and T. Lomo (1985). "Firing patterns of motor units in normal rats." Nature **314**(6007): 164-166.
Hickey, M. S., J. O. Carey, J. L. Azevedo, J. A. Houmard, W. J. Pories, R. G. Israel and G. L. Dohm (1995). "Skeletal muscle fiber composition is related to adiposity and in vitro glucose transport rate in humans." Am J Physiol **268**(3 Pt 1): E453-457.
Hogan, P. G., L. Chen, J. Nardone and A. Rao (2003). "Transcriptional regulation by calcium, calcineurin, and NFAT." Genes Dev **17**(18): 2205-2232.
Hood, D. A. (2001). "Invited Review: contractile activity-induced mitochondrial biogenesis in skeletal muscle." J Appl Physiol **90**(3): 1137-1157.

Horsley, V., B. B. Friday, S. Matteson, K. M. Kegley, J. Gephart and G. K. Pavlath (2001). "Regulation of the growth of multinucleated muscle cells by an NFATC2-dependent pathway." J Cell Biol **153**(2): 329-338.
Horsley, V., K. M. Jansen, S. T. Mills and G. K. Pavlath (2003). "IL-4 acts as a myoblast recruitment factor during mammalian muscle growth." Cell **113**(4): 483-494.
Houmard, J. A., M. L. Weidner, K. E. Gavigan, G. L. Tyndall, M. S. Hickey and A. Alshami (1998). "Fiber type and citrate synthase activity in the human gastrocnemius and vastus lateralis with aging." J Appl Physiol **85**(4): 1337-1341.
Huang, S. and M. P. Czech (2007). "The GLUT4 glucose transporter." Cell Metab **5**(4): 237-252.
Hughes, S. M., K. Koishi, M. Rudnicki and A. M. Maggs (1997). "MyoD protein is differentially accumulated in fast and slow skeletal muscle fibres and required for normal fibre type balance in rodents." Mech Dev **61**(1-2): 151-163.
Hughes, S. M., J. M. Taylor, S. J. Tapscott, C. M. Gurley, W. J. Carter and C. A. Peterson (1993). "Selective accumulation of MyoD and myogenin mRNAs in fast and slow adult skeletal muscle is controlled by innervation and hormones." Development **118**(4): 1137-1147.
Huijbregts, J., J. D. White and M. D. Grounds (2001). "The absence of MyoD in regenerating skeletal muscle affects the expression pattern of basement membrane, interstitial matrix and integrin molecules that is consistent with delayed myotube formation." Acta Histochem **103**(4): 379-396.
Jansen, J. K. and T. Fladby (1990). "The perinatal reorganization of the innervation of skeletal muscle in mammals." Prog Neurobiol **34**(1): 39-90.
Jarvis, J. C., T. Mokrusch, M. M. Kwende, H. Sutherland and S. Salmons (1996). "Fast-to-slow transformation in stimulated rat muscle." Muscle Nerve **19**(11): 1469-1475.
Jiang, H., T. Jordan, J. Li, H. Li and J. X. DiMario (2004). "Innervation-dependent and fiber type-specific transcriptional regulation of the slow myosin heavy chain 2 promoter in avian skeletal muscle fibers." Dev Dyn **231**(2): 292-302.
Kablar, B., A. Asakura, K. Krastel, C. Ying, L. L. May, D. J. Goldhamer and M. A. Rudnicki (1998). "MyoD and Myf-5 define the specification of musculature of distinct embryonic origin." Biochem Cell Biol **76**(6): 1079-1091.
Kassar-Duchossoy, L., B. Gayraud-Morel, D. Gomes, D. Rocancourt, M. Buckingham, V. Shinin and S. Tajbakhsh (2004). "Mrf4 determines skeletal muscle identity in Myf5:Myod double-mutant mice." Nature **431**(7007): 466-471.
Kegley, K. M., J. Gephart, G. L. Warren and G. K. Pavlath (2001). "Altered primary myogenesis in NFATC3(-/-) mice leads to decreased muscle size in the adult." Dev Biol **232**(1): 115-126.
Kim, J. S., D. J. Kosek, J. K. Petrella, J. M. Cross and M. M. Bamman (2005). "Resting and load-induced levels of myogenic gene transcripts differ between older adults with demonstrable sarcopenia and young men and women." J Appl Physiol **99**(6): 2149-2158.
Kitzmann, M. and A. Fernandez (2001). "Crosstalk between cell cycle regulators and the myogenic factor MyoD in skeletal myoblasts." Cell Mol Life Sci **58**(4): 571-579.
Koopman, R., L. Verdijk, R. J. Manders, A. P. Gijsen, M. Gorselink, E. Pijpers, A. J. Wagenmakers and L. J. van Loon (2006). "Co-ingestion of protein and leucine

stimulates muscle protein synthesis rates to the same extent in young and elderly lean men." Am J Clin Nutr **84**(3): 623-632.
Kosek, D. J., J. S. Kim, J. K. Petrella, J. M. Cross and M. M. Bamman (2006). "Efficacy of 3 days/wk resistance training on myofiber hypertrophy and myogenic mechanisms in young vs. older adults." J Appl Physiol **101**(2): 531-544.
Kothary, R., S. Clapoff, S. Darling, M. D. Perry, L. A. Moran and J. Rossant (1989). "Inducible expression of an hsp68-lacZ hybrid gene in transgenic mice." Development **105**(4): 707-714.
Lassar, A. B., R. L. Davis, W. E. Wright, T. Kadesch, C. Murre, A. Voronova, D. Baltimore and H. Weintraub (1991). "Functional activity of myogenic HLH proteins requires hetero-oligomerization with E12/E47-like proteins in vivo." Cell **66**(2): 305-315.
Le Grand, F. and M. Rudnicki (2007). "Satellite and stem cells in muscle growth and repair." Development **134**(22): 3953-3957.
Li, H. and Y. Capetanaki (1993). "Regulation of the mouse desmin gene: transactivated by MyoD, myogenin, MRF4 and Myf5." Nucleic Acids Res **21**(2): 335-343.
Li, J. B. and A. L. Goldberg (1976). "Effects of food deprivation on protein synthesis and degradation in rat skeletal muscles." Am J Physiol **231**(2): 441-448.
Lillioja, S., A. A. Young, C. L. Culter, J. L. Ivy, W. G. Abbott, J. K. Zawadzki, H. Yki-Jarvinen, L. Christin, T. W. Secomb and C. Bogardus (1987). "Skeletal muscle capillary density and fiber type are possible determinants of in vivo insulin resistance in man." J Clin Invest **80**(2): 415-424.
Lin, J., H. Wu, P. T. Tarr, C. Y. Zhang, Z. Wu, O. Boss, L. F. Michael, P. Puigserver, E. Isotani, E. N. Olson, B. B. Lowell, R. Bassel-Duby and B. M. Spiegelman (2002). "Transcriptional co-activator PGC-1 alpha drives the formation of slow-twitch muscle fibres." Nature **418**(6899): 797-801.
Liu, D., B. L. Black and R. Derynck (2001). "TGF-beta inhibits muscle differentiation through functional repression of myogenic transcription factors by Smad3." Genes Dev **15**(22): 2950-2966.
Liu, L. N., P. Dias and P. J. Houghton (1998). "Mutation of Thr115 in MyoD positively regulates function in murine fibroblasts and human rhabdomyosarcoma cells." Cell Growth Differ **9**(9): 699-711.
Liu, Y. and M. F. Schneider (1998). "Fibre type-specific gene expression activated by chronic electrical stimulation of adult mouse skeletal muscle fibres in culture." J Physiol **512 (Pt 2)**: 337-344.
Livak, K. J. and T. D. Schmittgen (2001). "Analysis of relative gene expression data using real-time quantitative PCR and the 2(-Delta Delta C(T)) Method". Methods **25**(4): 402-408
Long, Y. C., S. Glund, P. M. Garcia-Roves and J. R. Zierath (2007). "Calcineurin regulates skeletal muscle metabolism via coordinated changes in gene expression." J Biol Chem **282**(3): 1607-1614.
Lowell, B. B. and G. I. Shulman (2005). "Mitochondrial dysfunction and type 2 diabetes." Science **307**(5708): 384-387.
Luquet, S., J. Lopez-Soriano, D. Holst, A. Fredenrich, J. Melki, M. Rassoulzadegan and P. A. Grimaldi (2003). "Peroxisome proliferator-activated receptor delta controls muscle development and oxidative capability." FASEB J **17**(15): 2299-2301.

Lyons, G. E., M. Ontell, R. Cox, D. Sassoon and M. Buckingham (1990). "The expression of myosin genes in developing skeletal muscle in the mouse embryo." J Cell Biol **111**(4): 1465-1476.

Macharia, R., A. Otto, P. Valasek and K. Patel (2010). "Neuromuscular junction morphology, fiber-type proportions, and satellite-cell proliferation rates are altered in MyoD(-/-) mice." Muscle Nerve **42**(1): 38-52.

Macian, F., C. Lopez-Rodriguez and A. Rao (2001). "Partners in transcription: NFAT and AP-1." Oncogene **20**(19): 2476-2489.

Mal, A., M. Sturniolo, R. L. Schiltz, M. K. Ghosh and M. L. Harter (2001). "A role for histone deacetylase HDAC1 in modulating the transcriptional activity of MyoD: inhibition of the myogenic program." EMBO J **20**(7): 1739-1753.

Matsakas, A. and K. Patel (2009). "Skeletal muscle fibre plasticity in response to selected environmental and physiological stimuli." Histol Histopathol **24**(5): 611-629.

McCullagh, K. J., E. Calabria, G. Pallafacchina, S. Ciciliot, A. L. Serrano, C. Argentini, J. M. Kalhovde, T. Lomo and S. Schiaffino (2004). "NFAT is a nerve activity sensor in skeletal muscle and controls activity-dependent myosin switching." Proc Natl Acad Sci U S A **101**(29): 10590-10595.

McKinsey, T. A., C. L. Zhang, J. Lu and E. N. Olson (2000). "Signal-dependent nuclear export of a histone deacetylase regulates muscle differentiation." Nature **408**(6808): 106-111.

McKinsey, T. A., C. L. Zhang and E. N. Olson (2002). "MEF2: a calcium-dependent regulator of cell division, differentiation and death." Trends Biochem Sci **27**(1): 40-47.

Megeney, L. A., B. Kablar, K. Garrett, J. E. Anderson and M. A. Rudnicki (1996). "MyoD is required for myogenic stem cell function in adult skeletal muscle." Genes Dev **10**(10): 1173-1183.

Miyazaki, M., Y. Hitomi, T. Kizaki, H. Ohno, S. Haga and T. Takemasa (2004). "Contribution of the calcineurin signaling pathway to overload-induced skeletal muscle fiber-type transition." J Physiol Pharmacol **55**(4): 751-764.

Molkentin, J. D., B. L. Black, J. F. Martin and E. N. Olson (1995). "Cooperative activation of muscle gene expression by MEF2 and myogenic bHLH proteins." Cell **83**(7): 1125-1136.

Molkentin, J. D., J. R. Lu, C. L. Antos, B. Markham, J. Richardson, J. Robbins, S. R. Grant and E. N. Olson (1998). "A calcineurin-dependent transcriptional pathway for cardiac hypertrophy." Cell **93**(2): 215-228.

Molkentin, J. D. and E. N. Olson (1996). "Combinatorial control of muscle development by basic helix-loop-helix and MADS-box transcription factors." Proc Natl Acad Sci U S A **93**(18): 9366-9373.

Morley, J. E., R. N. Baumgartner, R. Roubenoff, J. Mayer and K. S. Nair (2001). "Sarcopenia." J Lab Clin Med **137**(4): 231-243.

Mu, X., L. D. Brown, Y. Liu and M. F. Schneider (2007). "Roles of the calcineurin and CaMK signaling pathways in fast-to-slow fiber type transformation of cultured adult mouse skeletal muscle fibers." Physiol Genomics **30**(3): 300-312.

Murre, C., P. S. McCaw and D. Baltimore (1989). "A new DNA binding and dimerization motif in immunoglobulin enhancer binding, daughterless, MyoD, and myc proteins." Cell **56**(5): 777-783.

Nabeshima, Y., K. Hanaoka, M. Hayasaka, E. Esumi, S. Li and I. Nonaka (1993). "Myogenin gene disruption results in perinatal lethality because of severe muscle defect." Nature **364**(6437): 532-535.

Narusawa, M., R. B. Fitzsimons, S. Izumo, B. Nadal-Ginard, N. A. Rubinstein and A. M. Kelly (1987). "Slow myosin in developing rat skeletal muscle." J Cell Biol **104**(3): 447-459.

Naya, F. J., B. Mercer, J. Shelton, J. A. Richardson, R. S. Williams and E. N. Olson (2000). "Stimulation of slow skeletal muscle fiber gene expression by calcineurin in vivo." J Biol Chem **275**(7): 4545-4548.

Naya, F. J., C. Wu, J. A. Richardson, P. Overbeek and E. N. Olson (1999). "Transcriptional activity of MEF2 during mouse embryogenesis monitored with a MEF2-dependent transgene." Development **126**(10): 2045-2052.

Neal, J. W. and N. A. Clipstone (2001). "Glycogen synthase kinase-3 inhibits the DNA binding activity of NFATc." J Biol Chem **276**(5): 3666-3673.

Niro, C., J. Demignon, S. Vincent, Y. Liu, J. Giordani, N. Sgarioto, M. Favier, I. Guillet-Deniau, A. Blais and P. Maire (2010). "Six1 and Six4 gene expression is necessary to activate the fast-type muscle gene program in the mouse primary myotome." Dev Biol **338**(2): 168-182.

Oberbach, A., Y. Bossenz, S. Lehmann, J. Niebauer, V. Adams, R. Paschke, M. R. Schon, M. Bluher and K. Punkt (2006). "Altered fiber distribution and fiber-specific glycolytic and oxidative enzyme activity in skeletal muscle of patients with type 2 diabetes." Diabetes Care **29**(4): 895-900.

Ogilvie, R. W. and D. L. Feeback (1990). "A metachromatic dye-ATPase method for the simultaneous identification of skeletal muscle fiber types I, IIA, IIB and IIC." Stain Technol **65**(5): 231-241.

Oh, M., Rybkin, II, V. Copeland, M. P. Czubryt, J. M. Shelton, E. van Rooij, J. A. Richardson, J. A. Hill, L. J. De Windt, R. Bassel-Duby, E. N. Olson and B. A. Rothermel (2005). "Calcineurin is necessary for the maintenance but not embryonic development of slow muscle fibers." Mol Cell Biol **25**(15): 6629-6638.

Okamura, H., J. Aramburu, C. Garcia-Rodriguez, J. P. Viola, A. Raghavan, M. Tahiliani, X. Zhang, J. Qin, P. G. Hogan and A. Rao (2000). "Concerted dephosphorylation of the transcription factor NFAT1 induces a conformational switch that regulates transcriptional activity." Mol Cell **6**(3): 539-550.

Olguin, H. C., Z. Yang, S. J. Tapscott and B. B. Olwin (2007). "Reciprocal inhibition between Pax7 and muscle regulatory factors modulates myogenic cell fate determination." J Cell Biol **177**(5): 769-779.

Olson, E. N. and R. S. Williams (2000). "Remodeling muscles with calcineurin." Bioessays **22**(6): 510-519.

Ornatsky, O. I., J. J. Andreucci and J. C. McDermott (1997). "A dominant-negative form of transcription factor MEF2 inhibits myogenesis." J Biol Chem **272**(52): 33271-33278.

Parker, M. H., P. Seale and M. A. Rudnicki (2003). "Looking back to the embryo: defining transcriptional networks in adult myogenesis." Nat Rev Genet **4**(7): 497-507.

Parsons, S. A., D. P. Millay, B. J. Wilkins, O. F. Bueno, G. L. Tsika, J. R. Neilson, C. M. Liberatore, K. E. Yutzey, G. R. Crabtree, R. W. Tsika and J. D. Molkentin (2004). "Genetic loss of calcineurin blocks mechanical overload-induced skeletal muscle fiber type switching but not hypertrophy." J Biol Chem **279**(25): 26192-26200.

Parsons, S. A., B. J. Wilkins, O. F. Bueno and J. D. Molkentin (2003). "Altered skeletal muscle phenotypes in calcineurin Aalpha and Abeta gene-targeted mice." Mol Cell Biol **23**(12): 4331-4343.

Patti, M. E., A. J. Butte, S. Crunkhorn, K. Cusi, R. Berria, S. Kashyap, Y. Miyazaki, I. Kohane, M. Costello, R. Saccone, E. J. Landaker, A. B. Goldfine, E. Mun, R. DeFronzo, J. Finlayson, C. R. Kahn and L. J. Mandarino (2003). "Coordinated reduction of genes of oxidative metabolism in humans with insulin resistance and diabetes: Potential role of PGC1 and NRF1." Proc Natl Acad Sci U S A **100**(14): 8466-8471.

Personius, K. E. and R. J. Balice-Gordon (2001). "Loss of correlated motor neuron activity during synaptic competition at developing neuromuscular synapses." Neuron **31**(3): 395-408.

Pette, D. (1998). "Training effects on the contractile apparatus." Acta Physiol Scand **162**(3): 367-376.

Pette, D. and R. S. Staron (2000). "Myosin isoforms, muscle fiber types, and transitions." Microsc Res Tech **50**(6): 500-509.

Pette, D. and R. S. Staron (2001). "Transitions of muscle fiber phenotypic profiles." Histochem Cell Biol **115**(5): 359-372.

Pette, D. and G. Vrbova (1985). "Neural control of phenotypic expression in mammalian muscle fibers." Muscle Nerve **8**(8): 676-689.

Pette, D. and G. Vrbova (1999). "What does chronic electrical stimulation teach us about muscle plasticity?" Muscle Nerve **22**(6): 666-677.

Polesskaya, A., A. Duquet, I. Naguibneva, C. Weise, A. Vervisch, E. Bengal, F. Hucho, P. Robin and A. Harel-Bellan (2000). "CREB-binding protein/p300 activates MyoD by acetylation." The Journal of biological chemistry **275**(44): 34359-34364.

Polesskaya, A., I. Naguibneva, A. Duquet, E. Bengal, P. Robin and A. Harel-Bellan (2001). "Interaction between acetylated MyoD and the bromodomain of CBP and/or p300." Mol Cell Biol **21**(16): 5312-5320.

Porter, C. M., M. A. Havens and N. A. Clipstone (2000). "Identification of amino acid residues and protein kinases involved in the regulation of NFATc subcellular localization." J Biol Chem **275**(5): 3543-3551.

Porter, M. M., A. A. Vandervoort and J. Lexell (1995). "Aging of human muscle: structure, function and adaptability." Scand J Med Sci Sports **5**(3): 129-142.

Potthoff, M. J., H. Wu, M. A. Arnold, J. M. Shelton, J. Backs, J. McAnally, J. A. Richardson, R. Bassel-Duby and E. N. Olson (2007). "Histone deacetylase degradation and MEF2 activation promote the formation of slow-twitch myofibers." J Clin Invest **117**(9): 2459-2467.

Puigserver, P. (2005). "Tissue-specific regulation of metabolic pathways through the transcriptional coactivator PGC1-alpha." Int J Obes (Lond) **29 Suppl 1**: S5-9.

Puri, P. L., M. L. Avantaggiati, C. Balsano, N. Sang, A. Graessmann, A. Giordano and M. Levrero (1997). "p300 is required for MyoD-dependent cell cycle arrest and muscle-specific gene transcription." EMBO J **16**(2): 369-383.

Puri, P. L., S. Iezzi, P. Stiegler, T. T. Chen, R. L. Schiltz, G. E. Muscat, A. Giordano, L. Kedes, J. Y. Wang and V. Sartorelli (2001). "Class I histone deacetylases sequentially interact with MyoD and pRb during skeletal myogenesis." Mol Cell **8**(4): 885-897.

Puri, P. L., V. Sartorelli, X. J. Yang, Y. Hamamori, V. V. Ogryzko, B. H. Howard, L. Kedes, J. Y. Wang, A. Graessmann, Y. Nakatani and M. Levrero (1997). "Differential roles of p300 and PCAF acetyltransferases in muscle differentiation." Mol Cell **1**(1): 35-45.

Rana, Z. A., K. Gundersen and A. Buonanno (2008). "Activity-dependent repression of muscle genes by NFAT." Proc Natl Acad Sci U S A **105**(15): 5921-5926.

Rana, Z. A., K. Gundersen and A. Buonanno (2009). "The ups and downs of gene regulation by electrical activity in skeletal muscles." J Muscle Res Cell Motil **30**(7-8): 255-260.

Ranger, A. M., M. J. Grusby, M. R. Hodge, E. M. Gravallese, F. C. de la Brousse, T. Hoey, C. Mickanin, H. S. Baldwin and L. H. Glimcher (1998). "The transcription factor NF-ATc is essential for cardiac valve formation." Nature **392**(6672): 186-190.

Rao, A., C. Luo and P. G. Hogan (1997). "Transcription factors of the NFAT family: regulation and function." Annu Rev Immunol **15**: 707-747.

Raue, U., D. Slivka, B. Jemiolo, C. Hollon and S. Trappe (2006). "Myogenic gene expression at rest and after a bout of resistance exercise in young (18-30 yr) and old (80-89 yr) women." J Appl Physiol **101**(1): 53-59.

Rudnicki, M. A., T. Braun, S. Hinuma and R. Jaenisch (1992). "Inactivation of MyoD in mice leads to up-regulation of the myogenic HLH gene Myf-5 and results in apparently normal muscle development." Cell **71**(3): 383-390.

Rudnicki, M. A., P. N. Schnegelsberg, R. H. Stead, T. Braun, H. H. Arnold and R. Jaenisch (1993). "MyoD or Myf-5 is required for the formation of skeletal muscle." Cell **75**(7): 1351-1359.

Ryder, J. W., R. Bassel-Duby, E. N. Olson and J. R. Zierath (2003). "Skeletal muscle reprogramming by activation of calcineurin improves insulin action on metabolic pathways." J Biol Chem **278**(45): 44298-44304.

Sabourin, L. A., A. Girgis-Gabardo, P. Seale, A. Asakura and M. A. Rudnicki (1999). "Reduced differentiation potential of primary MyoD-/- myogenic cells derived from adult skeletal muscle." J Cell Biol **144**(4): 631-643.

Sabourin, L. A. and M. A. Rudnicki (2000). "The molecular regulation of myogenesis." Clin Genet **57**(1): 16-25.

Sandri, M., J. Lin, C. Handschin, W. Yang, Z. P. Arany, S. H. Lecker, A. L. Goldberg and B. M. Spiegelman (2006). "PGC-1alpha protects skeletal muscle from atrophy by suppressing FoxO3 action and atrophy-specific gene transcription." Proc Natl Acad Sci U S A **103**(44): 16260-16265.

Sartorelli, V., J. Huang, Y. Hamamori and L. Kedes (1997). "Molecular mechanisms of myogenic coactivation by p300: direct interaction with the activation domain of MyoD and with the MADS box of MEF2C." Mol Cell Biol **17**(2): 1010-1026.

Sartorelli, V., P. L. Puri, Y. Hamamori, V. Ogryzko, G. Chung, Y. Nakatani, J. Y. Wang and L. Kedes (1999). "Acetylation of MyoD directed by PCAF is necessary for the execution of the muscle program." Mol Cell **4**(5): 725-734.

Schiaffino, S. and C. Reggiani (2011). "Fiber types in mammalian skeletal muscles." Physiol Rev **91**(4): 1447-1531.

Schiaffino, S., M. Sandri and M. Murgia (2007). "Activity-dependent signaling pathways controlling muscle diversity and plasticity." Physiology (Bethesda) **22**: 269-278.

Schuierer, M. M., C. J. Mann, H. Bildsoe, C. Huxley and S. M. Hughes (2005). "Analyses of the differentiation potential of satellite cells from myoD-/-, mdx, and PMP22 C22 mice." BMC Musculoskelet Disord **6**: 15.

Schultz, E. (1996). "Satellite cell proliferative compartments in growing skeletal muscles." Dev Biol **175**(1): 84-94.

Schulz, R. A. and K. E. Yutzey (2004). "Calcineurin signaling and NFAT activation in cardiovascular and skeletal muscle development." Dev Biol **266**(1): 1-16.

Seale, P. and M. A. Rudnicki (2000). "A new look at the origin, function, and "stem-cell" status of muscle satellite cells." Dev Biol **218**(2): 115-124.

Shaw, K. T., A. M. Ho, A. Raghavan, J. Kim, J. Jain, J. Park, S. Sharma, A. Rao and P. G. Hogan (1995). "Immunosuppressive drugs prevent a rapid dephosphorylation of transcription factor NFAT1 in stimulated immune cells." Proc Natl Acad Sci U S A **92**(24): 11205-11209.

Shen, T., Y. Liu, Z. Cseresnyes, A. Hawkins, W. R. Randall and M. F. Schneider (2006). "Activity- and calcineurin-independent nuclear shuttling of NFATc1, but not NFATc3, in adult skeletal muscle fibers." Mol Biol Cell **17**(4): 1570-1582.

Sheridan, C. M., E. K. Heist, C. R. Beals, G. R. Crabtree and P. Gardner (2002). "Protein kinase A negatively modulates the nuclear accumulation of NF-ATc1 by priming for subsequent phosphorylation by glycogen synthase kinase-3." J Biol Chem **277**(50): 48664-48676.

Short, K. R., J. L. Vittone, M. L. Bigelow, D. N. Proctor, J. M. Coenen-Schimke, P. Rys and K. S. Nair (2005). "Changes in myosin heavy chain mRNA and protein expression in human skeletal muscle with age and endurance exercise training." J Appl Physiol **99**(1): 95-102.

Simone, C., S. V. Forcales, D. A. Hill, A. N. Imbalzano, L. Latella and P. L. Puri (2004). "p38 pathway targets SWI-SNF chromatin-remodeling complex to muscle-specific loci." Nat Genet **36**(7): 738-743.

Slater, C. R. (1982). "Postnatal maturation of nerve-muscle junctions in hindlimb muscles of the mouse." Dev Biol **94**(1): 11-22.

Smith, C. K., 2nd, M. J. Janney and R. E. Allen (1994). "Temporal expression of myogenic regulatory genes during activation, proliferation, and differentiation of rat skeletal muscle satellite cells." J Cell Physiol **159**(2): 379-385.

Snider, L. and S. J. Tapscott (2003). "Emerging parallels in the generation and regeneration of skeletal muscle." Cell **113**(7): 811-812.

Sorrentino, V., R. Pepperkok, R. L. Davis, W. Ansorge and L. Philipson (1990). "Cell proliferation inhibited by MyoD1 independently of myogenic differentiation." Nature **345**(6278): 813-815.

Spangenburg, E. E. and F. W. Booth (2003). "Molecular regulation of individual skeletal muscle fibre types." Acta Physiol Scand **178**(4): 413-424.

Stellingwerff, T., M. K. Boit and P. T. Res (2007). "Nutritional strategies to optimize training and racing in middle-distance athletes." J Sports Sci **25 Suppl 1**: S17-28.
Swoap, S. J., R. B. Hunter, E. J. Stevenson, H. M. Felton, N. V. Kansagra, J. M. Lang, K. A. Esser and S. C. Kandarian (2000). "The calcineurin-NFAT pathway and muscle fiber-type gene expression." Am J Physiol Cell Physiol **279**(4): C915-924.
Tajbakhsh, S. (2003). "Stem cells to tissue: molecular, cellular and anatomical heterogeneity in skeletal muscle." Curr Opin Genet Dev **13**(4): 413-422.
Tajbakhsh, S. and M. Buckingham (2000). "The birth of muscle progenitor cells in the mouse: spatiotemporal considerations." Curr Top Dev Biol **48**: 225-268.
Tajbakhsh, S., D. Rocancourt and M. Buckingham (1996). "Muscle progenitor cells failing to respond to positional cues adopt non-myogenic fates in myf-5 null mice." Nature **384**(6606): 266-270.
Tanner, C. J., H. A. Barakat, G. L. Dohm, W. J. Pories, K. G. MacDonald, P. R. Cunningham, M. S. Swanson and J. A. Houmard (2002). "Muscle fiber type is associated with obesity and weight loss." Am J Physiol Endocrinol Metab **282**(6): E1191-1196.
Tapscott, S. J. (2005). "The circuitry of a master switch: Myod and the regulation of skeletal muscle gene transcription." Development **132**(12): 2685-2695.
Tapscott, S. J., R. L. Davis, M. J. Thayer, P. F. Cheng, H. Weintraub and A. B. Lassar (1988). "MyoD1: a nuclear phosphoprotein requiring a Myc homology region to convert fibroblasts to myoblasts." Science **242**(4877): 405-411.
Termin, A., R. S. Staron and D. Pette (1989). "Changes in myosin heavy chain isoforms during chronic low-frequency stimulation of rat fast hindlimb muscles. A single-fiber study." Eur J Biochem **186**(3): 749-754.
Thayer, M. J., S. J. Tapscott, R. L. Davis, W. E. Wright, A. B. Lassar and H. Weintraub (1989). "Positive autoregulation of the myogenic determination gene MyoD1." Cell **58**(2): 241-248.
Torgan, C. E. and M. P. Daniels (2001). "Regulation of myosin heavy chain expression during rat skeletal muscle development in vitro." Mol Biol Cell **12**(5): 1499-1508.
Tothova, J., B. Blaauw, G. Pallafacchina, R. Rudolf, C. Argentini, C. Reggiani and S. Schiaffino (2006). "NFATc1 nucleocytoplasmic shuttling is controlled by nerve activity in skeletal muscle." J Cell Sci **119**(Pt 8): 1604-1611.
Vandervoot, A. A. and T. B. Symons (2001). "Functional and metabolic consequences of sarcopenia." Can J Appl Physiol **26**(1): 90-101.
Verdijk, L. B., R. Koopman, G. Schaart, K. Meijer, H. H. Savelberg and L. J. van Loon (2007). "Satellite cell content is specifically reduced in type II skeletal muscle fibers in the elderly." Am J Physiol Endocrinol Metab **292**(1): E151-157.
Verdijk, L. B., T. Snijders, M. Beelen, H. H. Savelberg, K. Meijer, H. Kuipers and L. J. Van Loon (2010). "Characteristics of muscle fiber type are predictive of skeletal muscle mass and strength in elderly men." J Am Geriatr Soc **58**(11): 2069-2075.
Verzi, M. P., J. P. Anderson, E. Dodou, K. K. Kelly, S. B. Greene, B. J. North, R. M. Cripps and B. L. Black (2002). "N-twist, an evolutionarily conserved bHLH protein expressed in the developing CNS, functions as a transcriptional inhibitor." Dev Biol **249**(1): 174-190.

Verzi, M. P., D. J. McCulley, S. De Val, E. Dodou and B. L. Black (2005). "The right ventricle, outflow tract, and ventricular septum comprise a restricted expression domain within the secondary/anterior heart field." Dev Biol **287**(1): 134-145.

Wang, D. Z., M. R. Valdez, J. McAnally, J. Richardson and E. N. Olson (2001). "The Mef2c gene is a direct transcriptional target of myogenic bHLH and MEF2 proteins during skeletal muscle development." Development **128**(22): 4623-4633.

Wang, Y. X. and M. A. Rudnicki (2012). "Satellite cells, the engines of muscle repair." Nat Rev Mol Cell Biol **13**(2): 127-133.

Wang, Y. X., C. L. Zhang, R. T. Yu, H. K. Cho, M. C. Nelson, C. R. Bayuga-Ocampo, J. Ham, H. Kang and R. M. Evans (2004). "Regulation of muscle fiber type and running endurance by PPARdelta." PLoS Biol **2**(10): e294.

Waters, D. L., R. N. Baumgartner and P. J. Garry (2000). "Sarcopenia: current perspectives." J Nutr Health Aging **4**(3): 133-139.

Weintraub, H., R. Davis, S. Tapscott, M. Thayer, M. Krause, R. Benezra, T. K. Blackwell, D. Turner, R. Rupp, S. Hollenberg and et al. (1991). "The myoD gene family: nodal point during specification of the muscle cell lineage." Science **251**(4995): 761-766.

Weintraub, H., V. J. Dwarki, I. Verma, R. Davis, S. Hollenberg, L. Snider, A. Lassar and S. J. Tapscott (1991). "Muscle-specific transcriptional activation by MyoD." Genes Dev **5**(8): 1377-1386.

Weintraub, H., S. J. Tapscott, R. L. Davis, M. J. Thayer, M. A. Adam, A. B. Lassar and A. D. Miller (1989). "Activation of muscle-specific genes in pigment, nerve, fat, liver, and fibroblast cell lines by forced expression of MyoD." Proc Natl Acad Sci U S A **86**(14): 5434-5438.

Wernig, A., A. Irintchev and P. Weisshaupt (1990). "Muscle injury, cross-sectional area and fibre type distribution in mouse soleus after intermittent wheel-running." J Physiol **428**: 639-652.

Wigston, D. J. and A. W. English (1992). "Fiber-type proportions in mammalian soleus muscle during postnatal development." J Neurobiol **23**(1): 61-70.

Wu, H., F. J. Naya, T. A. McKinsey, B. Mercer, J. M. Shelton, E. R. Chin, A. R. Simard, R. N. Michel, R. Bassel-Duby, E. N. Olson and R. S. Williams (2000). "MEF2 responds to multiple calcium-regulated signals in the control of skeletal muscle fiber type." EMBO J **19**(9): 1963-1973.

Yablonka-Reuveni, Z., M. A. Rudnicki, A. J. Rivera, M. Primig, J. E. Anderson and P. Natanson (1999). "The transition from proliferation to differentiation is delayed in satellite cells from mice lacking MyoD." Dev Biol **210**(2): 440-455.

Yan, Z., M. Okutsu, Y. N. Akhtar and V. A. Lira (2011). "Regulation of exercise-induced fiber type transformation, mitochondrial biogenesis, and angiogenesis in skeletal muscle." J Appl Physiol **110**(1): 264-274.

Yang, T. T., Q. Xiong, H. Enslen, R. J. Davis and C. W. Chow (2002). "Phosphorylation of NFATc4 by p38 mitogen-activated protein kinases." Mol Cell Biol **22**(11): 3892-3904.

Zammit, P. S., F. Relaix, Y. Nagata, A. P. Ruiz, C. A. Collins, T. A. Partridge and J. R. Beauchamp (2006). "Pax7 and myogenic progression in skeletal muscle satellite cells." J Cell Sci **119**(Pt 9): 1824-1832.

Zhu, J. and F. McKeon (1999). "NF-AT activation requires suppression of Crm1-dependent export by calcineurin." Nature **398**(6724): 256-260.
Zurlo, F., P. M. Nemeth, R. M. Choksi, S. Sesodia and E. Ravussin (1994). "Whole-body energy metabolism and skeletal muscle biochemical characteristics." Metabolism **43**(4): 481-486.

Publishing Agreement

It is the policy of the University to encourage the distribution of all theses, dissertations, and manuscripts. Copies of all UCSF theses, dissertations, and manuscripts will be routed to the library via the Graduate Division. The library will make all theses, dissertations, and manuscripts accessible to the public and will preserve these to the best of their abilities, in perpetuity.

I hereby grant permission to the Graduate Division of the University of California, San Francisco to release copies of my thesis, dissertation, or manuscript to the Campus Library to provide access and preservation, in whole or in part, in perpetuity.

Melissa Ihlen Stewart 12/31/12

Author Signature Date